

**GEOLOGY AND PETROPHYSICAL CHARACTERIZATION OF
THE FERRON SANDSTONE FOR 3-D SIMULATION OF A
FLUVIAL-DELTAIC RESERVOIR**

Annual
October 1, 1996 - September 30, 1997

By
Thomas C. Chidsey, Jr.
Paul B. Anderson
Thomas H. Morris
John A. Dewey, Jr.
Ann Mattson
Craig B. Foster
S. H. Snelgrove
Thomas A. Ryer

May 1998

Performed Under Contract No. DE-AC22-93BC14896

Utah Geological Survey
Salt Lake City, Utah



**National Petroleum Technology Office
U. S. DEPARTMENT OF ENERGY
Tulsa, Oklahoma**

DISCLAIMER

This report was prepared as an account of work sponsored by an agency of the United States Government. Neither the United States Government nor any agency thereof, nor any of their employees, makes any warranty, expressed or implied, or assumes any legal liability or responsibility for the accuracy, completeness, or usefulness of any information, apparatus, product, or process disclosed, or represents that its use would not infringe privately owned rights. Reference herein to any specific commercial product, process, or service by trade name, trademark, manufacturer, or otherwise does not necessarily constitute or imply its endorsement, recommendation, or favoring by the United States Government or any agency thereof. The views and opinions of authors expressed herein do not necessarily state or reflect those of the United States Government.

This report has been reproduced directly from the best available copy.

Available to DOE and DOE contractors from the Office of Scientific and Technical Information, P.O. Box 62, Oak Ridge, TN 37831; prices available from (615) 576-8401.

Available to the public from the National Technical Information Service, U.S. Department of Commerce, 5285 Port Royal Rd., Springfield VA 22161

DOE/BC/14896-22
Distribution Category UC-122

Geology And Petrophysical Characterization Of The Ferron Sandstone For 3-D
Simulation Of A Fluvial-Deltaic Reservoir

Annual Report
October 1, 1996 - September 30, 1997

By
Thomas C. Chidsey, Jr.
Paul B. Anderson
Thomas H. Morris
John A. Dewey, Jr.
Ann Mattson
Craig B. Foster
S. H. Snelgrove
Thomas A. Ryer

May 1998

Work Performed Under Contract No. DE-AC22-93BC14896

Prepared for
U.S. Department of Energy
Assistant Secretary for Fossil Energy

Robert Lemmon, Project Manager
National Petroleum Technology Office
P.O. Box 3628
Tulsa, OK 74101

Prepared by:
Utah Geological Survey
PO Box 146100
Salt Lake City, UT 84114-6100

CONTENTS

ABSTRACT	ix
EXECUTIVE SUMMARY	xi
ACKNOWLEDGMENTS	xv
1. INTRODUCTION	1-1
1.1 Project Purpose	1-1
1.2 Project Background	1-2
1.3 Approach	1-4
1.4 Annual Report Organization	1-4
1.5 References	1-5
2. REGIONAL STRATIGRAPHY	2-1
2.1 Surface Mapping/Interpretation of the Outcrop Belt	2-1
2.2 Preliminary Regional Stratigraphic Interpretations	2-3
2.3 References	2-4
3. CASE STUDIES	3-1
3.1 Ivie Creek Case-Study Area	3-1
3.1.1 Lithofacies and Depositional Environment Determination	3-2
3.1.1.1 Kf-1-Iv-a Parasequence	3-2
3.1.1.2 Kf-2 Parasequence Set	3-3
3.1.2 Clinoform Characterization	3-5
3.1.2.1 Field Methods	3-6
3.1.2.2 Clinoform Geostatistical Analysis	3-7
3.1.2.3 Clinoform Characteristics:	3-8
3.1.2.4 Depositional History	3-9
3.1.3 Geostatistical Analysis	3-9
3.1.4 Parasequence Characterization from Cross Sections, and Elevation and Isopach Maps	3-13
3.1.5 Development of Three-Dimensional Facies Models	3-19
3.2 Willow Springs Wash Case-Study Area	3-19
3.3 References	3-24
4. RESERVOIR MODELING	4-1
4.1 Assumed Reservoir Conditions	4-3
4.2 Fluid and Rock Properties	4-3
4.2.1 Relative Fluid-Permeability Curves	4-3
4.2.2 Capillary Pressure	4-4

4.2.3 Pressure-Volume Data	4-5
4.3 Two-Dimensional Simulations	4-5
4.4 Three-Dimensional Simulations	4-8
4.5 References	4-18
5. TECHNOLOGY TRANSFER	5-1
5.1 Utah Geological Survey <i>Petroleum News</i> , <i>Survey Notes</i> , and Internet Web Site ..	5-2
5.2 Presentations	5-2
5.3 Publications	5-3

FIGURES

Figure 1.1. Location of the Ferron Sandstone project area	1-1
Figure 1.2. Ferron Sandstone stratigraphy	1-3
Figure 2.1. Diagram showing relative positions of Ferron parasequences and parasequence sets	2-2
Figure 3.1. Data collection point locations in the Ivie Creek case-study area	3-2
Figure 3.2. Example of Ferron Sandstone reservoir gamma-ray type log, core description, and lithofacies	3-4
Figure 3.3. Stratigraphic nomenclature and hierarchical units of the Kf-1 parasequence set, Ivie Creek case-study area	3-6
Figure 3.4. Measurements used for clinoform characterization and bedform thickness vs. position in the Kf-1-Iv-a parasequence, Ivie Creek amphitheater	3-7
Figure 3.5. Time steps during deposition of the lower subcycle of the Kf-1-Iv-a parasequence	3-10
Figure 3.6. Ivie Creek amphitheater two-dimensional deterministic model for the Kf-1-Iv-a parasequence using mean permeability	3-11
Figure 3.7. Cumulative probability curves of lithofacies vs. permeability	3-12
Figure 3.8. Variograms of selected parasequence surfaces in the Kf-1 and Kf-2, Ivie Creek case-study area	3-14
Figure 3.9. Cumulative percent plots of grain size, and permeability vs. potential reservoir facies of Kf-2 and Kf-1-Iv-a	3-15
Figure 3.10. Stratigraphic cross section through the Ivie Creek case-study area	3-16
Figure 3.11. Kriged surface elevation maps, Ivie Creek case-study area	3-17
Figure 3.12. Isopach maps, Ivie Creek case-study area	3-18
Figure 3.13. Schematic, discretized three-dimensional volume from selected block of the Kf-1-Iv-a parasequence within the Ivie Creek case-study area	3-20
Figure 3.14. Cross sections for three-dimensional clinoform facies model	3-21
Figure 3.15. Kf-1-Iv-a three-dimensional facies model, 60-foot elevation layer	3-22
Figure 3.16. Paleogeographic map of the Kf-1-Indian Canyon-c parasequence, Willow Springs Wash case-study area	3-24
Figure 4.1. Location of modeling domains used to simulate fluid flow through clinoform lithofacies of the Kf-1-Iv-a parasequence	4-1
Figure 4.2. Cross sections of Kf-1-Iv-a within the three-dimensional model region	4-2
Figure 4.3. Prototypical two-dimensional modeling domain showing geometry of clinoform lithofacies	4-6
Figure 4.4. Distributions of oil saturation as a function of time within a domain with homogeneous permeability and porosity	4-7
Figure 4.5. Distributions of oil saturation as a function of time within the prototypical, heterogeneous model domain	4-9
Figure 4.6. Clinoform lithofacies distributions in the detailed three-dimensional lithofacies model	4-10

Figure 4.7. Inferred structure of lithofacies along cross sections cut diagonally through the four-well pattern	4-11
Figure 4.8. Production scenario used when simulating the three-dimensional homogeneous case	4-12
Figure 4.9. Grid spacings used in the 1/4-volume three-dimensional model domain	4-13
Figure 4.10. Distribution of oil saturation as a function of time for variable grid within the three-dimensional model domain.	4-14
Figure 4.11. Summary plots of water-injection rate, water cut, and oil-production rate as a function of time	4-15
Figure 4.12. Detailed permeability distribution assigned in the detailed case for the Kf-1-Iv-a parasequence	4-16
Figure 4.13. Layered heterogeneous permeability distribution for the Kf-1-Iv-a parasequence simplified from the detailed style model	4-17
Figure 4.14. Sample plot of oil saturation at five years after the start of production from simulation of the detailed style model	4-19
Figure 4.15. Sample plot of oil saturation at five years after the start of production from simulation of the layered heterogeneous style model	4-20

TABLES

Table 3.1. Depositional facies of the Kf-1 parasequence set in the Willow Springs Wash case-study area	3-23
Table 4.1. Capillary pressure as a function of water saturation	4-4
Table 4.2. Pressure-volume data	4-5

ABSTRACT

The objective of the Ferron Sandstone project is to develop a comprehensive, interdisciplinary, quantitative characterization of a fluvial-deltaic reservoir to allow realistic inter-well and reservoir-scale models to be developed for improved oil-field development in similar reservoirs world-wide. Quantitative geological and petrophysical information on the Cretaceous Ferron Sandstone in east-central Utah was collected. Both new and existing data is being integrated into a three-dimensional model of spatial variations in porosity, storativity, and tensorial rock permeability at a scale appropriate for inter-well to regional-scale reservoir simulation. Simulation results could improve reservoir management through proper infill and extension drilling strategies, reduction of economic risks, increased recovery from existing oil fields, and more reliable reserve calculations. Transfer of the project results to the petroleum industry is an integral component of the project. This report covers research activities for fiscal year 1996-97, the fourth year of the project. Most work consisted of interpreting the large quantity of data collected over two field seasons.

The project is divided into four tasks: (1) regional stratigraphic analysis, (2) case studies, (3) reservoirs models, and (4) field-scale evaluation of exploration strategies. The primary objective of the regional stratigraphic analysis is to provide a more detailed interpretation of the stratigraphy and gross reservoir characteristics of the Ferron Sandstone as exposed in outcrop. The primary objective of the case-studies work is to develop a detailed geological and petrophysical characterization, at well-sweep scale or smaller, of the primary reservoir lithofacies typically found in a fluvial-dominated deltaic reservoir. Work on tasks 3 and 4 consisted of developing two- and three-dimensional reservoir models at various scales. The bulk of the work on these tasks is being completed primarily during the last year of the project, and is incorporating the data and results of the regional stratigraphic analysis and case-studies tasks.

Regionally, the Ferron Sandstone consists of at least seven delta-front sandstone bodies or parasequence sets. Our work focuses on two parasequence sets (Kf-1 and Kf-2) in the lower part of the Ferron. The Kf-1 represents a river-dominated delta deposit which changes from proximal to distal. The Kf-2 contains more and cleaner sand, indicating a more wave-influenced environment of deposition.

During fiscal year 1996-97, lithofacies, measured sections, vertical and horizontal scales, and other data were plotted on photomosaics of the Ferron Sandstone outcrop belt within the study area for both the regional analyses. Interpretive work also continued in two case-study areas: Ivie Creek and Willow Springs Wash. This work included describing the lithofacies found in each parasequence, constructing stratigraphic cross sections, and producing paleogeographic maps.

In the Ivie Creek case-study area, the bounding surfaces between delta-front clinoform deposits were investigated in detail to fully understand how such features affect fluid flow in a reservoir. Data from permeability transects and measured sections in the Kf-1 and Kf-2 were used to determine the statistical structure of the spatially variable permeability field within the delta front and to investigate how geological processes control the spatial distribution of permeability. Detailed

architectural and permeability models based on the high-resolution field work were used to conduct two- and three-dimensional reservoir simulations.

Technology transfer during the fourth project year consisted of booth displays for various professional conventions, technical presentations, publications, maintaining a project home page on the Internet, and preparing for field trips to the area.

EXECUTIVE SUMMARY

Understanding reservoir heterogeneity is the key to increasing oil recovery from existing fields in the United States. Fluvial-deltaic reservoirs have the largest developed oil reserves, and due to the high degree of reservoir heterogeneity, the largest amount of untapped and unrecovered oil within developed reservoirs. Reservoir heterogeneity is dramatically exposed in the fluvial-deltaic Ferron Sandstone Member of the Cretaceous Mancos Shale in east-central Utah.

The Utah Geological Survey (UGS) leads a multidisciplinary team to develop a comprehensive and quantitative characterization of the Ferron Sandstone as an example of a fluvial-deltaic reservoir which will allow realistic interwell and reservoir-scale modeling. These models may be used for improved oil-field development in similar reservoirs world-wide. The Ferron Sandstone project team consists of the UGS (prime contractor), University of Utah, Brigham Young University, Utah State University, Amoco Production Company, Mobil Exploration and Producing Company, and several geologic contractors. This research is performed under the Geoscience/Engineering Reservoir Characterization Program of the U.S. Department of Energy, National Petroleum Technology Office, Tulsa, Oklahoma. This report covers research activities for fiscal year 1996-97, the fourth year of the project. Most work consisted of interpreting large quantities of data collected over two field seasons.

The project is divided into four tasks: (1) regional stratigraphic analysis, (2) case studies, (3) development of reservoirs models, and (4) field-scale evaluation of exploration strategies. The primary objective of the regional stratigraphic analysis is to provide a more detailed interpretation of the sequence stratigraphy and gross reservoir characteristics of the Ferron Sandstone as exposed in outcrop. This regional study includes determining the dimensions and depositional environment of important sandstone reservoir bodies and the nature of contacts with adjacent rocks. The primary objective of the case-studies work is to develop a detailed geological and petrophysical characterization of some of the primary reservoir lithofacies typically found in a fluvial-dominated deltaic reservoir. The bulk of the work on tasks 3 and 4, (reservoir models and field-scale evaluation of exploration strategies), is being conducted primarily during the last year of the project, and is incorporating the data and results of Tasks 1 and 2 (the regional stratigraphic analysis and case-studies tasks).

During the 1996-97 project year, lithofacies, measured sections, vertical and horizontal scales, and other data were plotted on photomosaics in the field for both the regional and case-study analyses. Regionally, the Ferron Sandstone consists of at least nine delta-front sandstone bodies or parasequence sets.

The focus of our work is two parasequence sets in the lower part of the Ferron designated as the Kf-1 and Kf-2. The Kf-1 represents a river-dominated delta deposit which changes from proximal to distal. The Kf-2 contains more and cleaner sand, indicating a more wave-influenced environment of deposition.

A hierarchical system of abbreviations is used to designate each mappable body of rock. Kf designates Cretaceous Ferron Sandstone. The first dash designates the next hierarchical subdivision or parasequence set, for example Kf-2. The next dash in the UGS hierarchical scheme designates

a higher frequency stratigraphic unit which is mappable and is separated from the rocks above and below by a flooding surface and/or transgressive surface of erosion, and makes up the highest frequency unit mapped within each larger stratigraphic unit or parasequence set (for example Kf-2-Muddy Canyon). In most cases these units would fit the definition of a parasequence.

Work continued in the two case-study areas: Ivie Creek and Willow Springs Wash in the central and southern parts respectively of the study area. Lithofacies were described and paleogeographic maps constructed for each parasequence in these areas. The Ferron Sandstone in the Ivie Creek case-study area consists of two regional-scale parasequence sets, the Kf-1 and Kf-2. The Ivie Creek case-study area was selected since it contains abrupt facies changes in the Kf-1 delta-front sandstones. Reservoir modeling is being conducted on data collected from and geological interpretations of the Kf-1 parasequence set in the Ivie Creek case-study area. The modeling effort is concentrating on: (1) variations in fluid flow between the lithofacies, (2) the amount of communication between each parasequence, and (3) the effects the various bounding surfaces within parasequences would have on fluid flow in these units.

Five primary activities were performed as part of the geological characterization of the Ferron Sandstone in the Ivie Creek case-study area: (1) construction of elevation and isopach maps, and cross sections, (2) lithofacies and depositional environment determination, (3) clinoform characterization, (4) geostatistical evaluation, and (5) development of three-dimensional facies models. Cross sections were constructed to tie into the regional picture and for use in the three-dimensional reservoir modeling effort. These cross sections display parasequence and parasequence set boundaries, measured sections, and correlations through geophysical logs and conventional core from five project drill holes. Depositional trends were estimated from parasequence surface elevation and isopach maps. Elevation and isopach maps provided insight into paleotopography, sediment source, and depositional patterns. Analysis of these two data types reveals delta evolution during the deposition of the Kf-1 and Kf-2 parasequence sets.

The Kf-1-Iv-a parasequence is characterized by clinoform geometries that dip basinward, recording an episode of delta progradation into a deeper water, fully marine bay. The clinoform outcrops together form an arcuate feature, which is interpreted as a delta-complex. Based on the geometry of the clinoform deposits, the source for the delta is believed to be from the southeast where outcrops contain numerous distributary channel deposits at the top of Kf-1. The wave-modified Kf-2 parasequence set in the Ivie Creek case-study area was deposited in seven depositional environments: (1) lower shoreface, (2) middle shoreface, (3) upper shoreface, (4) foreshore, (5) distributary complex, (6) distributary channel, and (7) distributary-mouth bar. The gamma-ray log characteristics of each facies were tied to core taken from project drill holes in the area.

The clinoform section of Kf-1-Iv-a parasequence was classified into four lithofacies: clinoform proximal, medial, distal, and cap. Descriptive field data were gathered to better define the flow characteristic across clinoform-to-clinoform boundaries. To characterize the clinoform bedforms, measurements were taken of the overall length of the clinoform body, the inclination angle from datum at quartiles along the bedform, and the bedform thickness at quartiles along the bedform.

Spatial variations in lithofacies, stratigraphic thickness, sedimentary structures, and permeability data were quantified through geostatistical analysis. Geostatistical work was devoted

to: (1) displaying in illustrations the deterministic permeability of Kf-1-Iv-a, (2) testing the permeability data set for log normality, and (3) analyzing permeability controls for both the Kf-1-Iv-a parasequence and Kf-2 parasequence set.

The Willow Springs Wash area is the largest of the study areas and was selected for the excellent three-dimensional aspect of exposures in the Willow Springs Wash and Indian Canyon areas. The focus of the work in the Willow Springs Wash case-study area was parasequences of the Kf-1 delta-front. No reservoir simulations will be conducted on data collected from the Willow Springs Wash area; however, the architectural elements interpreted from the outcrops will be incorporated into the overall reservoir model for the Ferron Sandstone.

Three primary activities were performed as part of the geological characterization of the Ferron Sandstone in the Willow Springs Wash case-study area: (1) photomosaic construction, (2) lithofacies determination, and (3) paleogeographic interpretation. Work during the project year consisted of processing and interpreting the data collected from the Indian Canyon portion of the Willow Springs Wash case-study area during the previous field seasons and detailed photomosaics. Outcrop-based paleogeographic maps were constructed for the various time steps of parasequences in the Kf-1 parasequence set. Eleven distinct depositional facies were described in the Kf-1 parasequence set.

During the project year two- and three-dimensional, fluid-flow modeling was begun on the Kf-1-Iv-1 parasequence in the Ivie Creek case-study area. The modeling strategy was finalized following completion of the field-based characterization activities needed to develop input to both geostatistical models and fluid-flow simulators. Input parameters for both fluid and rock properties have been finalized for a plausible set of reservoir conditions.

The vertical, two-dimensional model domains capture important elements of the transition from proximal to distal fluvial-deltaic lithofacies. In particular, these model domains enable one to explore how clinoform geometry and the inferred properties of the intervening bounding layers might influence the flow of oil and water at the interwell scale. Detailed geological mapping and the results of outcrop-based permeability testing provide a foundation for assigning petrophysical properties within the model domains.

The three-dimensional model domain measures 2,000 feet by 2,000 feet by 80 feet (610x610x24 m). Within this volume, the detailed distribution of lithofacies types of the Kf-1-Iv-a parasequence has been inferred from a three-dimensional grid of 20 feet by 20 feet by 4-foot (6x6x1.2 m) cells using discretized cross sections. Simulations are being made to explore the way that outcrop-based data might be used to improve predictive simulations that, in turn, are needed to plan reservoir development.

Technology transfer during the fourth project year consisted of: (1) displaying project materials at the UGS booth during the national and regional conventions of the American Association of Petroleum Geologists, (2) presenting four technical project lectures to various professional and academic organizations, (3) publishing abstracts, technical progress reports, field trip road logs, and newsletter articles detailing project progress and results, and maintaining a home page for the Ferron Sandstone project on the UGS' Internet web site.

ACKNOWLEDGMENTS

The Ferron Sandstone project is performed under the Geoscience/Engineering Reservoir Characterization Program of the U.S. Department of Energy (DOE), National Petroleum Technology Office, Tulsa, Oklahoma, contract number DE-AC22-93BC14896. The Contracting Officer's Representative is Robert Lemmon.

Project Contributors:

Principal Investigator: M.L. Allison; Utah Geological Survey, Salt Lake City, UT

Program Manager: T.C. Chidsey, Jr.; Utah Geological Survey, Salt Lake City, UT

Task Contributing Scientists and Organizations:

R.L. Bon, T.C. Chidsey, Jr., K.P. McClure, D.E. Tabet, B.T. Tripp, K.A. Waite; Utah Geological Survey, Salt Lake City, UT

P.B. Anderson; Geologic Consultant, Salt Lake City, UT

T.A. Ryer; The ARIES Group, Louisville, CO

M.A. Chan, C.B. Forster, Richard Jarrard, Ann Mattson, S.H. Snelgrove; University of Utah, Salt Lake City, UT

J.A. Dewey, Jr., and T.H. Morris; Brigham Young University, Provo, UT

J.V. Koebbe; Utah State University, Logan, UT

Don Best, Bruce Welton, F.M. Wright III; Mobil Exploration/Producing Technical Center, Dallas, TX

R.L. Chambers, Chandra Rai, and Carl Sondergeld; Amoco Production Company, Tulsa, OK

1. INTRODUCTION

Thomas C. Chidsey, Jr.; Utah Geological Survey

1.1 Project Purpose

Nationwide, fluvial-deltaic reservoirs have the largest developed oil reserves, and due to the high degree of reservoir heterogeneity, the largest amount of untapped and unrecovered oil within developed reservoirs. The purpose of this multi-year project is to use the Ferron Sandstone to develop a comprehensive, interdisciplinary, and quantitative characterization of an outcrop analogue to fluvial-deltaic reservoir which will allow realistic inter-well and reservoir-scale modeling to be used for improved oil-field development in actual reservoirs world-wide. This information should help to improve reserve estimates in fluvial-dominated deltaic reservoir systems and aid in designing more efficient production strategies.

The fluvial-deltaic Ferron Sandstone Member of the Cretaceous Mancos Shale in east-central Utah (figure 1.1) is a perfect analog since its reservoir heterogeneity is dramatically exposed in outcrop. The results may benefit industry by: (1) **increasing recoverable reserves** by identifying untapped compartments created by reservoir heterogeneity, (2) **reducing development costs** by more efficiently siting infill drilling locations, (3) **increasing deliverability** by exploiting the reservoir along optimal fluid-flow paths, (4) **enhancing the application of new technologies**, such as horizontal drilling, by identifying optimal drilling directions to maximize fluid-flow, and (5) **identifying reservoir trends** for field extension drilling.

The geological and petrophysical properties of the Ferron Sandstone are being quantitatively determined by a multidisciplinary team. To evaluate the Ferron Sandstone as a model for fluvial-

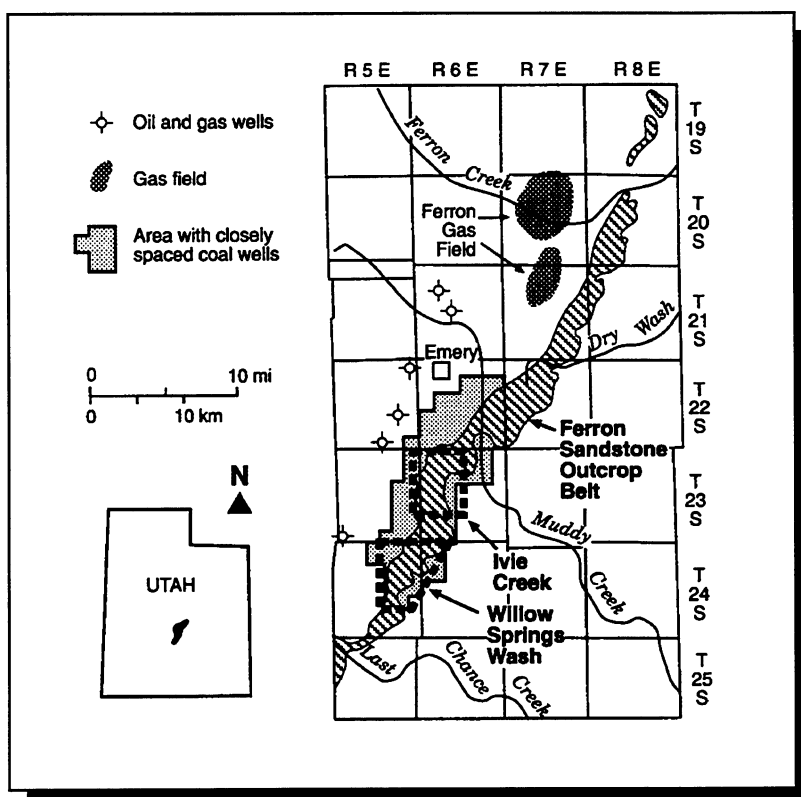


Figure 1.1. Location map of the Ferron Sandstone project area (outcrop belt is cross-hatched) showing detailed case-study areas (outlined by heavy dashed lines).

deltaic reservoirs, the UGS, University of Utah, Brigham Young University, Utah State University, Amoco Production Company, Mobil Exploration/Producing Technical Center, The ARIES Group, and geologic consultant Paul B. Anderson entered into a cooperative agreement with the U.S. Department of Energy as part of its Geoscience/Engineering Reservoir Characterization program.

1.2 Project Background

The Ferron Sandstone Member of the Cretaceous Mancos Shale is well exposed along the west flank of the San Rafael uplift of east-central Utah (figure 1.1). The Ferron Sandstone is a fluvial-deltaic deposit with excellent exposures of a variety of delta facies along the margins of a rapidly subsiding basin (figure 1.2a). The Ferron Sandstone is an analogue for many of the highly productive reservoirs in the Alaskan North Slope, Gulf Coast, and Rocky Mountain regions.

The Ferron Sandstone is an eastward-thinning clastic wedge deposited during Upper Cretaceous time. The Ferron and equivalent portions of the Frontier Formation in northern Utah and Wyoming record a pronounced and widespread regression of the Cretaceous Western Interior seaway. In the study area, these deposits accumulated on a deltaic shoreline in a rapidly subsiding portion of the Cretaceous foreland basin. The Ferron consists of a series of stacked, transgressive-regressive cycles (deltaic-front sets) which are well displayed in outcrop (figure 1.2b). These various deltaic-front sets define a hierarchical pattern of seaward-stepping, vertically-stacked, and landward-stepping depositional geometries. This architecture indicates an initial strong supply of sediment relative to available space where sediment could accumulate, followed by near-balance and then a relative decrease in sediment supply. Each deltaic-front set contains in outcrop all, or portions of each of the complex lithofacies that make up a typical fluvial-dominated deltaic deposit. Such lithofacies include meander channels, distributary channels, tidal channels, mouth-bar complexes, wave-modified strandlines, bar-finger sandstones, prodelta and delta-front deposits, transgressive sandstones, as well as bayfill, lagoonal, and flood-plain deposits.

The excellent exposures and accessibility of the three-tiered, hierarchical stacking pattern and associated complex lithofacies of the deltaic-front sets make the Ferron Sandstone of Utah the best analogue for petroleum reservoirs in fluvial-dominated deltas throughout the world. The Ferron Sandstone is a good analogue for the Triassic Ivishak Formation (the principal reservoir at Prudhoe Bay field, Alaska) and for the Tertiary Wilcox and Frio Formations of south Texas. The Ferron Sandstone is also an excellent model for and is correlative to, the Cretaceous Frontier Formation which produces petroleum throughout Wyoming. The Ferron lithofacies are also a good analogue for the Tertiary Green River and Wasatch Formations, the major oil and gas producing reservoirs in the Uinta Basin, Utah. In addition to its value as a reservoir analogue, sands and coalbeds of the Ferron Sandstone produce gas north of the study area in the Wasatch Plateau and along the west-northwest flank of the San Rafael uplift, currently the most active gas play in Utah.

This project is motivated by the need to deal with complex reservoir heterogeneities on an interwell to field scale. These scales are difficult to resolve in reservoir exploration and development activities. Standard industry approaches to field development rely on generic depositional models constrained primarily by data obtained in petrophysical (logging and coring) evaluations of exploration and development wells. The quantity, quality, and distribution of these data are typically insufficient to adequately model the reservoir. Work on the Ferron Sandstone is predicated on the

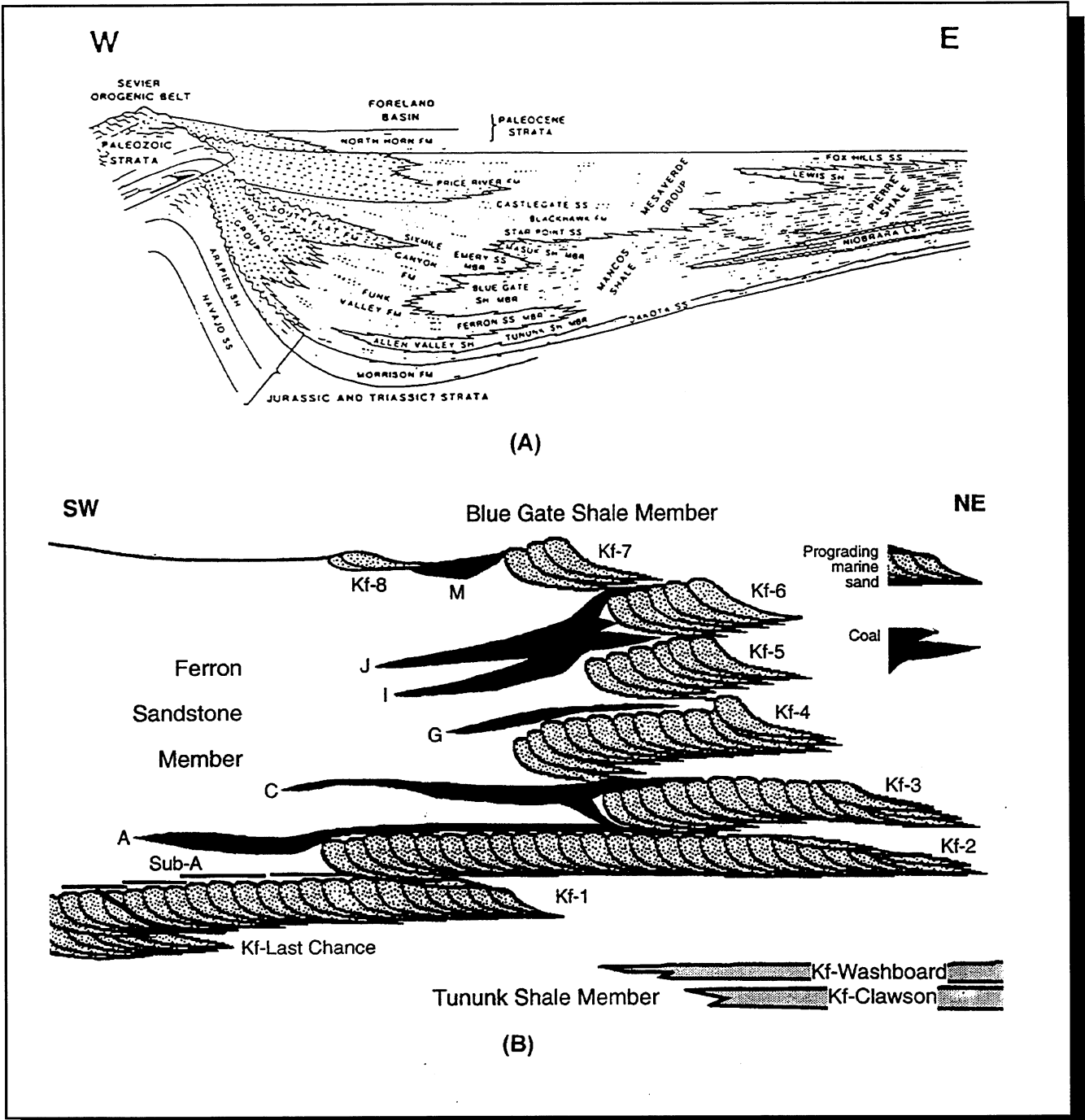


Figure 1.2. Ferron Sandstone stratigraphy: (A) cross section of the Cretaceous foreland basin across Utah (from Ryer, 1981), and (B) diagrammatic cross section of the Ferron Sandstone and adjacent members of the Mancos Shale showing the numbering and stacking of the deltaic-front sets (from Ryer, 1991; Anderson and others, 1997). Coal horizons (black) are designated by letters.

assumption that detailed outcrop mapping of petrophysical and geological properties of this analogue reservoir will provide an unusually comprehensive database and reservoir simulation. Simulation results can be used to guide exploration and development strategies in reservoirs found in similar depositional environments.

1.3 Approach

The primary approach of the study is to quantitatively determine geological and petrophysical properties of the Ferron Sandstone. The project is divided into four tasks: (1) regional stratigraphic analysis, (2) case studies, (3) development of reservoirs models, and (4) field-scale evaluation of exploration strategies. Transfer of the project results to the petroleum industry is an integral component of the project. Both new and existing data are being integrated into a three-dimensional representation of spatial variations in porosity, storativity, and tensorial rock permeability at a scale appropriate for inter-well to regional-scale reservoir simulation.

During the 1996-97 project year (the fourth year of the project), mapping of regional facies refined current models for the architecture, geometry, and distribution of lithofacies in the Ferron Sandstone. Case-study areas provided more detailed mapping and analysis of specific lithofacies important to reservoir production (figure 1.1). Extensive vertical and lateral exposures offered excellent opportunity for investigation. The existing database was augmented with additional detailed mapping of the three-dimensional geologic structure and determination of petrophysical properties of various lithofacies at case-study locations within the Ferron Sandstone outcrop belt to serve as reservoir analogues. Determining permeability anisotropy within each facies was an important consideration and was accomplished by mapping lithofacies, grain sizes, and sedimentary structures.

Information collected is being used to identify flow units within each case-study area at the scale of a single production well. Three-dimensional gridded databases were developed that contain the best estimates of the distributions of both scalar (porosity and storativity) and tensorial (permeability) petrophysical properties of flow units found within the various lithofacies of the Ferron Sandstone. Standard geostatistical approaches were used to extrapolate between the detailed study areas and other observation points.

Reservoir modeling at the field scale was performed to evaluate how a detailed understanding of the geological and petrophysical structure of the Ferron Sandstone will enhance exploration and development strategies in similar reservoir systems. Numerical simulations of reservoir response to multiple-well production strategies are being used to quantitatively assess the effectiveness of both standard and modified strategies.

1.4 Annual Report Organization

This report is organized into five sections: Introduction, Regional Stratigraphy, Case Studies, Reservoir Modeling, and Technology Transfer. It is a progress report of on-going research and is not intended as a final report. Whenever possible, preliminary conclusions have been drawn based on available data and field observations.

1.5 References

- Anderson, P.B., Chidsey, T.C., Jr., and Ryer, T.A., 1997, Fluvial-deltaic sedimentation and stratigraphy of the Ferron Sandstone, *in* Link, P.K., and Kowallis, B.J., editors, Mesozoic to Recent geology of Utah: Provo, Brigham Young University Geology Studies, v. 42, pt. 11, p. 135-154.
- Ryer, T.A., 1981, Deltaic coals of Ferron Sandstone Member of Mancos Shale: predictive model for Cretaceous coal-bearing strata of Western Interior: American Association of Petroleum Geologists Bulletin, v. 65, no. 11, p. 2323-2340.
- 1991, Stratigraphy, facies, and depositional history of the Ferron Sandstone in the canyon of Muddy Creek, east-central Utah: *in* Chidsey, T.C., Jr., editor, Geology of east-central Utah: Utah Geological Association Publication 19, p. 45-54.

2. REGIONAL STRATIGRAPHY

Paul B. Anderson; Geological Consultant
Thomas A. Ryer; The ARIES Group
and
Thomas C. Chidsey, Jr.; Utah Geological Survey

The regional stratigraphy of the Ferron Sandstone has been described by Anderson (1991), Anderson and others (1997), Barton and Angle (1995), Barton and Tyler (1991), Chidsey (1997), Chidsey and Allison (1996), Cotter (1971, 1975a, 1975b, 1976), Davis (1954), Gardner (1991, 1993, 1995), Hodder and Jewell (1979), and Ryer (1981a, 1981b, 1982a, 1982b, 1983, 1991). The primary objective of additional study of regional stratigraphy is to provide a more detailed interpretation of the stratigraphy of the Ferron Sandstone outcrop belt from Last Chance Creek to Ferron Creek (figure 1.1). This area is similar in scale to a moderate to large oil reservoir. The regional study includes determining the dimensions and depositional environment of each sandstone body, and the nature of the contacts with adjacent rocks or flow units. The regional study provides a basis for selecting prime outcrops for detailed case studies of the major reservoir types (mouth-bar complex, wave-modified and river-dominated delta front, distributary channel, and tidal channels). Toward the end of the project, the regional stratigraphic data will be incorporated into model simulations at the oil and gas field scale.

2.1 Surface Mapping/Interpretation of the Outcrop Belt

The main Ferron Sandstone cliff and its deeply incised canyons together provide a three-dimensional view of lithofacies variations and transitions. The Ferron Sandstone has excellent exposures along strike and numerous canyons that cut perpendicular to strike offer excellent exposures along the depositional dip direction. Most of the Ferron Sandstone cliffs within the study area was photographed on the ground and from the air during the 1994 field season. Outcrop photographs then scanned and assembled into 138 photomosaics using image-editing software; these photomosaics cover 80 miles (129 km) of Ferron Sandstone outcrop (figure 1.1).

Each photomosaic is being annotated with the following data collected during the 1994 and 1995 field seasons: (1) flooding surfaces (transgressive surfaces of erosion), (2) possible parasequence boundaries (surfaces which may be a flooding surface, but for which there is not clear evidence of transgression), (3) base of channels, (4) depositional tops of shoreline and bay-fill units, (5) significant bedding surfaces of shoreline units, (6) lateral accretion in tidal inlet and fluvial channel deposits, and (7) bedding surfaces in slump features (figure 2.1). A scale bar is included on the photomosaics and is based on the measurements made in the field on location points which are visible in the photographs. Field-based topographic map tie points and match points for adjacent photomosaics are also included on the photomosaics.

When completed, these annotated photomosaics will be used for correlation, for development of cross sections, and for placement of the case-study areas into the regional setting. The photomosaics will be available on compact discs to researchers.

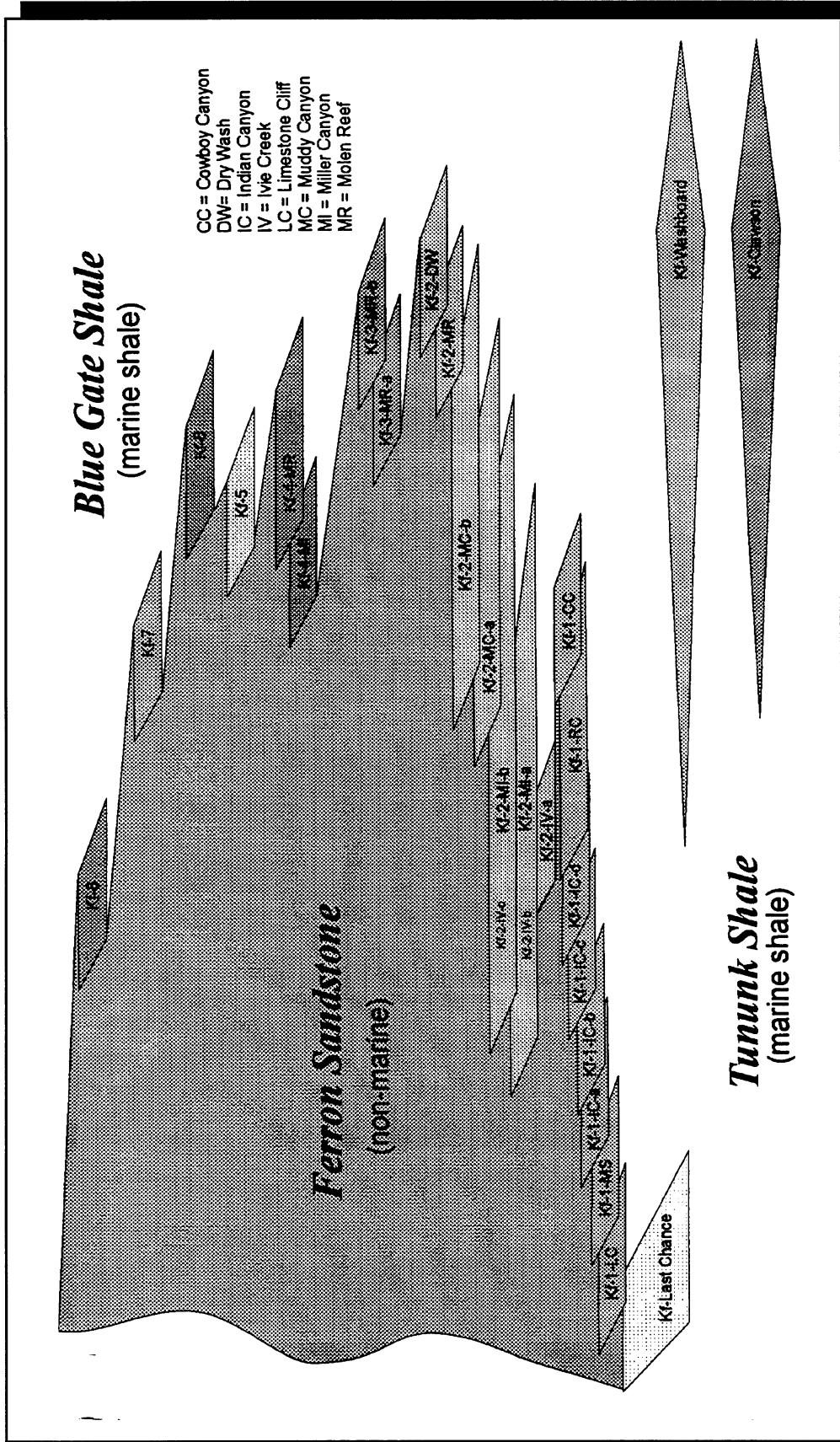


Figure 2.1. Diagram showing relative positions of Ferron parasequences and parasequence sets. The diagram has no scale. Landward is to the left, seaward to the right. The vertical axis is probably better equated to time than to rock section. Note that parasequence sets Kf-5 through Kf-8 are presently not divided into parasequences.

2.2 Preliminary Regional Stratigraphic Interpretations

Ferron Sandstone is recognized as a member of the Mancos Shale. No type section has been designated. The name is derived from the town of Ferron, Utah, but it is clear from Lupton's work (1916) that he would have chosen the outcrops southeast of the town of Emery (figure 1.1) as representative of the member where it is most typically developed. The name Ferron Sandstone is presently used on outcrops around the San Rafael Swell, in the Henry Mountains basin, and beneath Castle Valley and the Wasatch Plateau.

During middle Turonian time, the relatively straight, north-trending western shoreline of the western interior seaway had reached about halfway across Utah (Williams and Stelck, 1975). The shoreline configuration changed as it prograded eastward. The rate of progradation was more rapid in northern and southern Utah, less rapid in central Utah, because of geographical variations in subsidence rates and volumes of sediment arriving from the Sevier orogenic belt to the west. The result was a shoreline bend to the west in the Castle Valley area of east-central Utah. Ryer and Lovekin (1986) concluded that this embayment was caused primarily by very rapid subsidence.

The Ferron Sandstone has been divided into mappable units or bodies of rock. Most of these units would be members of the Ferron, if it were elevated to formation status. Eleven mappable units have been recognized on outcrop from project work (figures 1.2 and 2.1). A hierarchical system of abbreviations is used to designate each mappable body of rock. Kf designates Cretaceous Ferron Sandstone. The first dash designates the next hierarchical subdivision, for example Kf-2, which is comparable to a member or informal "tongue." Most of these "members" are separated by major flooding surfaces and include smaller-scale progradational units that display distinctive stacking patterns; in essence they are parasequence sets, as defined by Van Wagoner and others (1990). The lowest two units, Kf-Clawson and Kf-Washboard (figure 2.1), have been separated and together informally designated "lower Ferron Sandstone" by Ryer and McPhillips (1983). Ryer and McPhillips' "upper Ferron Sandstone" consists of delta-front units 1-7 (Kf-1 through 7 on figures 1.2 and 2.1). Based on UGS project work, their delta-front unit 1 can be divided into Kf-Last Chance (Kf-LC) below and Kf-1 above; in addition, a Kf-8 unit is recognized above Kf-7.

The next dash in the UGS hierarchical scheme (for example Kf-2-Muddy Canyon) designates a higher frequency stratigraphic unit which is mappable and is separated from the rocks above and below by a flooding surface and/or transgressive surface of erosion, and makes up the highest frequency unit mapped within each larger stratigraphic unit or parasequence set. In most cases these units would fit the definition of a parasequence (Van Wagner and others, 1990), but in some cases these units do not strictly fit Van Wagner's definition. With these qualifications, the term parasequence is used to designate the highest frequency stratigraphic unit recognized and mapped.

Other recent studies (Gardner, 1991, 1993, 1995; Barton and Angle, 1995) have not distinguished parasequences in Kf-Clawson, Kf-Washboard, and Kf-7 and 8, although they may exist. Kf-LC contains several parasequences, but it is arguable whether or not a "major" flooding surface is present between it and Kf-1. Internal morphology of Kf-LC indicates it is more aggradational than Kf-1. It is possible for the stacking pattern of a group of parasequences to change from aggradational to progradational without a "major flooding surface." Other characteristics of Kf-LC are distinctive from Kf-1, hence its hierarchical designation. Kf-1 through 7 have associated coal beds, which carry letter designations originally assigned by Lupton (1916).

The oldest unit exposed on the Ferron outcrop belt in Castle Valley is Kf-LC. This unit contains parasequences that are relatively short in overall dip length (1.3 to 0.75 miles [2.1-1.2 km]), rapidly thickening (0 to 60 feet [0-18 m]) with steeply seaward-inclined bed sets (about 5°). The contact with the underlying Tununk Shale is sharp. Unit Kf-LC was deposited in a steeper gradient shoreline topography, than other Ferron stratigraphic units, and with abundant sediment supply.

Progradation of Kf-1 and Kf-2 was characterized by an abundant supply of sediment compared to the creation of accommodation space (Gardner, 1995). A relatively small amount of sediment was required to aggrade the coastal plain and a considerable amount of sediment passed north and east through the fluvial systems to reach the shoreline. Rapid supply of sediment at the river mouths promoted the building of fluvial-dominated deltas, the deposits of which are conspicuously more abundant in Kf-1 and Kf-2 than they are in Kf-3 through Kf-7 (Gardner, 1993). It is highly probable that relative sea level rise caused either by eustatic fluctuations or by pulses of basin subsidence, continually affected the area and are the underlying mechanism for inducing both parasequence-set and parasequence-level transgressions and regressions. A delta is very much "at risk" should even a minor rise of relative sea level occur. Transgression of the coast adjacent to a delta diminishes the river's already inefficient gradient, leading inevitably to avulsion of the river, abandonment of the delta, and rapid transgression across the delta plain. Many such transgressions are recognizable in Kf-LC, Kf-1, and Kf-2.

The earliest, proximal part of each parasequence set consists of parasequences deposited on wave-dominated coasts. The relative sea level rise that brought about the parasequence-level transgressions caused reduction of sediment supply to the coast. As the rise slowed and the balance shifted back to progradation, the supply of sediment to the coast increased. Initially, the supply was low, allowing extensive wave reworking. This also explains the pronounced seaward stratigraphic rise of many parasequences just seaward of their pinchouts. The younger, more distal parasequences of Kf-1 and Kf-2 commonly contain more fluvial-dominated deltaic deposits. At these times, the rate of rise of relative sea level was slower and the amount of sediment delivered to the shoreline was correspondingly greater. The supply was great enough to allow progradation of recognizable deltas.

2.3 References

- Anderson, P.B., 1991, Landward pinch-out of Cretaceous marine nearshore clastics in the Ferron Sandstone Member of the Mancos Shale and Blackhawk Formation, east-central Utah; potential stratigraphic traps: Utah Geological Survey Contract Report 91-12, 110 p.
- Anderson, P.B., Chidsey, T.C., Jr., and Ryer, T.A., 1997, Fluvial-deltaic sedimentation and stratigraphy of the Ferron Sandstone, *in* Link, P.K., and Kowallis, B.J., editors, Mesozoic to Recent geology of Utah: Provo, Brigham Young University Geology Studies, v. 42, pt. 11, p. 135-154.
- Barton, M.D., and Angle, E.S., 1995, Comparative anatomy and petrophysical property structure of seaward- and landward-stepping deltaic reservoir analogs, Ferron Sandstone, Utah: Gas Research Institute Topical Report GRI - 95/0167, 59 p.

- Barton, M.D., and Tyler, Noel, 1991, Quantification of permeability structure in distributary channel deposits Ferron Sandstone, Utah, *in* Chidsey, T.C., Jr., editor, Geology of east-central Utah: Utah Geological Association Publication 19, p. 273-282.
- Chidsey, T.C., Jr., compiler, 1997, Geological and petrophysical characterization of the Ferron Sandstone for 3-D simulation of a fluvial-deltaic reservoir - annual report for the period October 1, 1995 to September 30, 1996: U.S. Department of Energy, DOE/BC/14896-15, 57 p.
- Chidsey, T.C., Jr., and Allison, M.L., compilers, 1996, Geological and petrophysical characterization of the Ferron Sandstone for 3-D simulation of a fluvial-deltaic reservoir - annual report for the period October 1, 1994 to September 30, 1995: U.S. Department of Energy, DOE/BC/14896-13, 104 p.
- Cotter, Edward, 1971, Paleoflow characteristics of a Late Cretaceous river in Utah from analysis of sedimentary structures in the Ferron Sandstone: *Journal of Sedimentary Petrology*, v. 41, no. 1, p. 129-138.
- 1975a, Deltaic deposits in the Upper Cretaceous Ferron Sandstone, Utah, *in* Broussard, M.L.S., editor, Deltas, models for exploration: Houston Geological Society, p. 471-484.
- 1975b, Late Cretaceous sedimentation in a low-energy coastal zone: the Ferron Sandstone of Utah: *Journal of Sedimentary Petrology*, v. 45, p. 15-41.
- 1976, The role of deltas in the evolution of the Ferron Sandstone and its coals: Provo, Brigham Young University Geology Studies, v. 22, pt. 3, p. 15-41.
- Davis, L.J., 1954, Stratigraphy of the Ferron Sandstone, *in* Grier, A.W., editor, Geology of portions of the high plateaus and adjacent canyon lands, central and south-central Utah: Intermountain Association of Petroleum Geologists, Fifth Annual Field Conference Guidebook, p. 55-58.
- Gardner, M.H., 1991, Siliciclastic facies architecture in foreland basin clastic wedges - field guide to the Ferron Sandstone Member of the Mancos Shale, east-central Utah: Boulder, Colorado School of Mines, unpublished report, 35 p.
- 1993, Sequence stratigraphy of the Ferron Sandstone (Turonian) of east-central Utah: Boulder, Colorado School of Mines Ph.D. dissertation, 406 p.
- 1995, The stratigraphic hierarchy and tectonic history of the mid-Cretaceous foreland basin of central Utah, *in* Dorobek, S.L., and Ross, G.M., editors, Stratigraphic evolution of foreland basins: SEPM (Society for Sedimentary Geology) Special Publication No. 52, p. 283-303.

- Hodder, D.T., and Jewell, R.C., editors, 1979, Reclaimability analysis of the Emery coal field, Emery County, Utah: U.S. Bureau of Land Management EMRI Report No. 16, 408 p.
- Lupton, C.T., 1916, Geology and coal resources of Castle Valley in Carbon, Emery, and Sevier Counties, Utah: U.S. Geological Survey Bulletin 628, 88 p.
- Ryer, T.A., 1981a, Deltaic coals of Ferron Sandstone Member of Mancos Shale: predictive model for Cretaceous coal-bearing strata of western interior: American Association of Petroleum Geologists Bulletin, v. 65, no. 11, p. 2323-2340.
- 1981b, The Muddy and Quitcupah Projects: a project report with descriptions of cores of the I, J, and C coal beds from the Emery coal field, central Utah: U.S. Geological Survey Open-File Report 81-460, 34 p.
- 1982a, Possible eustatic control on the location of Utah Cretaceous coal fields, *in* Gurgel, K.D., editor, Proceedings of the 5th Symposium on the Geology of Rocky Mountain Coal: Utah Geological and Mineralogical Survey Bulletin 118, p. 89-93.
- 1982b, Cross section of the Ferron Sandstone Member of the Mancos Shale in the Emery coal field, Emery and Sevier Counties, central Utah: U.S. Geological Survey Map MF-1357, vertical scale: 1 inch = 30 meters, horizontal scale: 1 inch = 1.25 kilometers.
- 1983, Transgressive-regressive cycles and the occurrence of coal in some Upper Cretaceous strata of Utah: *Geology*, v. 11, p. 207-210.
- 1991, Stratigraphy, facies, and depositional history of the Ferron Sandstone in the canyon of Muddy Creek, east-central Utah, *in* Chidsey, T.C., Jr., editor, Geology of east-central Utah: Utah Geological Association Publication 19, p. 45-54.
- Ryer, T.A., and Lovekin, J.R., 1986, The Upper Cretaceous Vernal delta of Utah--depositional or paleotectonic feature?, *in* Peterson, J.A., editor, Paleotectonics and sedimentation in the Rocky Mountain region, United States: American Association of Petroleum Geologists, Memoir 41, p. 497-510.
- Ryer, T.A., and McPhillips, Maureen, 1983, Early Late Cretaceous paleogeography of east-central Utah, *in* Reynolds, W.M., and Dolly, E.D., editors, Mesozoic paleogeography of the west-central United States: SEPM (Society of Sedimentary Geology), Rocky Mountain Section, Rocky Mountain Paleogeography Symposium 2, p. 253-272.
- Van Wagoner, J.C., Mitchum, R.M., Campion, K.M., and Rahmanian, V.D., 1990, Siliciclastic sequence stratigraphy in well-logs, cores, and outcrop: American Association of Petroleum Geologists Methods in Exploration Series 7, p. 1-55.

Williams, G.D., and Stelck, C.R., 1975, Speculation on the Cretaceous paleogeography of North America, *in* Caldwell, W.G.E., editor, The Cretaceous System in the western interior of North America: Geological Association of Canada Special Paper 13, p. 1-20.

3. CASE STUDIES

Paul B. Anderson; Geological Consultant
Thomas C. Chidsey, Jr.; Utah Geological Survey
Ann Mattson; University of Utah
and

Thomas H. Morris and John A. Dewey, Jr.; Brigham Young University

The primary objective of the case studies is to develop a detailed geological and petrophysical characterization, at well-sweep scale or smaller, of the primary reservoir lithofacies typically found in a fluvial-dominated deltaic reservoir. Two case-study areas were selected in 1994 for the project: **Ivie Creek** and **Willow Springs Wash**, in the central and southern parts respectively of the project study area (figure 1.1). The Ivie Creek case-study area was selected since it contains abrupt facies changes in the lower Ferron delta-front sandstones or parasequence sets in outcrops north of Ivie Creek, east of the mouth of Ivie Creek Canyon. Access to the area is excellent because of proximity to Interstate 70 (I-70). Field trips to this area, as part of technology transfer activities, will be easily conducted. Willow Springs Wash is the larger of the two case-study areas. It covers an area 3.5 miles (5.6 km) long and 4 miles (6.4 km) wide (figure 1.1). The site was selected because of the excellent three-dimensional exposures in the Willow Springs Wash and Indian Canyon areas.

The Ferron Sandstone in the Ivie Creek case-study area consists of two regional scale parasequence sets, the Kf-1 and Kf-2. In the Ivie Creek case-study area the Kf-1 parasequence set represents a river-dominated delta deposit which changes from proximal to distal from east to west. The Kf-2 parasequence set represents a wave-modified deposit consisting of lower, middle, and upper shoreface, foreshore, and stream-mouth bar environments of deposition. Reservoir modeling is being conducted on data and geological interpretations of the Kf-1-Ivie Creek-a (Kf-1-Iv-a) parasequence, in the Ivie Creek case-study area. Recommendations will be made on how bounding surfaces can be identified from core and well-log data and, ultimately, how such features should be considered in field development and secondary or enhanced oil recovery programs.

The focus of the work in the Willow Springs Wash case-study area is the parasequences of the Kf-1 parasequence set in Indian Canyon. These rocks represent wave-modified shoreline deposition. No reservoir simulations will be conducted on data collected from the Willow Springs Wash area. However, the architectural elements interpreted from the outcrops here and the Kf-2 at Ivie Creek will be incorporated into the overall reservoir model for the Ferron Sandstone.

3.1 Ivie Creek Case-Study Area

Sedimentary structures, lithofacies, bounding surfaces, and permeabilities measured along closely spaced traverses (both vertical and horizontal) were combined with data from core drilling to develop a three-dimensional view of the reservoirs within each case-study area. In developing the characterization, an evaluation was conducted on how variations in sedimentary structures, bounding surfaces, and lithofacies influence both compartmentalization and anisotropy of permeability.

Five primary activities were performed as part of the geological characterization of the Ferron Sandstone in the Ivie Creek case-study area: (1) lithofacies and depositional environment determination, (2) clinoform characterization, (3) geostatistics, (4) construction of elevation and isopach maps, and cross sections, and (5) development of three-dimensional facies models. Scaled photomosaic panels from the Ivie Creek amphitheater (south-facing outcrop belt) and Quitchupah Canyon (figure 3.1) provide a deterministic framework for two apparent-dip cross sections. These panels along with other photomosaic coverage and data from five drill holes, 15 stratigraphic sections, and 22 permeability transects (figure 3.1), acquired during two field seasons, provided the necessary information for this geologic evaluation and creation of the models to be used in reservoir simulations.

3.1.1 Lithofacies and Depositional Environment Determination

The Kf-1-Iv-a parasequence is characterized by clinoform geometries that dip basinward. The fluvial-dominated bodies were deposited into an area with minimal wave influence, therefore, the primary bedforms are preserved. In contrast, the Kf-2 parasequence set is characterized by more tabular bedforms that are laterally more extensive than those in the Kf-1-Iv-a. The Kf-2 parasequences were deposited into an area with moderate wave energy which reworked the sediments to create more tabular shapes.

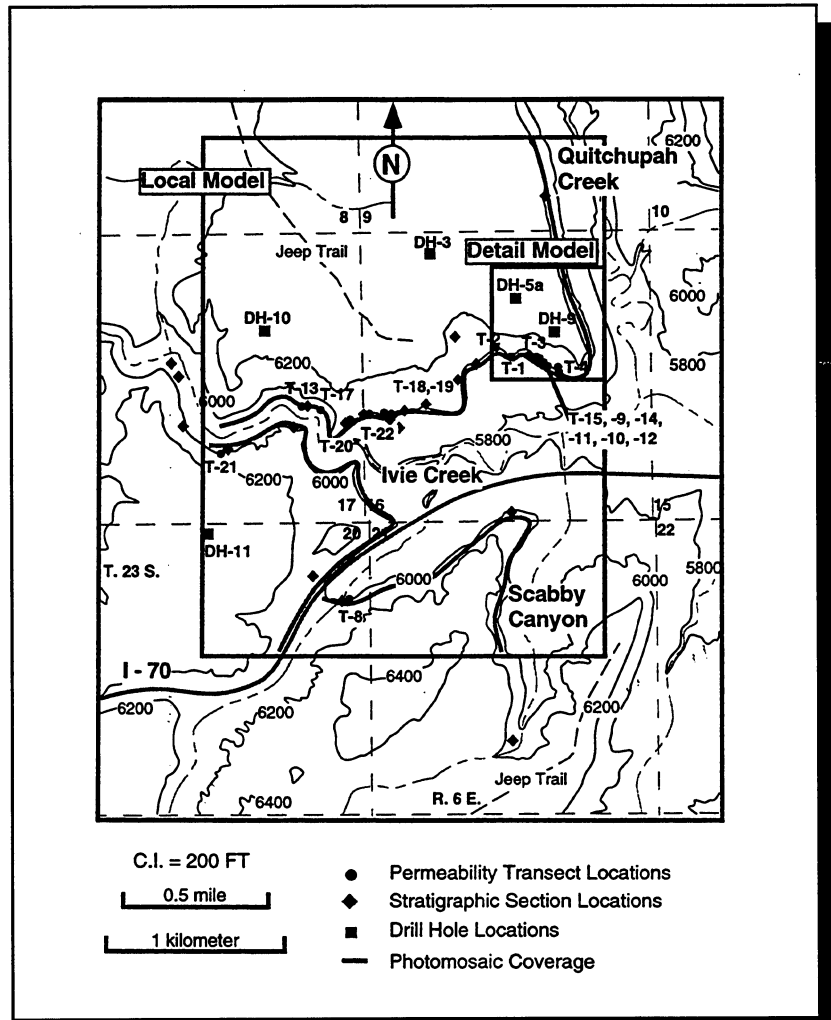


Figure 3.1. Data collection point locations in the Ivie Creek case-study area.

3.1.1.1 Kf-1-Iv-a Parasequence: The clinoform section of Kf-1-Iv-a parasequence was classified into four lithofacies: clinoform proximal (cp), clinoform medial (cm), clinoform distal (cd), and clinoform cap (cc). Lithofacies cp, cm, and cd are assigned to clinoforms only, and lithofacies cc is a bounding facies above the clinoforms (Chidsey, 1997; Anderson and others, 1997).

Lithofacies cp is mostly fine- to medium-grained sandstone. The chief sedimentary structure is low-angle cross-stratification with minor horizontal and trough cross-stratification and rare hummocky bedding. The lithofacies is dominantly thick- to medium-bedded, well to moderately indurated, with permeabilities ranging from 2 to 600 millidarcies (md) and a mean of about 10 md. The inclination of bed boundaries is generally greater than 10°. This lithofacies is interpreted to be the highest energy and most proximal to the sediment input point. The steep inclinations are interpreted to represent deposition into a relatively localized deep area in an open bay environment. The dominance of low-angle cross-stratification with inclinations within the bed or clinoforms in an up-depositional dip direction indicates the influence of on-shore wave energy.

Lithofacies cm is dominantly sandstone with about 5 percent shale. The sandstone is primarily fine-grained with slightly more fine- to very-fine-sized grains than fine- to medium-sized grains. Horizontal beds dominate with some rippled, trough, and low-angle cross-stratified beds. Bed thicknesses range from laminated to very thick, but most are medium. The beds are generally well to moderately indurated, but are occasionally friable. The permeability values range from non-detectable to 100 md with the mean about 3 md. Inclination on the clinoform boundaries is between 2 and 10°. Lithofacies cm is generally transitional between lithofacies cp and cd, but occasionally is present at the erosional truncation or off-lapping boundary of the clinoforms, with no visible connection to lithofacies cp.

Lithofacies cd is sandstone (sometimes silty) with about 10 percent shale. The sandstone grain size is dominantly fine to very fine grained, with considerable variation. Sedimentary structures in this lithofacies are chiefly horizontal laminations and ripples in medium to thin beds. Induration of the beds ranges from well cemented to friable. Average lithofacies cd permeability is just at the detection limit of 2 md, but ranges up to 80 md. This lithofacies is gradational with lithofacies cm and represents the deepest water and lowest energy deposition within the clinoform. It can be traced distally into prodelta to offshore lithofacies.

Lithofacies cc consists of very-fine- to fine-grained, thick- to medium-bedded sandstone. The beds are horizontal, with some trough and low-angle cross-stratification. Burrowing is rare. The sandstone is mostly well indurated, with permeabilities ranging from non-detectable to 100 millidarcies (md) and a mean of about 2 md. This lithofacies is present stratigraphically above the truncated clinoforms near the top of the parasequence and where bed boundaries show little to no inclination. The cc lithofacies is interpreted to represent an eroded and reworked delta top.

The paleogeographic interpretation of Kf-1-Iv-a suggests that the main delta lobe was located to the east and northeast (Chidsey, 1997; Anderson and others, 1997). That delta lobe allowed a protected embayment to develop in the northwest part of the case-study area. The clinoforms represent deposition into the embayment fed by river channels to the southeast. The distributary complexes/delta front, shallow marine, and deep marine environments produced the clinoform proximal, medial, and distal lithofacies respectively.

3.1.1.2 Kf-2 Parasequence Set: The wave-modified Kf-2 parasequence set in the Ivie Creek case-study area was deposited in seven depositional environments: (1) lower shoreface, (2) middle shoreface, (3) upper shoreface, (4) foreshore, (5) distributary complex, (6) distributary channel, and (7) distributary-mouth bar. The gamma-ray log characteristics of each facies were tied to core taken from project drill holes in the area (figure 3.2).

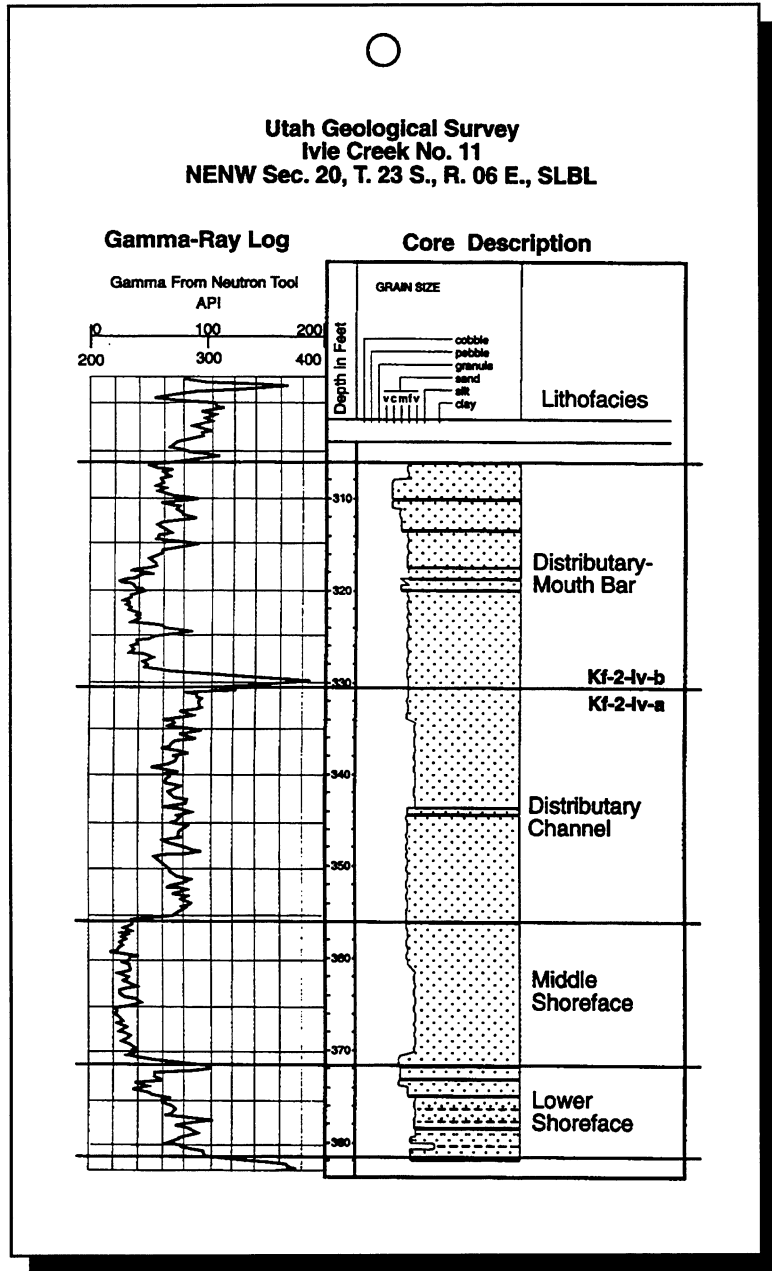


Figure 3.2. Example of Ferron Sandstone reservoir gamma-ray type log, core description, and lithofacies.

The lower shoreface facies consists of thinly interbedded shale to siltstone and very fine- to fine-grained sandstone. Wave ripples to horizontal laminations dominate this facies. Burrowing is generally found on the top of thin sandstone beds and the shale is often bioturbated. This facies is very similar to the transition facies but sandstone is more abundant than shale and siltstone. Hummocky stratification is common.

The middle shoreface facies is very fine- to fine-grained sandstone composed of hummocky, swaley, and planar laminations with minor ripple laminations. This facies is generally thick, representing 50 percent or more of the shoreface sequence. The most common burrow types are *Thalassinoides* and *Ophiomorpha* and the amount of burrowing varies from moderate to highly bioturbated.

The upper shoreface facies is characterized by fine- to medium-grained multidirectionally cross-stratified sandstone, in sets that are commonly separated by planar laminations. This facies is generally about 10 feet (3 m) thick; but greater in the vicinities of the landward pinchouts of the parasequences, where the upper shoreface may reach 20 feet (6.1 m)

in thickness. The facies is slightly to moderately burrowed, with *Ophiomorpha* as the most common trace fossil.

The foreshore facies consists of fine- to medium-grained sandstone which is planar to inclined bedded, slightly to intensely burrowed, and sometimes rooted. This facies is not always present at the top of the shoreface sequence but when present ranges up to a few feet in thickness.

The distributary complex facies is characterized by a predominance of sandstone and trough-cross stratification which is typically unidirectional. In places, this facies can be subdivided into

distributary channel and mouth-bar facies. This facies is often characterized by the complex geometry of bedsets and large-scale bounding surfaces in contrast to the flat to very gently inclined surfaces of the lower delta-front.

The distributary channel facies is common in river-dominated delta-fronts and is also found within the wave-modified shoreline of the Ferron. It is characterized by channels with high height-to-width ratios, and unidirectionally trough-cross-stratified and current-ripple-cross laminations. Channel fills are sandstone dominated, but heterolithic channel fills are common. Troughs in the channel base generally contain mud rip-up clasts, woody fragments, and rare sharks' teeth. This facies grades seaward into the distributary-mouth bar facies.

The distributary-mouth bar facies is found in the upper parts of delta-front sequences and is associated with distributary channels. This facies is characterized by fine-grained or coarser, trough-cross-stratified sandstone, and moderate to intense burrowing associated with lower flow velocities and decreased sedimentation rate, with some completely bioturbated intervals between trough sets. *Ophiomorpha* is common; escape burrows are less common. Paleoflow directions show a strong offshore component with the amount of scatter increasing with increased wave influence and distance from the distributary channel. Traced laterally and seaward, the facies commonly grades into middle shoreface or lower delta-front facies (fluvial-dominated shoreline).

3.1.2 Clinoform Characterization

Smaller sedimentary packages than the parasequence were recognized within Kf-1-Iv-a. Figure 3.3 illustrates these smaller units. In descending order they are: (1) subcycle, (2) clinoform, and (3) bounding layer.

A **subcycle** divides the parasequence into a smaller recognizable coarsening-upward, bed-thickening-upward unit. The mappable extent of the subcycle is distinctively smaller than the parasequence. It is possible that the unit's formation is in response to a localized relative sea-level change, or to a change in sediment supply from an actively forming delta or longshore drift.

Cli-no-form is used to identify a group of beds and bedsets which are inclined seaward in an echelon pattern and generally separated from one another by a distinctive bounding surface observable on outcrop. The clinoforms are visually defined on photomosaics of the outcrop. The clinoform shape is defined on the photomosaics based on a slightly more recessive break in the cliff face chiefly along the bounding surfaces of the clinoform. The resolution of the photography allows only a bounding surface to be drawn with no third dimension. Upon closer examination, it is clear that the line work representing the boundaries of clinoforms are drawn on a unit that generally does have some thickness. In order to clarify this difference, the term **bounding layer** is used to describe the thin rock layer which creates the erosive contrast on the cliff face and is appropriately called a bounding surface at the scale of the subcycle or parasequence. The bounding layer is important as a element of the flow characteristics of a clinoform-type reservoir because it generally contains beds and laminae which are finer grained, mud and carbonaceous-detritus rich, and probably have distinctly lower permeability than the main sand body of the clinoform.

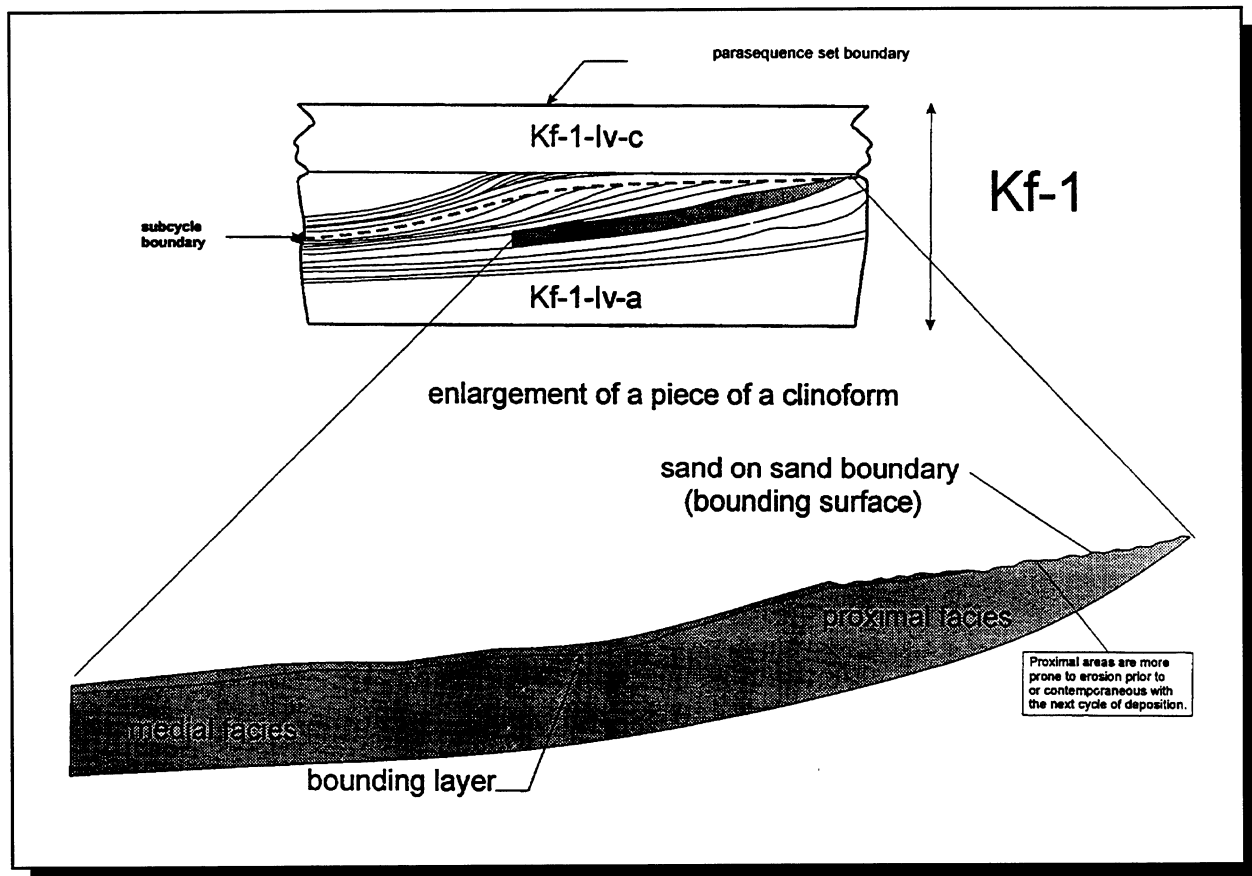


Figure 3.3. Stratigraphic nomenclature and hierarchical units of the Kf-1 parasequence set, Ivie Creek case-study area.

3.1.2.1 Field Methods: Descriptive field data were gathered to better define the flow characteristic across clinoform-to-clinoform boundaries in the Kf-1-Iv-a parasequence in the Ivie Creek case-study area. The emphasis was on bounding layers in portions of the clinoforms which are designated proximal or medial lithofacies. It was assumed that the distal lithofacies in the clinoforms are all similar in permeability and essentially act as strong baffles or barriers to flow.

The measured section data, photomosaics, and overlaying line work (which defines the clinoforms and lithofacies), and permeability transect data were used to target specific clinoforms for study. Bounding layers were described with the following information: location (plotted on the photomosaic), type of bounding surface (between what lithofacies), thickness of the bounding, slope profile, detailed description of lithology, a general description of the rocks above and below the bounding layer, photographs of the layer and the overlying and underlying rock, and geologists' in-field opinion of the cause of the bounding layer.

Twenty-two bounding-layer locations were examined and described. From these field examinations, it was determined that what has been referred to as a surface has a third dimension and varies from a true two-dimensional plane at the tops of the clinoforms to a tabular body with increasing thickness in a down-depositional dip direction.

3.1.2.2 Clinoform Geostatistical Analysis: To characterize the clinoform bedforms, measurements were taken of: (1) the overall length of the clinoform body, (2) the inclination angle from datum at quartiles along the bedform, and (3) the bedform thickness at quartiles along the bedform (figure 3.4A). Some interesting observations arise from the quantitative analysis of the apparent inclination angle data. Upon visual inspection, apparent inclination angles appear to be the same for the Ivie Creek amphitheater and Quitchupah Canyon for a given clinoform facies. However, when the apparent inclination angles are averaged, the angles found in Quitchupah Canyon ($\sim 14^\circ$) are steeper than those in the amphitheater ($\sim 11^\circ$). This implies that Quitchupah Canyon is closer to being a “true dip section” than the amphitheater.

The other parameters necessary to create a typical clinoform shape are the length and thickness of the body. Clinoform lengths range from 40 feet (12.2 m) to greater than 2,000 feet (610 m). A plot of thickness as a function of quartile shows that the first quartile is the thickest part of the clinoform (figure 3.4B). Quartile thickness as a function of facies decreases from clinoform proximal facies to clinoform distal facies. The thickness data combined with the apparent inclination angle data present a two-dimensional picture of the geometry of a typical clinoform.

Climoform facies can also be described as a function of position within a clinoform bedform. For the clinoform bodies analyzed, the dominant facies at the initial position in a bedform are clinoform proximal and clinoform medial. At the final position, the dominant facies is clinoform distal. The facies percentage at each quartile can provide rules to populate clinoform bodies with facies data.

When clinoform facies, permeability, and geometric data are brought together, a “typical clinoform” is constructed. This is a two-dimensional building block that may be used to create a reservoir simulation model based on facies.

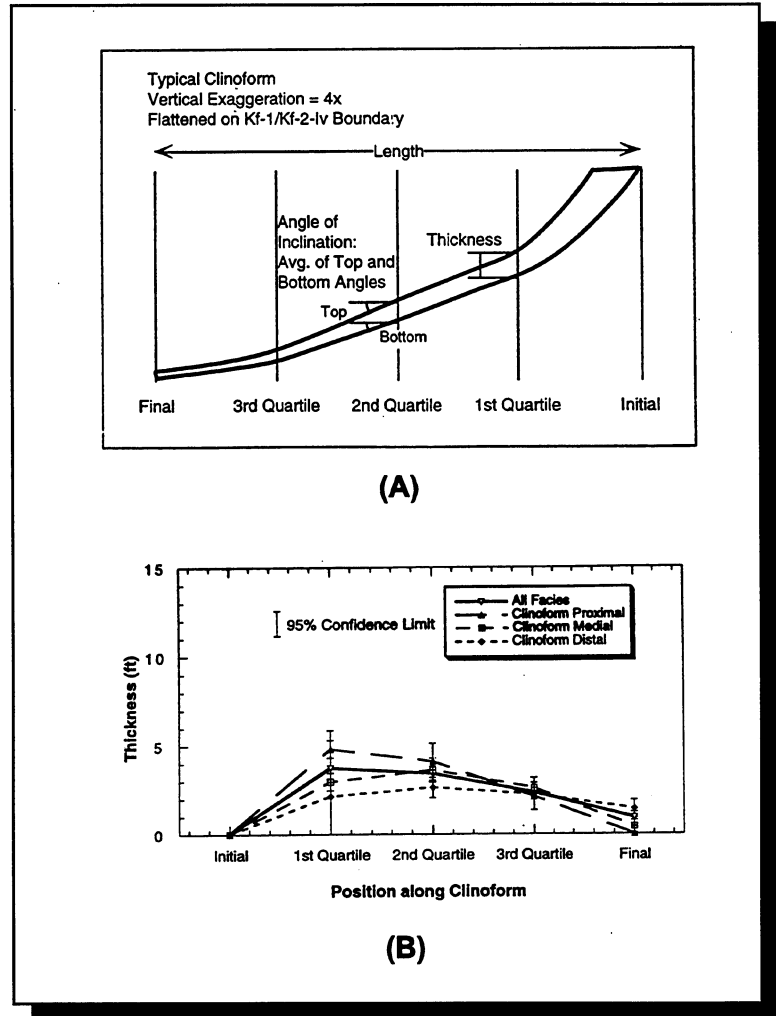


Figure 3.4. (A) Diagram of measurements used for clinoform characterization. (B) Bedform thickness vs. position along clinoforms in the Kf-1-Iv-a parasequence, Ivie Creek amphitheater.

3.1.2.3 Clinoform Characteristics: The clinoforms in the Ivie Creek case-study area change characteristics from the shallower water and more proximal location to the deeper water and more distal locations. Clinoform facies designations (described in section 3.1.1.1) were based on grain size, sedimentary structures, bedding thickness, inclination angle, and stratigraphic position. The abrupt end of the medial facies in figure 3.3 (end of shading) is representative of most of the contacts between proximal, medial, and distal clinoform facies used in this study. Polygon-shaped packages of rock are necessary for reservoir modeling and simulation. In reality, the transition from medial to distal (as well as medial to proximal) is gradational.

The smallest sedimentary package is the bounding layer (figure 3.3). This unit is defined by the base of the overlying clinoform and by the top of the underlying main sand body of the genetically associated clinoform. The lower surface of the bounding layer is generally sharp, but occasionally is gradational over a thin interval. Most of the bounding layers examined contained two common elements: (1) they are finer-grained, less cemented, and less resistant than the overlying and underlying clinoforms, (2) they contain laminations of carbonaceous material, which are consistently poorly cemented and more easily eroded, hence, are expressed as recesses on outcrop. The bounding layer ranges in thickness from less than an inch to a few feet thick. The unit generally decreases in grain size in a down-depositional-dip direction with a corresponding increase in thickness. The bounding layers generally range from fine-grained sandstone to mudstone and commonly contain bedding planes with laminae rich in carbonaceous debris. The bounding layer is chiefly horizontal to slightly irregular bedded with minor oscillation ripples and flaser bedding. Bed thickness is generally thin to laminated. Occasionally some portion of the bounding layer contains gypsum veinlets which are probably related to weathering since they have not been observed in bounding layers examined in core. The lithologic nature of the bounding layer is generally very similar to the clinoform distal facies.

As the bounding layers are followed on outcrop up the inclined surface of the clinoform, the last visible evidence of the bounding layer is often one or several laminae of carbonaceous material forming a very slight recess in the outcrop. On rare occasions the bounding layer does not reach the upper termination of the clinoform, forming a true sand-on-sand contact between clinoforms.

The generally abrupt nature of the contact between the clinoform below and the bounding layer above raises the question: which clinoform is the bounding layer most closely related to? Most of the bottoms of clinoforms (top of the underlying bounding layer) exhibit a smooth, sharp, concave up contact. Occasionally erosional truncation of the underlying bounding layer and/or the underlying clinoform (figure 3.3) is evident, particularly in the more proximal part of the clinoforms, hence, the conclusion that the bounding layer is more closely related to the depositional episode of the underlying clinoform. Sand-on-sand contacts represent either an area of no deposition of the finer-grained sediment during the waning stage of deposition of the underlying clinoform or, an area of erosion prior to, and associated with the deposition of the next clinoform.

The abrupt end of clinoform sand-dominated deposition is interpreted to represent the temporary change in sand distribution at the delta. During the temporary cessation of rapid sedimentation the small amount of wave-energy at the delta front continues to move and rework some bedload sediments. Suspended load (and associated carbonaceous debris) is “raining down” on the delta front almost continuously. Mud, silt, and carbonaceous debris dominance in the deeper water portions of Kf-1-Iv-a indicates the ability of wave-energy to winnow the “fines” to deeper and

lower energy environments. The presence of the bounding layer/clinoform couplet is indicative of high frequency depositional cyclicity during deposition of the subcycle.

3.1.2.4 Depositional History: The Kf-1-Iv-a parasequence in the Ivie Creek case-study area records an episode of delta progradation into a deeper water, fully marine bay. The clinoform outcrops together form an arcuate feature (convex surface to the northwest), which is interpreted as a delta-complex. Based on the geometry of the clinoform deposits, the source for the delta is believed to be from the southeast. Outcrops to the southeast of the study area contain numerous distributary channel deposits at the top of Kf-1.

Figure 3.5 illustrates a map view interpretation of the depositional history through time of a portion of the lower subcycle of Kf-1-Iv-a. Time Step 1 begins during active progradation of delta deposits and after the establishment of a major delta-front deposit prograding into the area. Minor erosion of the uppermost portion of the delta-front (clinoform proximal facies) is portrayed in Time Step 2. Time Steps 3 to 6 illustrate the addition of several clinoforms with some minor erosion. At Time Step 7 a significant change in deposition occurs. Either a relative rise of sea level at this location (most likely caused by minor tectonics or compaction and subsidence of the delta lobe) or a change in the wave-energy regime of the bay resulted in reworking of the previous upper portion of the delta and deposition of the cap facies during Time Step 8. It is likely that this change, marked by the cap facies, was related to a change in the volume or point of discharge of sediments as well. The recognition of an overall fining of the Kf-1-Iv-a at this stratigraphic level points to some change in the depositional regime. This event marks the base of the next subcycle. Distributary channel switching is the most probable mechanism for clinoform cyclicity in figure 3.5; however, no distributary channel deposits have been located juxtaposed with the clinoforms.

3.1.3 Geostatistical Analysis

Spatial variations in lithofacies, stratigraphic thickness, sedimentary structures, and permeability data were quantified through geostatistical analysis. The statistical variability of this information is needed for defining individual petrophysical units within the Ivie Creek case-study area and for predicting the three-dimensional distribution of each unit. The statistical modeling is an important step in developing procedures for "scaling up" from the observational scale to that of a typical reservoir.

Geostatistical work was devoted to: (1) displaying in illustrations the deterministic permeability of Kf-1-Iv-a, (2) testing the permeability data set for log normality, and (3) analysis of permeability controls for both the Kf-1-Iv-a parasequence and Kf-2 parasequence set. Geostatistical analysis required quantification of field data and synthesis of defined lithofacies. The UGS database, composed of geological and petrophysical megascopic observations within the defined lithofacies, was used to generate graphical representations showing spatial variations and relationships of sedimentary structures, grain size, and sand/shale ratios. Statistical analyses included: (1) summary statistics (mean, median, and others) for each parasequence and lithofacies, (2) histograms, (3) cumulative probability plots, (4) relative percentage bar plots, (5) cross plots, and variograms (Mattson, 1997).

Deterministic permeability panels consisted of two models (figure 3.6). The first model incorporated clinoform proximal, medial, and distal lithofacies as the sole control on permeability

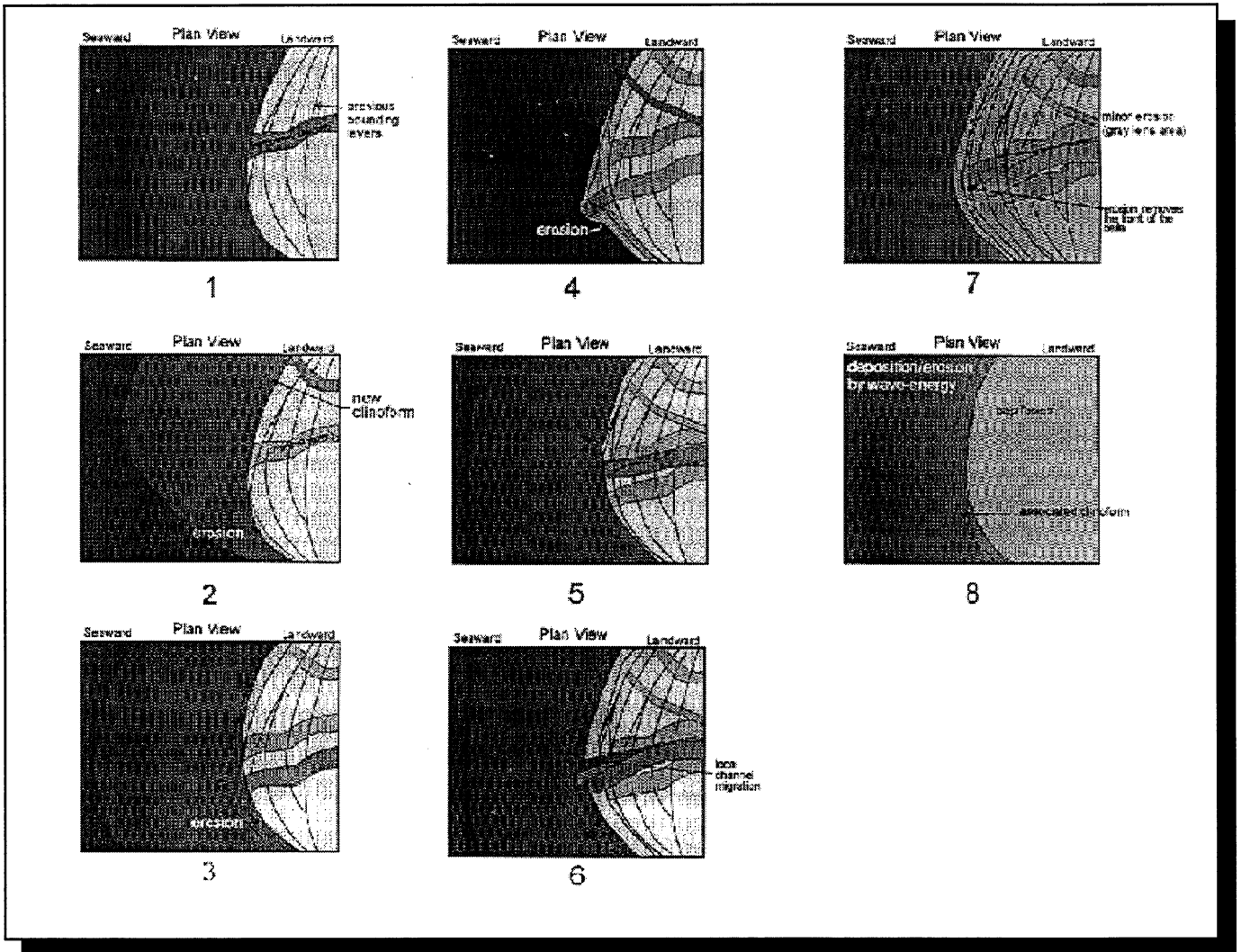


Figure 3.5. Plan view of eight time steps during deposition of the lower subcycle of the Kf-1-Iv-a parasequence. These views emphasize the switching of a distributary channel. Changes in the amount of wave-energy or sediment reaching the shore also influenced clinoform cyclicity.

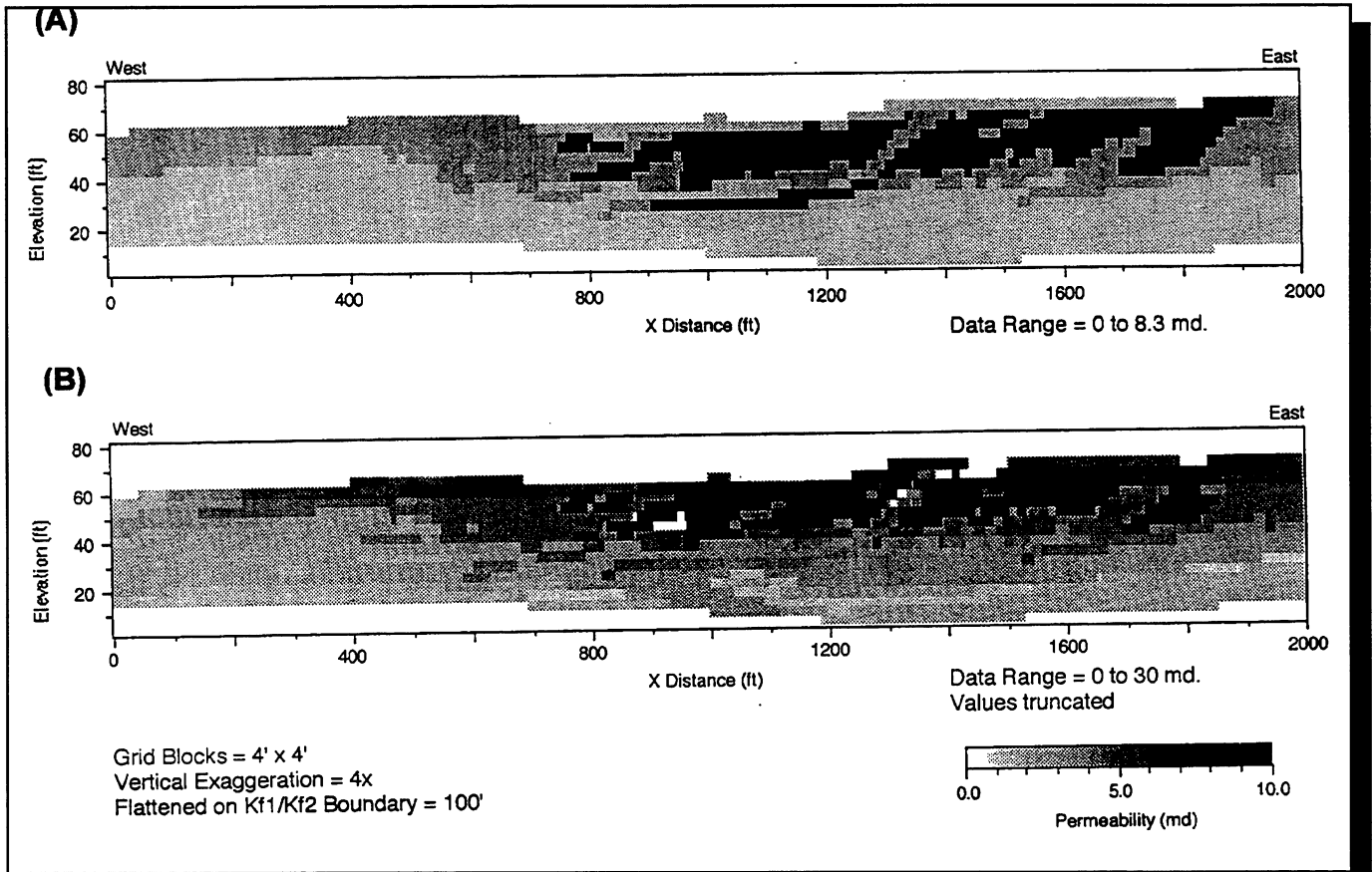


Figure 3.6. Ivie Creek amphitheater two-dimensional deterministic model for the Kf-1-Iv-a parasequence. (A) Geometric mean permeability distribution incorporating only lithofacies. (B) Geometric mean permeability distribution incorporating lithofacies, sedimentary structure, and average grain size.

distribution (figure 3.6A). The second model incorporated lithofacies, sedimentary structure, and average grain size to distribute permeability values (figure 3.6B). Each block in the model was populated with the geometric mean of the permeability data.

The Lilliefors test was used to analyze the permeability data set for log normality since it could handle the large number of data points involved and is considered to be one of the more robust tests available. Of the 41 categories (combinations of clinoform facies, sedimentary structure, and average grain size) that permeability data were divided into, only nine categories met the criteria of log normality. Categories failed due to two factors: (1) the large number of data points which cause the cumulative probability curve to be highly constrained so even a small deviation away from log normality will result in test failure, and (2) the limits of the permeability instruments (0.5 and 2.0 md) which create step increases in the cumulative probability curves. The influence of the second factor is evident when Kf-1-Iv-a permeability data were modeled to remove instrument effects. Three Kf-1-Iv-a modeled data sets from the nine categories (figure 3.7) pass the log-normality test.

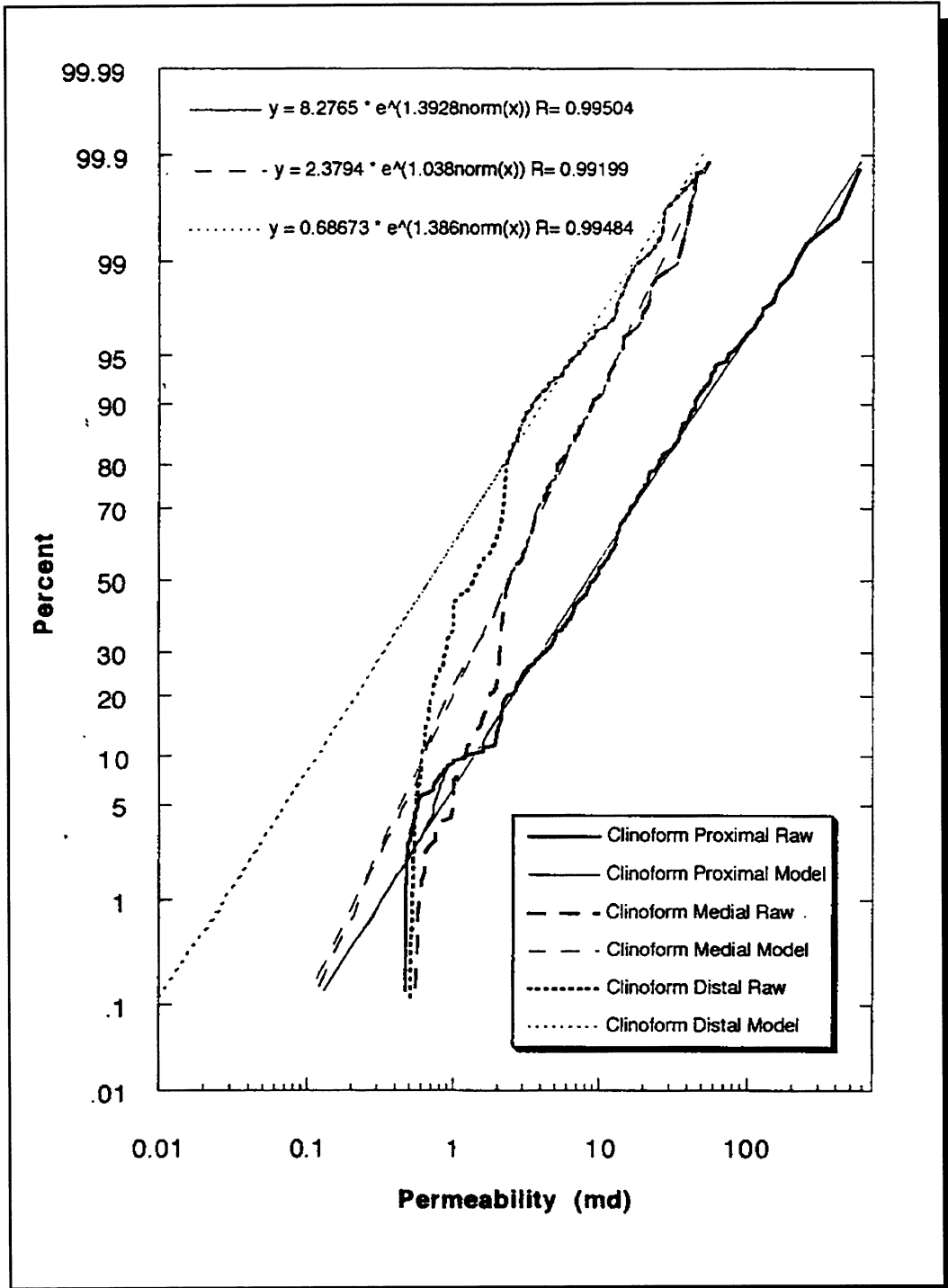


Figure 3.7. Cumulative probability curves of lithofacies vs. permeability model and raw data for the Kf-1-Iv-a parasequence of the detailed scale model.

Variograms of selected parasequence surfaces mapped in Kf-1 and Kf-2 parasequence sets were generated (figure 3.8). The variograms provided spatial relationships as an input to ordinary kriging. Each of the surfaces was kriged and then smoothed (500 foot [152.4 m] operator) in an attempt to remove artifacts. The results were used to construct the elevation and isopach maps (described in section 3.1.4).

From data collected in the Ivie Creek case-study area, a statistical comparison of grain size (figure 3.9A) and permeability (figure 3.9B) vs. facies was conducted. This comparison indicates grain size is not the only control on permeability. Facies and associated sedimentary structures have a major impact on permeability. In general the fluvial-dominated facies of Kf-1-Iv-a have lower permeability values than wave-modified facies of the Kf-2 exhibit similar grain-size distributions. For example, clinof orm proximal facies of Kf-1-Iv-a have a similar grain-size distribution as upper shoreface facies of Kf-2. However, the permeability distribution for the clinof orm proximal facies is much lower and is comparable to the middle shoreface facies of Kf-2. Other factors that probably influence permeability distributions are grain sorting, mineralogical composition, and rock type.

3.1.4 Parasequence Characterization from Cross Sections, and Elevation and Isopach Maps

Scaled photomosaic panels from the Ivie Creek amphitheater and Quitcupah Canyon were annotated with the same information as the regional photomosaics. Five cross sections through the Ivie Creek case-study area were constructed to tie into the regional picture and for use in the three-dimensional reservoir modeling effort. These cross sections display: (1) parasequence and parasequence set boundaries, (2) 15 measured sections which include lithology, sedimentary structures, and ichnofossils, and (3) correlations of parasequences through geophysical logs and conventional core from five project drill holes. An example is shown in figure 3.10.

Depositional trends may be estimated from parasequence surface elevation and isopach maps generated by ordinary kriging. Elevation maps provide insight to paleotopography as referenced to a datum. Isopach maps provide insight into the sediment source and depositional patterns. Analysis of these two data types is used to interpret the delta evolution during the deposition of the Kf-1 and Kf-2 parasequence sets (Mattson, 1997).

In general, surface elevation maps show the fluvial-dominated deltaic lobes of the Kf-1 parasequences dipping to the north-northwest (figure 3.11A). By contrast, surface elevation maps of the wave-modified, prograding shoreline of the Kf-2 parasequences show dip to the east (figure 3.11B).

Isopach maps show parasequence shape which indicates sediment source of the parasequence. These maps show great variability in sediment deposition of Kf-1 parasequences. The Kf-1-Iv-a parasequence is a fan-like deposit which thickens to the east (figure 3.12A). The Kf-2-Iv-a parasequence is wedge-shaped and thins to the east (figure 3.12B). The Kf-2-Iv-b and the Kf-2-Iv-c parasequences are generally tabular, but the Kf-2-Iv-c pinches out to the southwest. The sediment source switches from the east to the west during deposition of Kf-1.

Most of the sediments in Kf-1 cycles accumulated as delta lobes, sourced from a point. The pods of sediment in Kf-1 cycles indicate deposition in a protected environment such as a bay. In contrast, Kf-2 cycles accumulated in sheet-like bodies that pinchout laterally forming a wedge due to wave-action along the delta front.

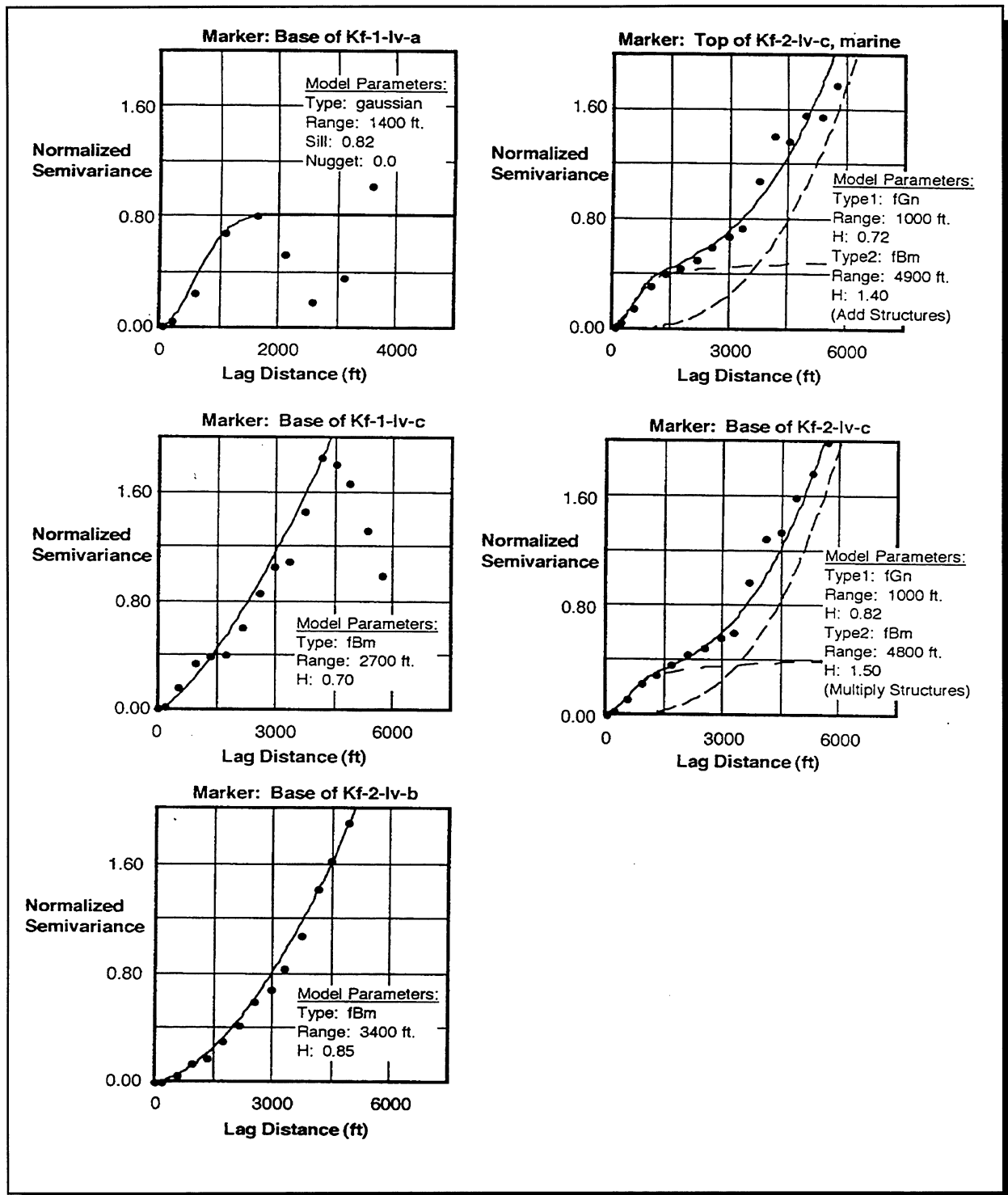


Figure 3.8. Variograms of selected parasequence surfaces mapped in the Kf-1 and Kf-2 parasequence sets, Ivie Creek case-study area. In variograms on right, the overall model is represented by a solid line generated by adding or multiplying the type 1 (fGn or fractile Gaussian model) and type 2 (fBm fractile Brownian model) models represented by the dashed lines.

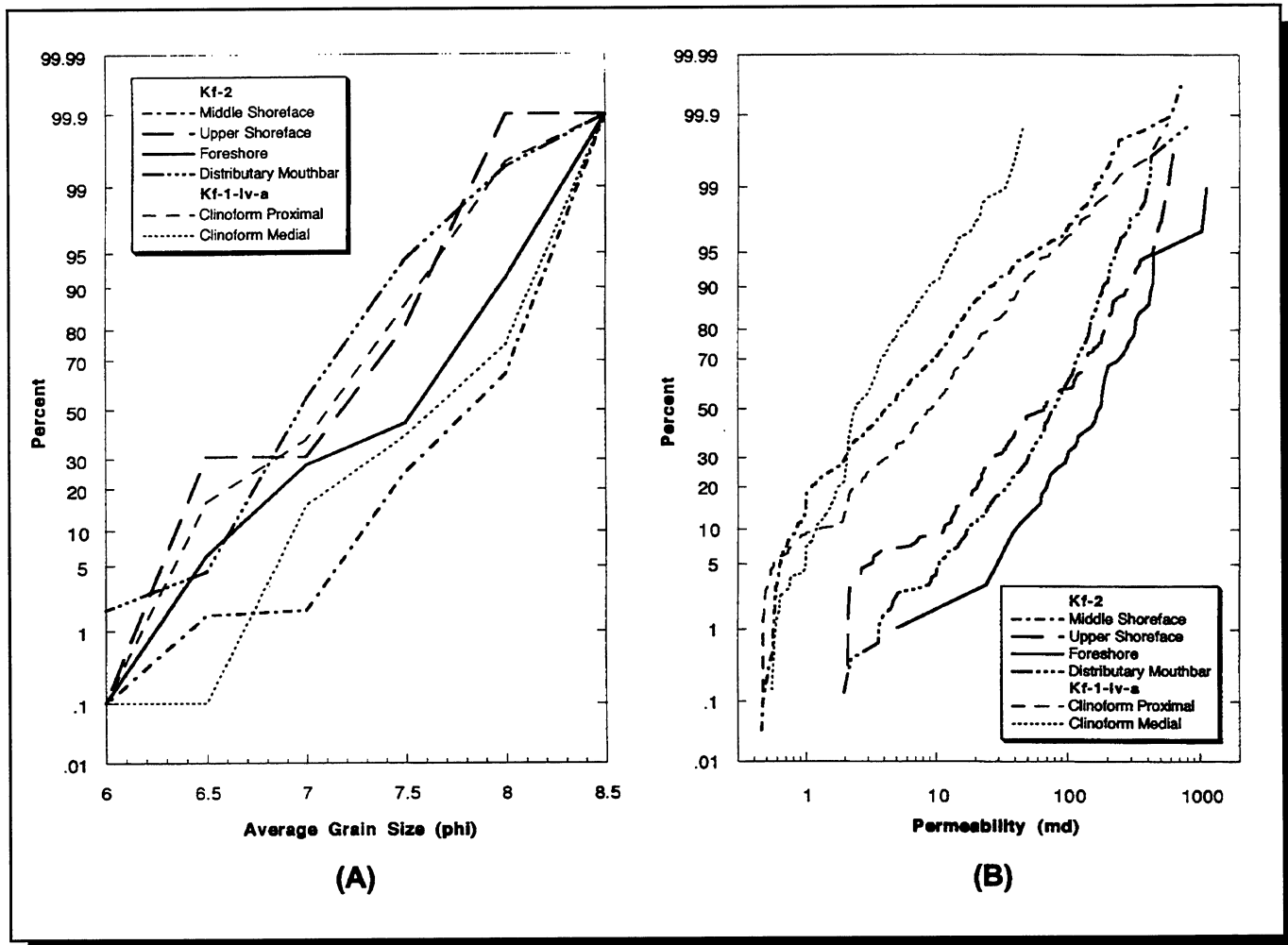


Figure 3.9. Cumulative percent plots of (A) grain size, and (B) permeability vs. potential reservoir facies of the Kf-2 parasequence set and the Kf-1-iv-a parasequence in the Ivie Creek case-study area.

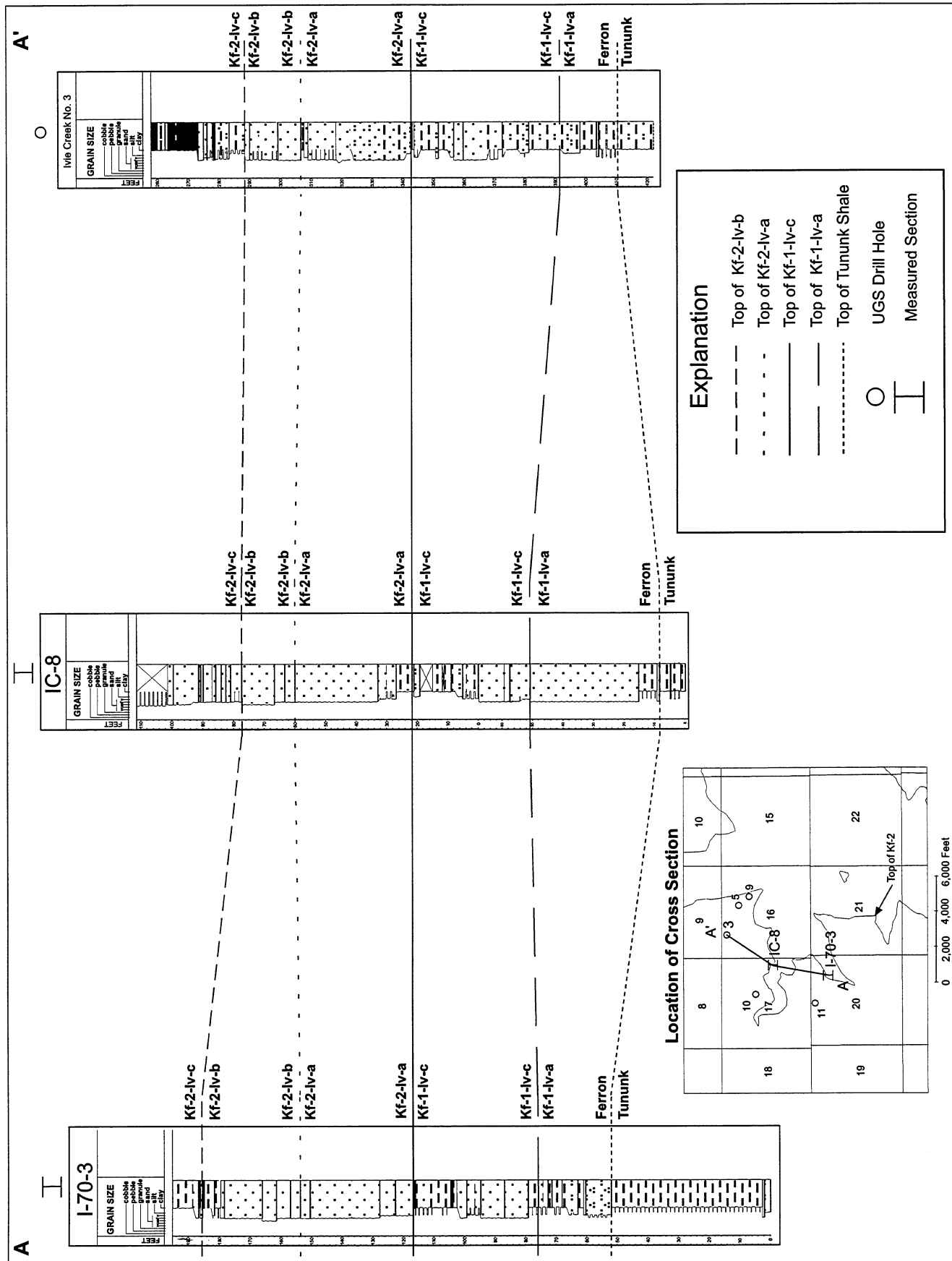


Figure 3.10. North-south stratigraphic cross section through the Ivie Creek case-study area showing correlation of lower Ferron Tununk.

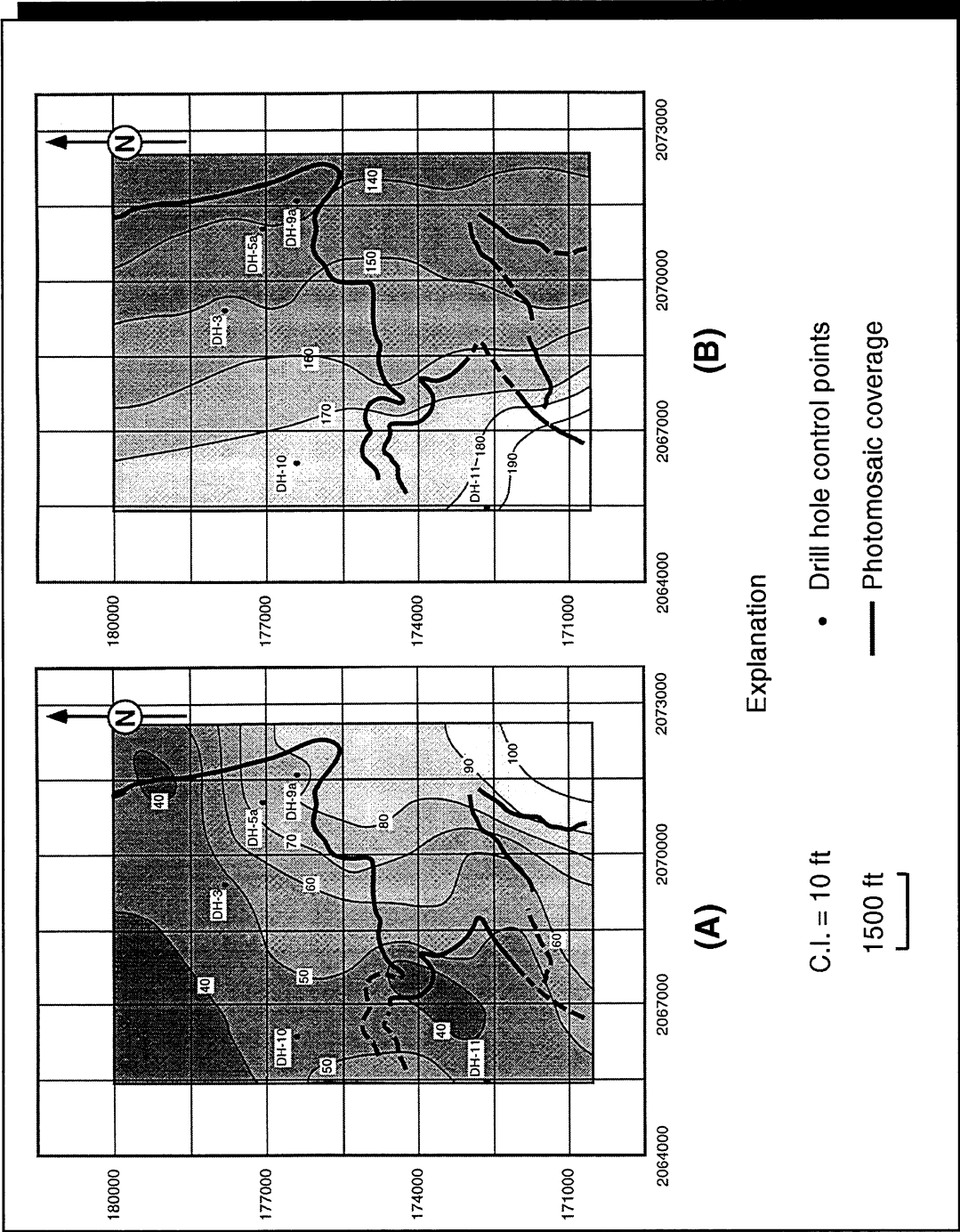
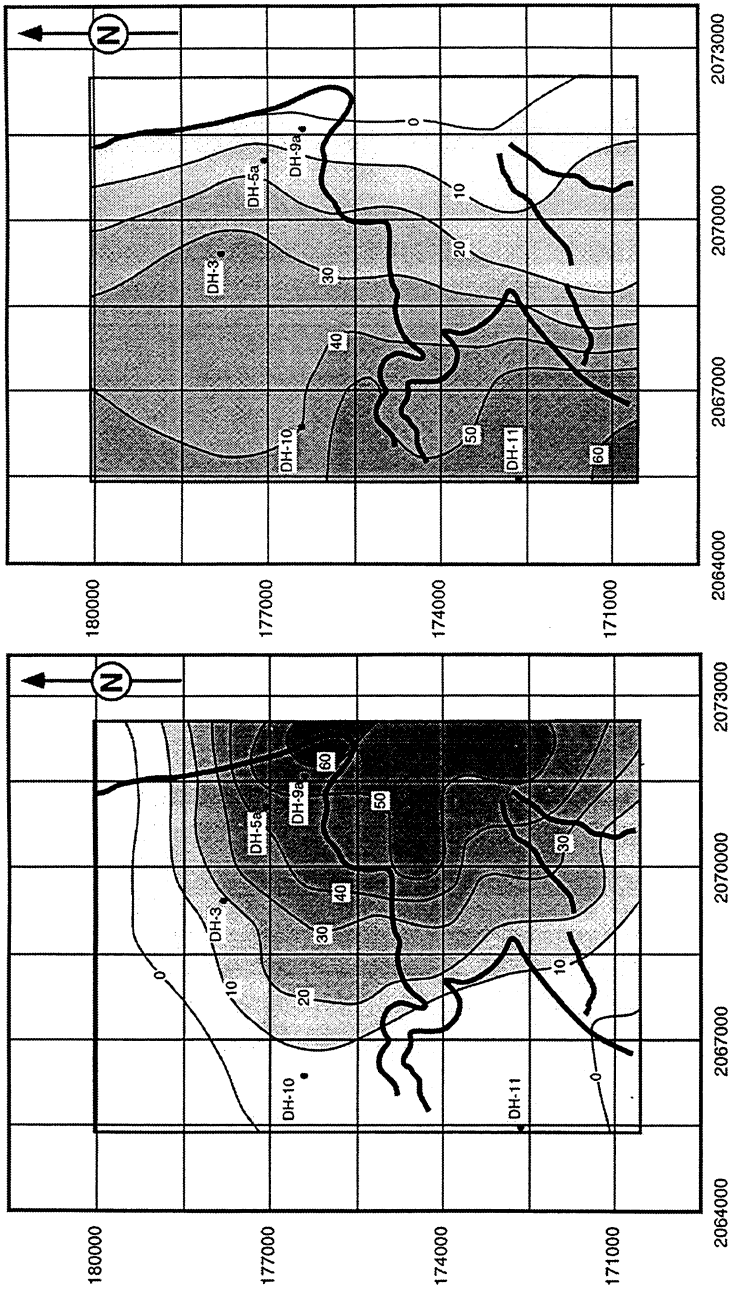


Figure 3.11. Kriged surface elevation maps for the local model using state plane coordinates. (A) Top of the Kf-1-Iv-a parasequence, and (B) base of the Kf-2-Iv-c parasequence. Extent of local model is shown in figure 3.1.



(A)

(B)

Explanation

- C.I. = 10 ft
- Drill hole control points
- 1500 ft
- Photomosaic coverage

Figure 3.12. Isopach maps for the local model using state plane coordinates. (A) Kf-1-Iv-a parasequence, (B) Kf-2-Iv-a parasequence. Extent of local model is shown in figure 3.1.

3.1.5 Development of Three-Dimensional Facies Models

An essential element for reservoir simulation is a three-dimensional facies model in which to distribute geological and petrophysical data. This model can be built in a deterministic or stochastic manner. The Kf-1-Iv-a parasequence three-dimensional facies model is a deterministic model based on clinoform facies and will be used for the reservoir simulation.

The three-dimensional facies model was created in several steps. First, general clinoform lithofacies categories were assigned to units (polygons) on the scaled photomosaic panels based on geometry, sedimentary structures, and apparent shale content. Graphic logs along permeability transects and measured sections were adjusted to fit the scaled line work to form the base for construction of cross sections used, ultimately, to develop the reservoir architecture of the three-dimensional facies model.

For the second step, a 2,000 foot by 2,000 foot by 80 foot (610x610x24 m) block of the Kf-1-Iv-a parasequence, within the Ivie Creek amphitheatre, was selected as the subject of the three-dimensional facies model which was developed as input to a series of reservoir simulations (figure 3.13). The properties of the three-dimensional facies model were derived from eight vertical cross sections which were discretized into 20 layers comprised of 20-foot- (6-m-) long, 4-foot- (1.2-m-) high blocks or cells of clinoform facies (figure 3.14). Facies data from the vertical sections were transferred to horizontal slices throughout the domain and the facies were interpolated between control points. This results in a modeling volume that is coherent from layer to layer, and agrees with the depositional hypothesis of arcuate lobes that were sourced from the east-southeast. The facies distribution in the model is most complex around the 60-foot (18.3-m) elevation layer (figure 3.15). The complexity decreases toward the top (dominantly proximal) and bottom (dominantly distal) portions of the model.

The final step before reservoir simulation was assigning petrophysical parameters to each cell in the model. Each cell represents one clinoform facies type. A permeability distribution is constructed by assigning the geometric mean of the clinoform facies permeability data to each cell in the model. This method is somewhat simplistic, but provides a means to compare fluid flow through a three-dimensional facies model with the two-dimensional facies model developed earlier.

The resulting three-dimensional facies model provides a realistic geologic model that can be used as an input to the reservoir simulation planned for the final quarter of the project. Because the model incorporates data from outcrop photomosaics, stratigraphic sections, and drill holes, it more accurately represents the reservoir than a model based only on drill-hole data. Although the high degree of detail may not be necessary for accurate reservoir predictions, a detailed image of the subsurface such as this provides a comparative case with more generalized models that are typically used in actual oil fields.

3.2 Willow Springs Wash Case-Study Area

Three primary activities were performed as part of the geological characterization of the Ferron Sandstone in the Willow Springs Wash case-study area (figure 1.1) interpretations of : (1) photomosaics, (2) lithofacies, and (3) paleogeography. Work during the project year consisted of processing the data collected from the Indian Canyon portion of the area during the previous field seasons and interpreting detailed photomosaics. Also, outcrop-based paleogeographic maps were constructed for the various time steps of parasequences in the Kf-1 parasequence set.

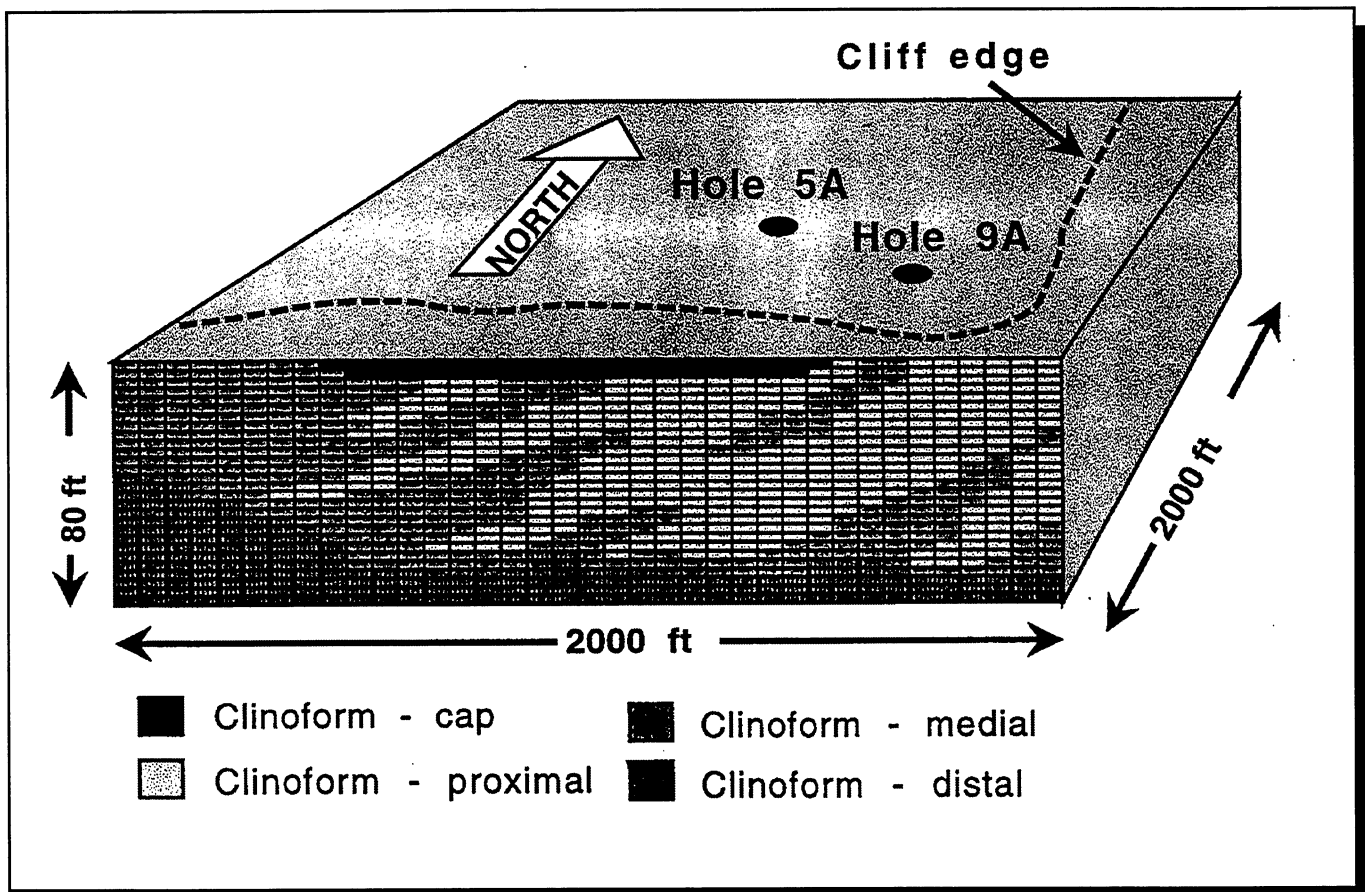


Figure 3.13. Schematic, discretized three-dimensional volume from the selected block of the Kf-1-Iv-a parasequence to be modeled within the Ivie Creek case-study area.

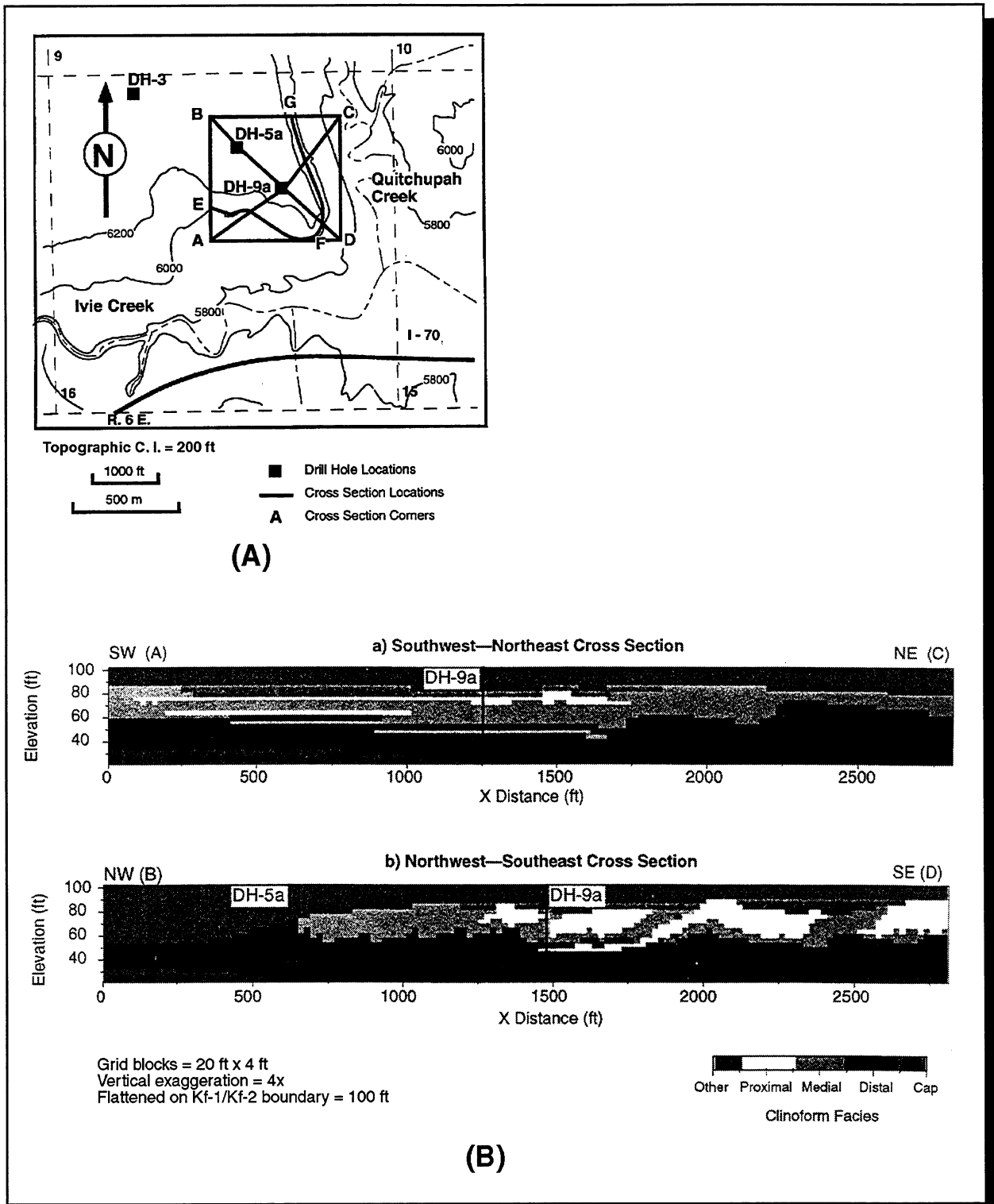


Figure 3.14. (A) Cross section locations for three-dimensional facies model, Kf-1-Iv-a detail model. (B) Southwest to northeast and northwest to southeast cross sections through drill hole No. 9a. Extent of local model is shown in figure 3.1.

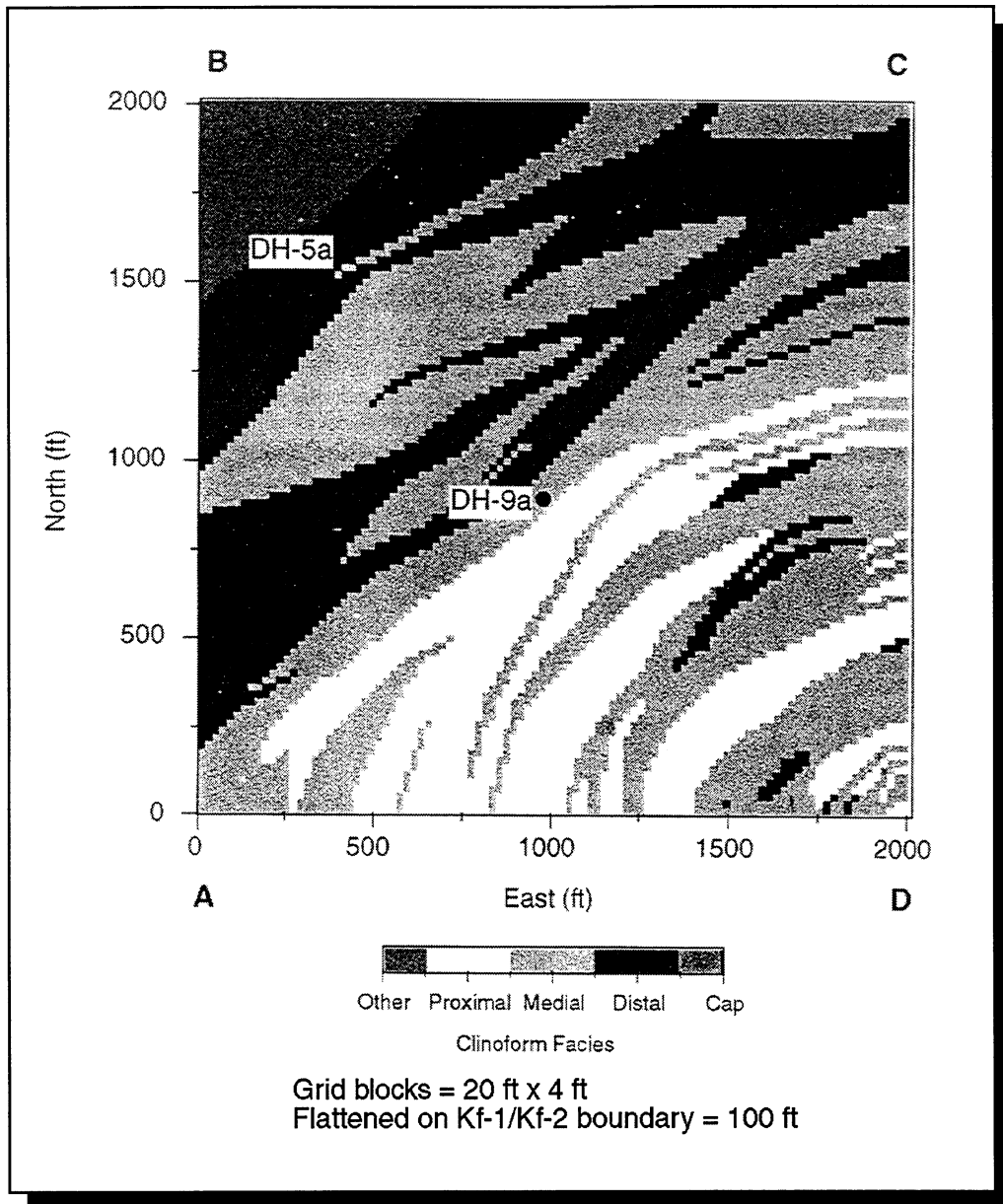


Figure 3.15. Kf-1-Iv-a three-dimensional facies model, 60-foot (18.3-m) elevation layer. Plan view of detailed model area shown in figure 3.14A index map.

Evaluation of the Indian Canyon data indicates eleven distinct depositional facies are recognized in the Kf-1 parasequence set in the Willow Springs Wash case-study area (table 3.1). These facies are: (1) prodelta-inner shelf, (2) lower shoreface, (3) middle shoreface, (4) upper shoreface-ebb tidal delta, (5) foreshore, (6) tidal inlet, (7) interdistributary bay-fill, (8) crevasse-splay, (9) multi-story channel, (10) multi-lateral channel, and (11) beach ridge. They can be grouped into two depositional systems: wave-dominated shoreline and fluvial-dominated delta.

Table 3.1. Depositional facies of the Kf-1 parasequence set in the Willow Springs Wash case-study area, Sevier County, Utah.

Depositional Facies	Characteristics	Wave-Dominated Shoreline	Fluvial-Dominated Delta
Prodelta-inner shelf	Interbedded silt and shale	x	x
Lower shoreface	Hummocky cross-stratified sand and silt	x	
Middle shoreface	Inclined bedded, planar-laminated sand	x	
Upper shoreface-ebb tidal delta	Thick-bedded, trough- and tabular-cross-stratified sand	x	
Foreshore	Thick-bedded, inclined planar-laminated sand	x	
Tidal inlet	Sigmoidal-bedded, cross-stratified sand	x	
Interdistributary bay-fill	Shale and interbedded sand		x
Crevasse splay	<i>En echelon</i> sand and interbedded silty shale		x
Multi-story channel	Multi-story, lensoidal sand		x
Multi-lateral channel	Multi-lateral, lensoidal sand		x
Beach ridge	Planar-laminated, cross-stratified sand and silt		x

Based on lateral and vertical facies associations, the rocks can be divided into four depositional units as Kf-1-Indian Canyon (IC)-a, -b, -c, and -d in ascending order. Marine-flooding surfaces, which are identified on the basis of vertical offset in landward pinch-outs, separate the a, b, and c depositional units. There is no flooding surface separating the c and d units. Because of this, the depositional units are divided into three parasequences. These are the Kf-1-IC-a and Kf-1-IC-b parasequences (which consist of depositional units a and b respectively) and the Kf-1-IC-c parasequence (which consists of depositional units c and d).

During the deposition of parasequences a, b, and the early part of c, the case-study area was characterized by northeastward progradation of a northwest-southeast striking shoreline. Kf-1-IC-a and the early part of Kf-1-IC-c represent longer pulses of progradation while Kf-1-IC-b represents a shorter pulse. During the first time step of deposition of the Kf-1-Indian Canyon-c parasequence, the shoreline trend was northwest-southeast (figure 3.16). A tidal inlet and associated ebb-tidal delta developed in the southwestern part of the case-study area. Measurements of paleocurrents within

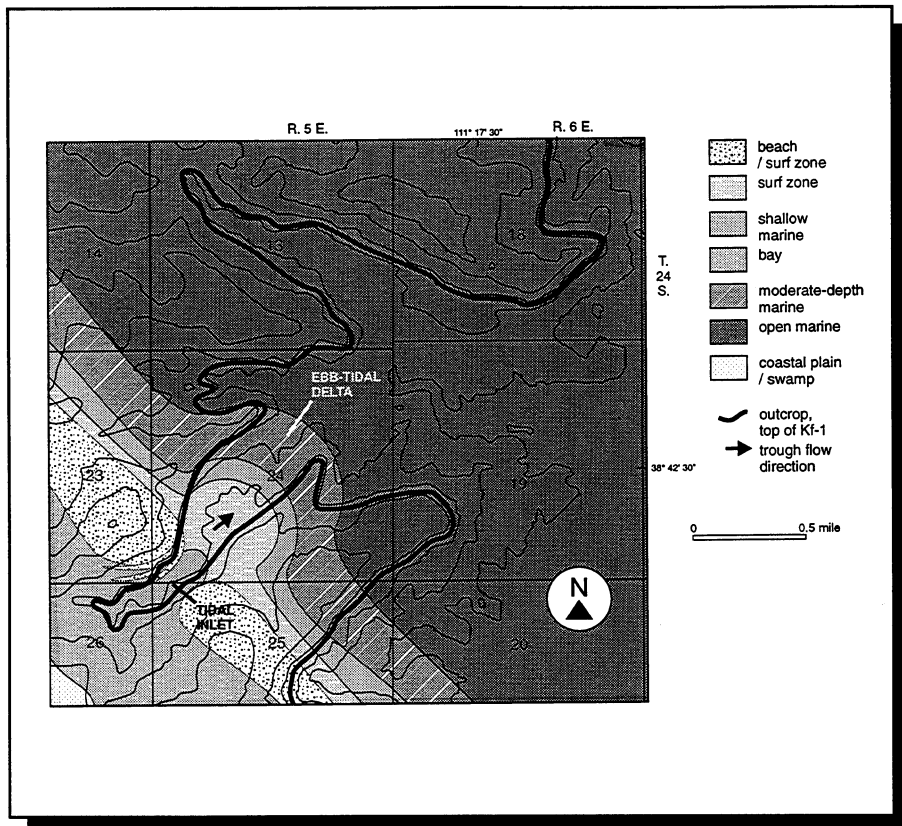


Figure 3.16. Paleogeographic interpretation of the Willow Springs Wash case-study area during deposition of the first step of the Kf-1-Indian Canyon-c parasequence. The ebb-tidal delta is in the SW1/4 section 24, T. 24 S., R. 5 E., of the Salt Lake Base Line.

the upper shoreface/ebb-tidal delta facies show northeast-directed flow. During the later part of Kf-1-IC-c, river avulsion created an autocyclic change in deposition that resulted in an “apparent parasequence” and sedimentation was characterized by deposition within an interdistributary bay.

The facies interpretations of the Willow Springs Wash case-study area suggest that “apparent parasequences” may result from autocyclic processes. These processes are independent of changes in relative sea level and as such, they are not parasequences in the strictest sense. Interpretation of these apparent parasequences

as true parasequences may help to visualize distinct compartments within a reservoir, but may not be beneficial in predicting facies distributions.

3.3 References

- Anderson, P.B., Chidsey, T.C., Jr., and Ryer, T.A., 1997, Fluvial-deltaic sedimentation and stratigraphy of the Ferron Sandstone, *in* Link, P.K., and Kowallis, B.J., editors, *Mesozoic to Recent geology of Utah*: Provo, Brigham Young University Geology Studies, v. 42, pt. 11, p. 135-154.
- Chidsey, T.C., Jr., compiler, 1997, Geological and petrophysical characterization of the Ferron Sandstone for 3-D simulation of a fluvial-deltaic reservoir - annual report for the period October 1, 1995 to September 30, 1996: U.S. Department of Energy, DOE/BC/14896-15, 57 p.

Mattson, Ann, 1997, Characterization, facies relationships, and architectural framework in a fluvial-deltaic sandstone - Cretaceous Ferron Sandstone, central Utah: Salt Lake City, University of Utah, M.S. thesis, 174 p.

4. RESERVOIR MODELING

C.B. Forster and S.H. Snelgrove; University of Utah

During the project year work focused on two- and three-dimensional, fluid-flow modeling. The modeling strategy was finalized following completion of the field-based characterization activities needed to develop input to both geostatistical models and fluid-flow simulators. All modeling work will be focused on the Kf-1-Iv-a parasequence, the fluvial-dominated deltaic unit exposed at the Ivie Creek case-study area (figure 1.1).

Input parameters for both fluid and rock properties have been created for a plausible set of reservoir conditions. Simulations are being run to explore the way that outcrop-based data might be used to improve predictive simulations that are needed to plan reservoir development. The location and size of the two- and three-dimensional simulation domains are shown in figures 4.1 and 4.2. All flow simulations are run using the TETRAD black oil simulator.

The vertical, two-dimensional model domains (figure 4.2A) capture important elements of the transition from proximal to distal fluvial-deltaic lithofacies exposed along Interstate 70 in the Ivie Creek case-study area. In particular, these model domains enable one to explore how clinoform geometry and the inferred properties of the intervening bounding layers might influence the flow of oil and water at the interwell scale. Detailed geological mapping and the results of outcrop-based permeability testing provide a foundation for assigning petrophysical properties within the model domains.

The three-dimensional model domain measures 2,000 feet by 2,000 feet by 80 feet (610x610x24 m) (figure 4.2B). Within this volume, the detailed distribution of lithofacies types of the Kf-1-Iv-a parasequence has been inferred from a three-dimensional grid of 20 feet by 20 feet by 4-feet (6x6x1.2 m) cells using the cross sections shown in figures 4.1 and 4.2A.

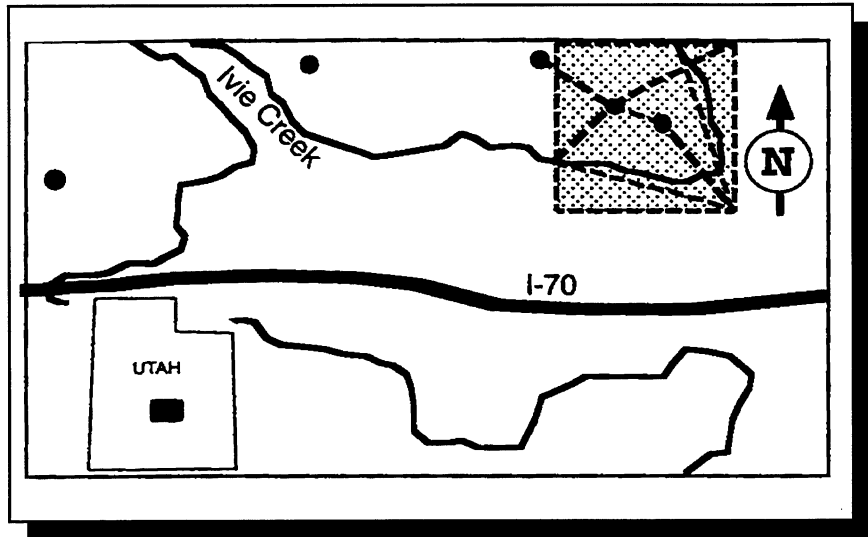


Figure 4.1. Sketch map of Ivie Creek case-study area showing the location of the modeling domains (shaded area) used to simulate fluid flow through clinoform lithofacies of the Kf-1-Iv-a parasequence. Black dots represent project drill-hole locations.

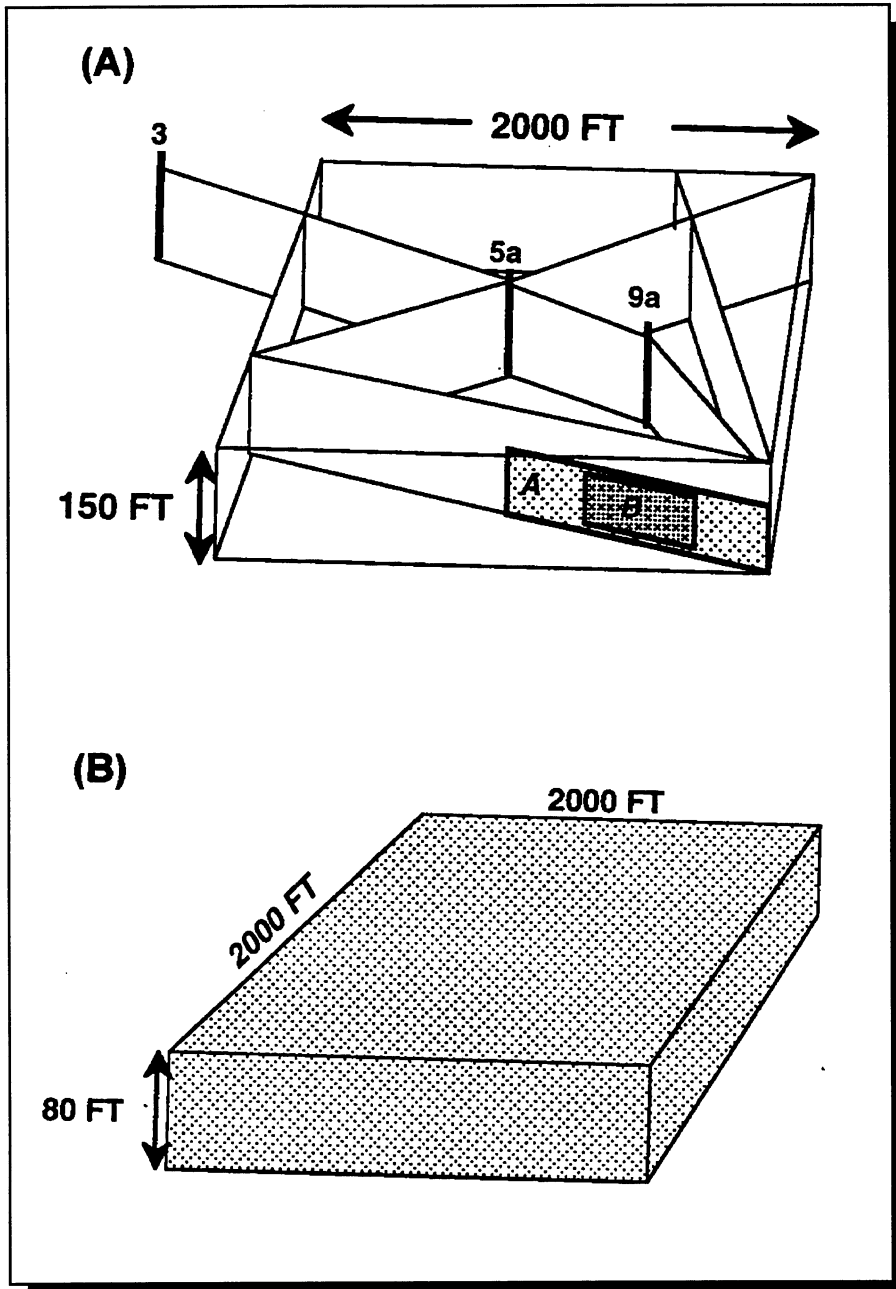


Figure 4.2. (A) Sketch showing geological cross sections constructed within the Kf-1-Iv-a parasequence within the three-dimensional model region. Two-dimensional, vertical modeling domains “A” and “B” are indicated along a geological cross section constructed from detailed photomosaic mapping. Drill holes Nos. 3, 5a, and 9a are tied into the cross section. (B) Sketch of three-dimensional modeling volume (the bottom 80 feet of A) used in simulating fluid flow through the Kf-1-Iv-a parasequence exposed at the Ivie Creek case-study area.

4.1 Assumed Reservoir Conditions

All simulations (both two- and three-dimensional modeling) are performed by imposing the hydraulic stresses associated with secondary recovery on a simulation volume having assumed uniform initial fluid pressures and saturations. This approach avoids the excessive computational burden associated with determining steady-state reservoir pressures and fluid saturations that would have prevailed prior to implementing primary recovery. Similarly, the computational cost associated with calculating oil saturations at the end of primary production is avoided by assuming a uniform oil saturation prior to simulating a waterflood. In addition to reducing the computational burden, these assumptions provide a simplified and uniform basis for comparing the results of waterflood simulations performed for a series of different petrophysical models. If the processes of reservoir filling and primary recovery were simulated for each petrophysical model, a different distribution of oil saturation would be computed as the initial conditions assigned when a simulated waterflood is initiated. The resulting variation in the initial conditions would complicate efforts to establish how each petrophysical structure influences the waterflooding process. Finally, by restricting these simulations only to the waterflood phase, the need to simulate gas production is avoided because fluid pressure reductions are minimal during waterflood which is not the case in the primary production phase. In these simulations the TETRAD simulator is operated in a mode that prohibits gas from coming out of solution. In order to justify this assumption, the minimum production-well, bottom-hole pressure is fixed at 2,685 pounds per square inch absolute (psia) (18,513 kpa) in the model. Because this pressure is the bubble point of black oil, it becomes impossible for pressure to drop below the bubble point anywhere in the reservoir at any time during a simulation (McCain, 1990).

The reservoir is assumed to be initially saturated with both oil and water but no gas. Oil and water densities are assigned values of 45.0 and 62.14 pounds/foot³ (729.6-1,007.6 kg/m³), respectively. A nominal reservoir pressure of 5,000 pounds per square inch (psi) (34,475 kpa) is assumed. This pressure corresponds to an approximate reservoir depth of 13,000 feet (3,962.2 m). A reservoir temperature of 166°F (60°C) is assumed.

4.2 Fluid and Rock Properties

4.2.1 Relative Fluid-Permeability Curves

Predicted reservoir performance can depend strongly on the shapes of oil and water relative-permeability curves, particularly when spatial and temporal variations in saturation are pronounced. Thus, defining relative permeability relationships typical of fluvial-deltaic reservoir rocks is crucial for obtaining reliable performance predictions at various scales of permeability averaging. The water-wet Berea Sandstone is used as the prototype relative-permeability model for assessing production performance in the Ferron Sandstone because its hydraulic properties are widely documented in the literature and it is believed to represent a typical example of a consolidated sandstone.

Prototype relative-permeability data for the Berea Sandstone are available from a series of laboratory tests using brine and air as the wetting and non-wetting fluid phases, respectively (Miller and others, 1993). Because these data were obtained for brine and air, they are not strictly

applicable to the water-oil system of interest during the reservoir simulations. Thus, the Berea data was used to transform brine-air relative-permeability data obtained for samples of Ferron Sandstone into usable quantities through a two-step approach. The first step involves relating Berea brine-air relative permeabilities to Ferron brine-air relative permeabilities through the parameter λ used to fit the Brooks-Corey relations:

$$\text{Eq. 4.1} \quad k_{rw} = S_e^{(2+3\lambda)/\lambda}$$

$$\text{Eq. 4.2} \quad k_{ro} = (1 - S_e)^2 * (1 - S_e)^{(2+\lambda)/\lambda}$$

where: $S_e = (S_w - S_{wc}) / (1 - S_{wc})$ is effective saturation, S_w and S_{wc} are actual and residual (connate) water saturations, and K_{rw} and K_{ro} are relative water and oil permeabilities.

After a value of λ was fit to the Berea brine-air relative permeability data and another value fit to the Ferron brine-air relative permeability data, the ratio of the two parameters was estimated in order to determine the fractional change in λ required to adjust the Berea curves for Ferron conditions. These fractional changes were obtained for 'average' Ferron brine-air data, as well as for proximal, medial, and distal subsets of the Ferron brine-air data, as determined from reported absolute brine permeabilities (Miller and others, 1993). Since λ is a measure of the degree of linear behavior in the Brooks-Corey relations and the Berea Sandstone is relatively well-sorted compared to the Ferron Sandstone, all λ -adjustment ratios were less than 1.0. The resulting ratios were then used to adjust λ estimated from fitting another Brooks-Corey curve to the Berea oil-water relative permeability data obtained from three-phase relative permeability plots with a gas saturation of 0 percent (Honarpour and others, 1986). Finally, the adjusted values of λ were used to generate Ferron Sandstone relative permeability curves for the average, proximal, medial, and distal clinofacies cases.

4.2.2 Capillary Pressure

Estimated values of capillary pressure in Ferron rocks, or the difference in pressure across the oil-water interface, were obtained from the standard water-wet Fatt and Dykstra relation provided in tabular form by Honarpour and others (1986). In a water-wet reservoir, a decrease in water saturation causes a decrease in curvature radius for water and a corresponding increase in capillary pressure. Table 4.1 shows the values of capillary pressure as a function of water saturation used in the Ferron Sandstone simulation studies.

Table 4.1. Capillary pressure (P_c) as a function of water saturation (S_w).

S_w	0.0	0.1	0.2	0.3	0.4	0.5	0.6	0.7	0.8	0.9	1.0
P_c (psi)	2.52	2.52	2.52	1.68	1.45	1.30	1.16	1.06	0.97	0.87	0.77

4.2.3 Pressure-Volume Data

Pressure-volume (PV) data relate oil production volumes at the ground surface to oil reservoir volumes at various reservoir pressures. The PV data used in this study (table 4.2) are the same as those used by Odeh (1981) in conducting a series of black oil simulations. Table 4.2 summarizes formation volume factors, solution-gas ratios, and fluid viscosities as a function of total reservoir pressure. Note that, because reservoir pressure is never allowed to drop below the bubble point during the simulations, much of the table was never needed during the TETRAD runs.

Table 4.2. Pressure-volume data.

Pressure (psia)	BW (stb/rb)	EG	BO (stb/rb)	RS	CR	μ_w (cP)	μ_g (cP)	μ_o (cP)
14.7	1.0410	1.069	1.062	1.0	0	0.31	1.0	1.040
264.7	1.0403	14.728	1.150	90.5	0	0.31	1.0	0.975
514.7	1.0395	28.388	1.207	180.0	0	0.31	1.0	0.910
1014.7	1.0380	55.711	1.295	371.0	0	0.31	1.0	0.830
2014.7	1.0350	110.352	1.435	636.0	0	0.31	1.0	0.695
2514.7	1.0335	137.641	1.500	775.0	0	0.31	1.0	0.641
3014.7	1.0320	164.914	1.565	930.0	0	0.31	1.0	0.594
4014.7	1.0290	219.615	1.695	1270.0	0	0.31	1.0	0.510
5014.7	1.0258	274.434	1.827	1618.0	0	0.31	1.0	0.449
9014.7	1.0130	461.419	2.357	2984.0	0	0.31	1.0	0.203

BW = water formation factor (standard stock tank barrels/reservoir barrels [stb/rb])
 EG = gas expansion factor
 BO = oil formation factor (stb/rb)
 RS = gas-solution ratio
 CR = condensate ratio
 μ_w = water viscosity (centipoise [cP])
 μ_g = gas viscosity (cP)
 μ_o = oil viscosity (cP)

4.3 Two-Dimensional Simulations

To October 1997, all two-dimensional simulations have been performed within a relatively small (330 feet [100.6 m] horizontal by 48 feet [14.6 m] vertical), prototypical model domain (figure 4.3) to gain confidence in the performance and use of TETRAD. Once the preliminary simulations are complete, simulations will be run in larger domains.

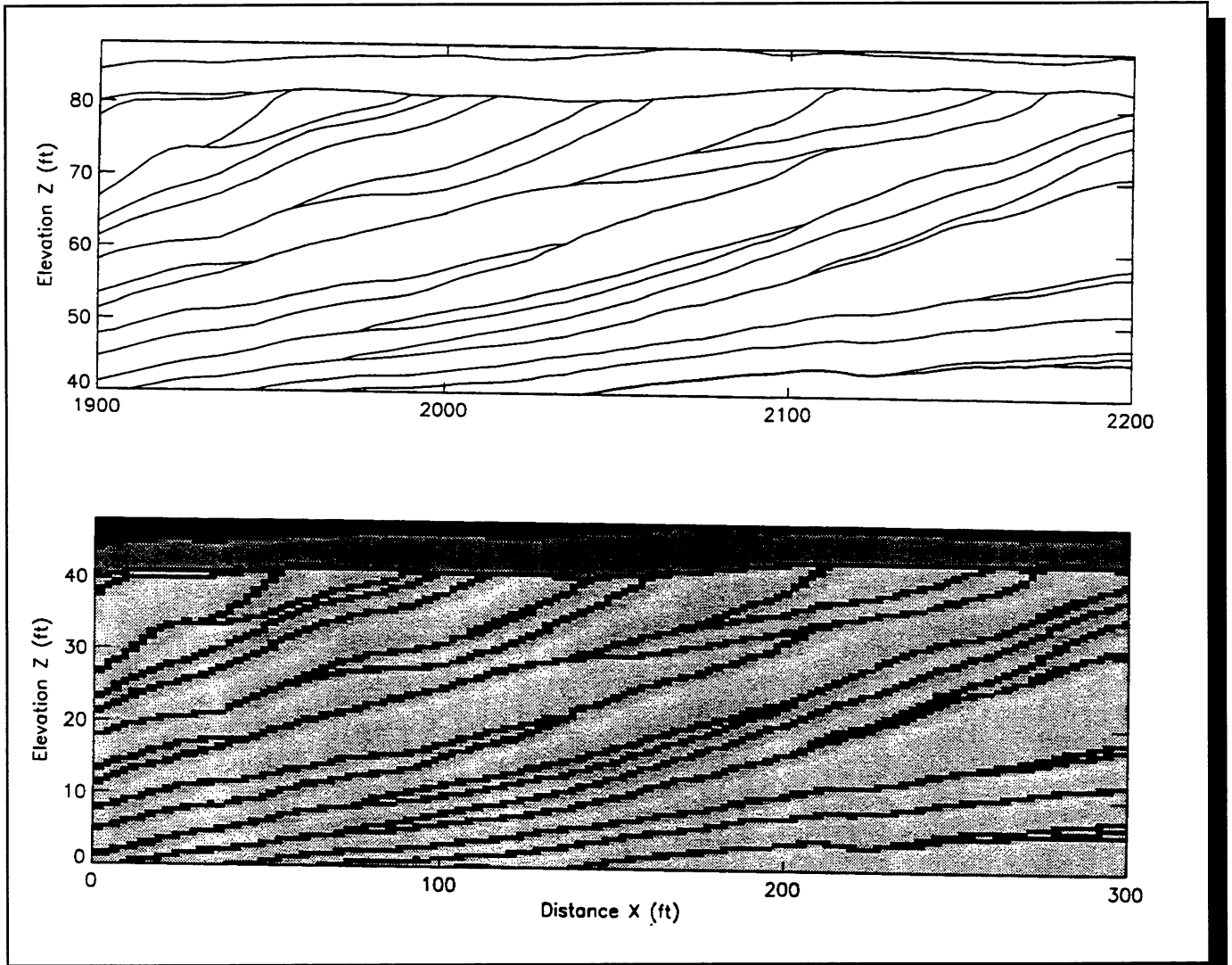


Figure 4.3. Prototypical two-dimensional modeling domain showing the scaled line drawing used to capture the geometry of the clinoform lithofacies and the corresponding, digitally gridded representation of the original line drawing.

The results of the TETRAD simulation are shown in figure 4.4. Water is injected from a well located on the left boundary. A short (single grid block) perforated interval is centered in the reservoir. Oil is produced from a short (single grid block), centered interval perforated in a well located on the right boundary. Figure 4.4 shows the distribution of oil saturation computed at several time steps using TETRAD.

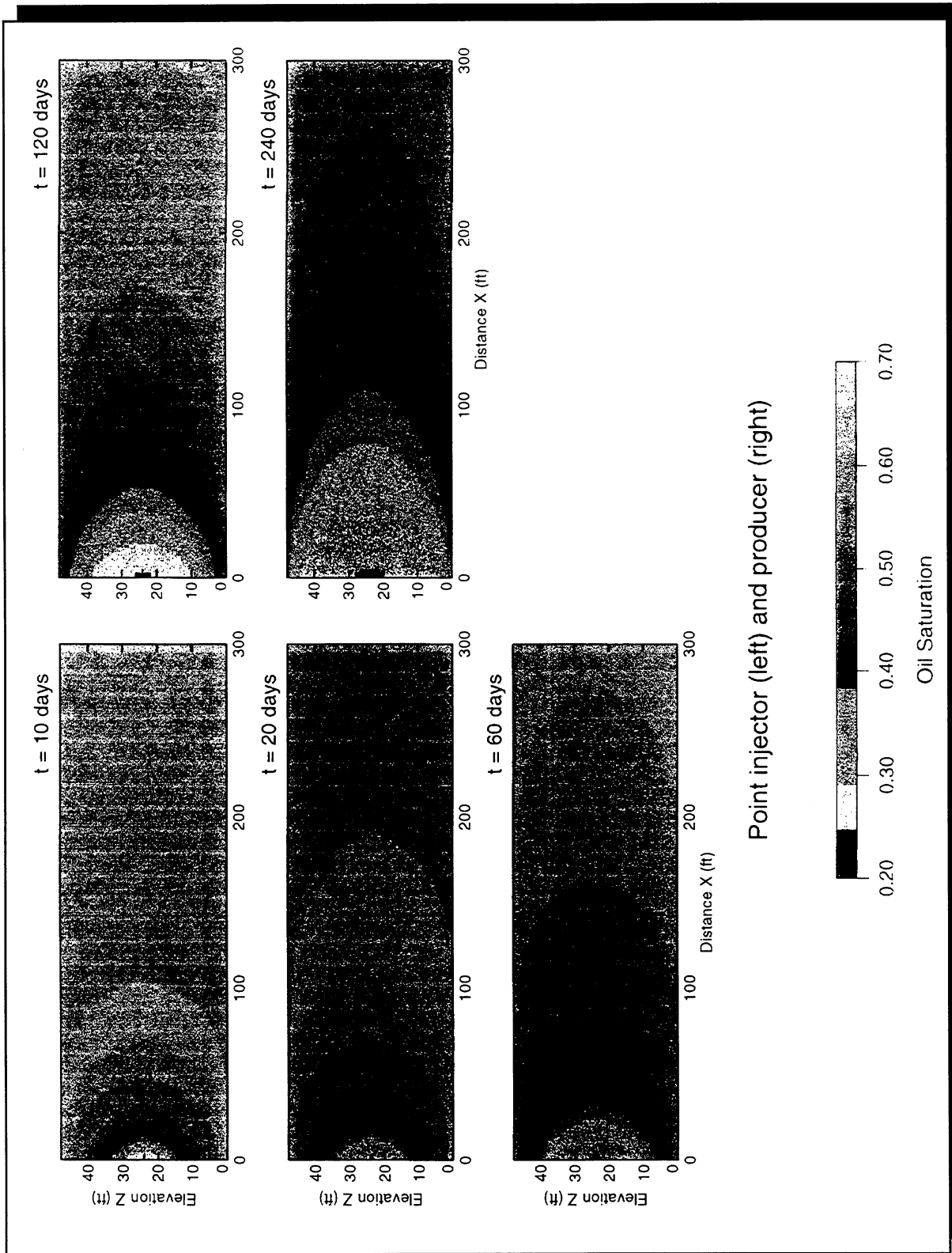


Figure 4.4. Distributions of oil saturation as a function of time, computed using TETRAD, within a domain with homogeneous permeability (20 md) and porosity (50 percent). Water is injected over a short interval centrally located along the left boundary and oil is produced over a similarly located interval on the right boundary.

The prototypical model domain shown in figure 4.3 represents a portion of the Ivie Creek case-study area evaluated in detail. The algorithms needed to translate the scaled line drawings of clinoform boundaries (represented in the upper half of figure 4.3) into a corresponding, gridded distribution of petrophysical parameters (shown in the lower half of figure 4.3) were developed using the data from this test domain. The algorithms provide an automated procedure for the following tasks:

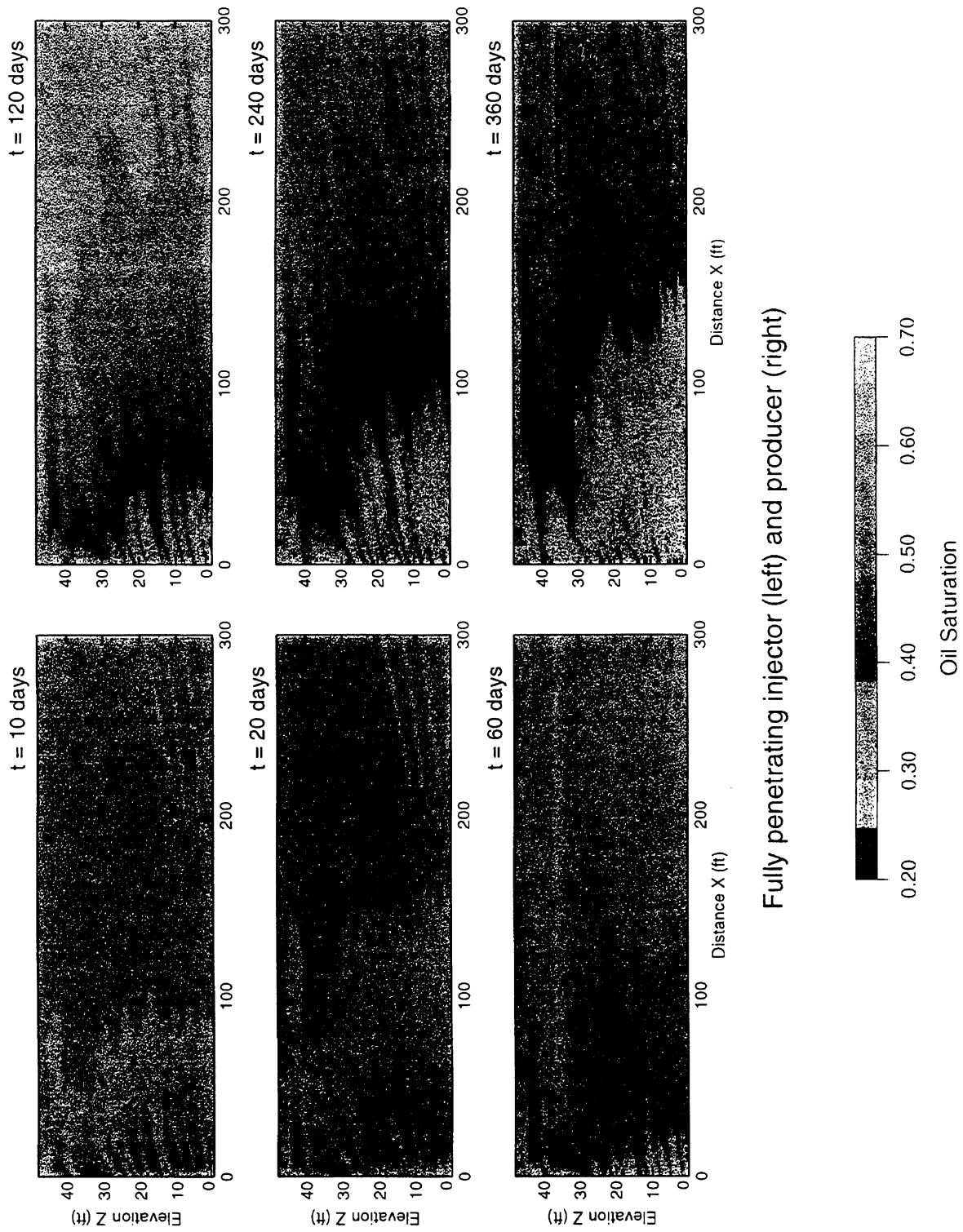
- converting the line drawings to individual polygonal elements (for example individual clinoform shapes),
- gridding the interiors of individual clinoforms,
- distinguishing between grid blocks representing clinoform boundaries and clinoform interiors,
- individually populating each clinoform with porosity values, relative permeability curves, and capillary pressure curves, and
- merging the gridded petrophysical distributions created for each clinoform into a single, heterogeneous model domain.

The lower half of figure 4.3 shows the results of this procedure. In this case, the parameter population is very simple; the gray clinoforms have a constant permeability of 20 md and the intervening, black boundary layers are assigned a constant permeability of 0.1 md. A porosity of 50 percent is assigned throughout the domain. Note that the black region at the top of the model domain is a null region that does not actively participate in the simulation. Improved algorithms that allow variable properties were assigned within each clinoform.

A second TETRAD waterflood simulation was run on the model domain shown in figure 4.3. This simulation by injected water along the left boundary of the domain and producing oil along the right boundary as in the first simulation test but the injector and producer are perforated across the entire thickness of the reservoir. A uniform, initial oil saturation of 70 percent is assumed with an inferred reservoir pressure of 5,000 psia (34,475 kpa). The results of the TETRAD simulation are shown in figure 4.5. The impact of the clinoform architecture on the progress of the waterflood is evident. For example, the permeability contrast between the clinoform interiors (20 md) and the boundary layers (0.1 md) focuses flow within individual, dipping clinoforms. Once flow is established within a clinoform the water moves up dip to the producing well. The presence of the dipping, lower permeability bounding layers cause cumulative oil production computed from this simulation to be 20 percent less than that computed for the corresponding homogenous domain subjected to the same injection/production conditions.

4.4 Three-Dimensional Simulations

The primary goals of the three-dimensional reservoir simulation studies are to: (1) assess the dependence of predicted reservoir performance on the scale at which the three-dimensional spatial distribution of permeability is averaged, and (2) explore and illustrate the impact of upscaled, clinoform-related permeability structures on secondary oil production. Three, three-dimensional styles of permeability structure are being simulated: homogeneous, layered heterogeneous, and detailed styles. If the measures of reservoir performance computed for each style are similar, one



Fully penetrating injector (left) and producer (right)

Figure 4.5. Distributions of oil saturation as a function of time, computed using TETRAD, within the prototypical, heterogeneous model domain shown in figure 4.3. Water is injected over the entire reservoir thickness on the left boundary and oil is produced over a similar interval on the right boundary.

would conclude that there is little added value to collecting the outcrop information that was used to construct the detailed petrophysical model. If, on the other hand, the computed measures of reservoir performance differ dramatically from style to style, outcrop-based reservoir analog studies may be valuable.

The three styles of permeability structures (homogeneous, layered heterogeneous, and detailed) are derived from the three-dimensional lithofacies distribution within the Kf-1-Iv-a, constructed during the course of the Ferron outcrop analog study. Both the homogeneous and layered heterogeneous permeability structures represent the results of relatively simple permeability averaging techniques commonly used by petroleum engineers. Absolute permeabilities are assigned to each facies as the geometric mean of values estimated from the field studies. In each case isotropic permeability tensors are assumed. Porosity values are computed from an empirical relationship between permeability and porosity that was derived from the laboratory tests performed on core plugs collected from outcrop.

The layered heterogeneous permeability structure is obtained by interpolating lithofacies sampled from four hypothetical wells “drilled” vertically at the corners of the gridded three-dimensional representation of the detailed lithofacies distribution (figure 4.6). These wells might be viewed as the four producers that would be installed in a reservoir prior to adding a central injection well to complete a five-spot production pattern. Unlike the detailed or homogeneous styles, the layered heterogeneous style contains an inherent layering imposed in the process of interpolating lithofacies between wells. Figure 4.7 shows the simple lithofacies structure inferred for the layered heterogeneous style along two diagonal cross sections cutting through the three-dimensional simulation volume shown in figure 4.2.

In the homogeneous permeability structure case, a single representative value of permeability is assigned to the entire simulation volume to yield an end-member case with maximum averaging of permeabilities associated with the detailed lithofacies distribution. This computed effective permeability for the model volume was not obtained by applying formal homogenization techniques. Instead, it was estimated as the geometric mean of the detailed permeability structure contained within the entire three-dimensional facies model.

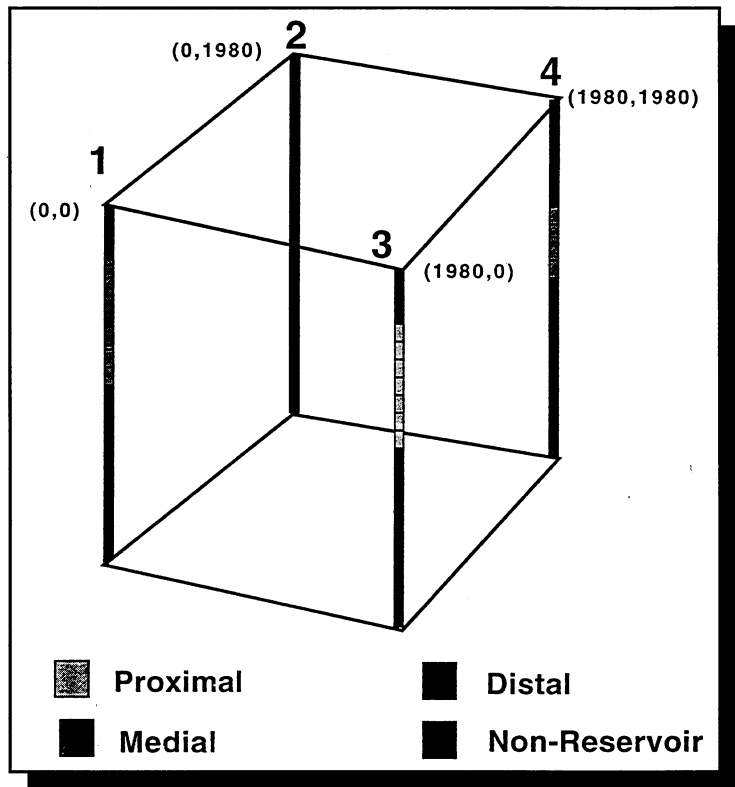


Figure 4.6. Clinoform lithofacies distributions obtained by “drilling” and sampling four vertical “wells” in the detailed three-dimensional lithofacies model.

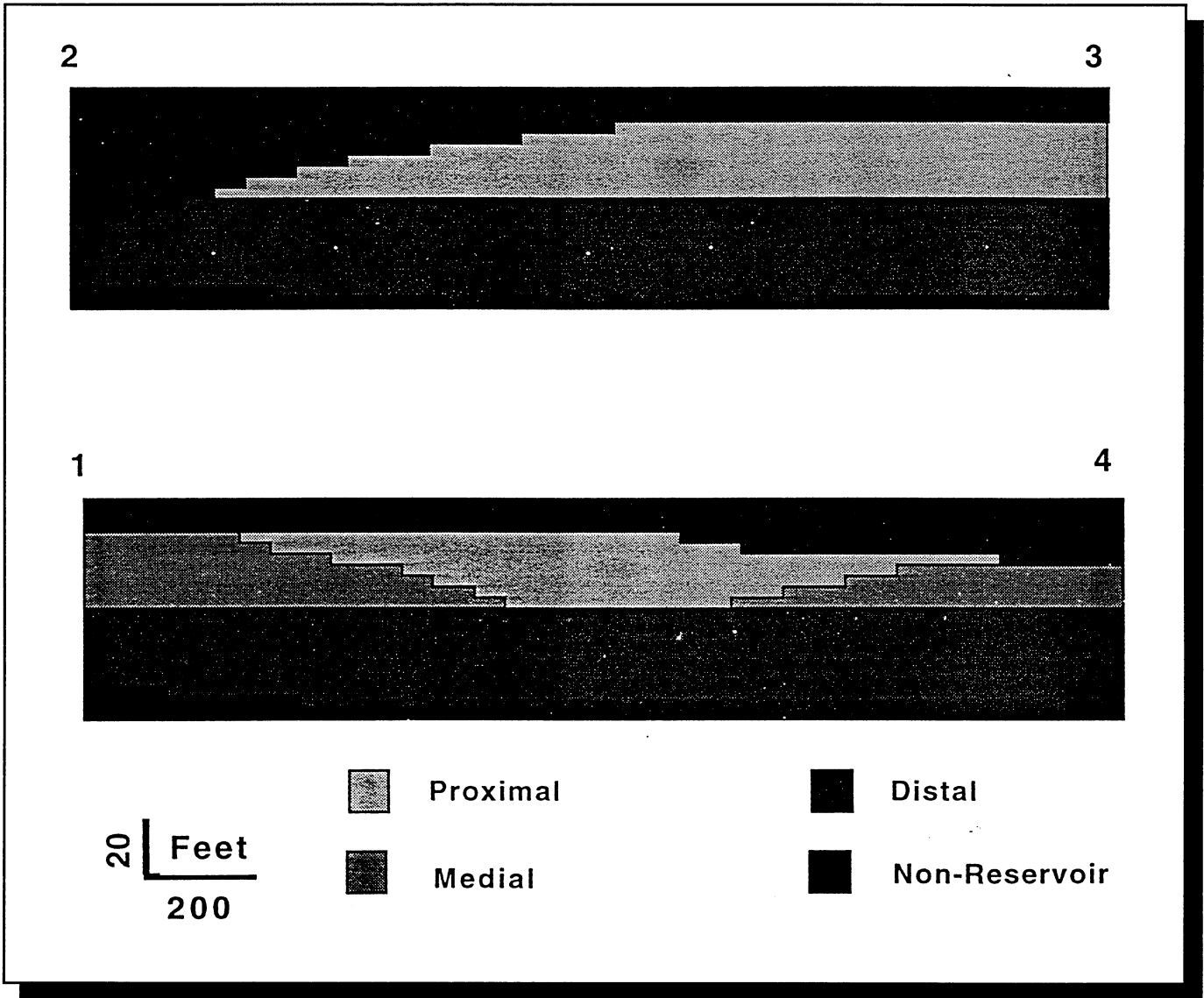


Figure 4.7. Inferred structure of lithofacies for the layer heterogeneous permeability style along cross sections cut diagonally through the four-well pattern shown in figure 4.6.

A single five-spot waterflood production strategy is used to impose the secondary recovery process within the homogeneous three-dimensional model domain. This five-spot pattern encompasses the entire three-dimensional volume which is 2,000 feet by 2,000 feet (610x610 m) in the horizontal plane with a vertical thickness of 80 feet (24 m) (figure 4.8). The symmetry of the five-spot well pattern, coupled with the intrinsic symmetry associated with the homogeneous reservoir properties, makes it possible to invoke $\frac{1}{4}$ -volume, horizontal symmetry considerations which reduces the computational burden. An initial uniform reservoir pressure of 5,000 psia (34,475 kpa) and initial uniform water and oil saturations of 50 percent were assigned throughout the $\frac{1}{4}$ -volume reservoir prior to each simulation. In each simulation, water is injected through the central well (corner well in the $\frac{1}{4}$ -volume domain) at a rate of 0.0001 pore volumes/day (PV/day),

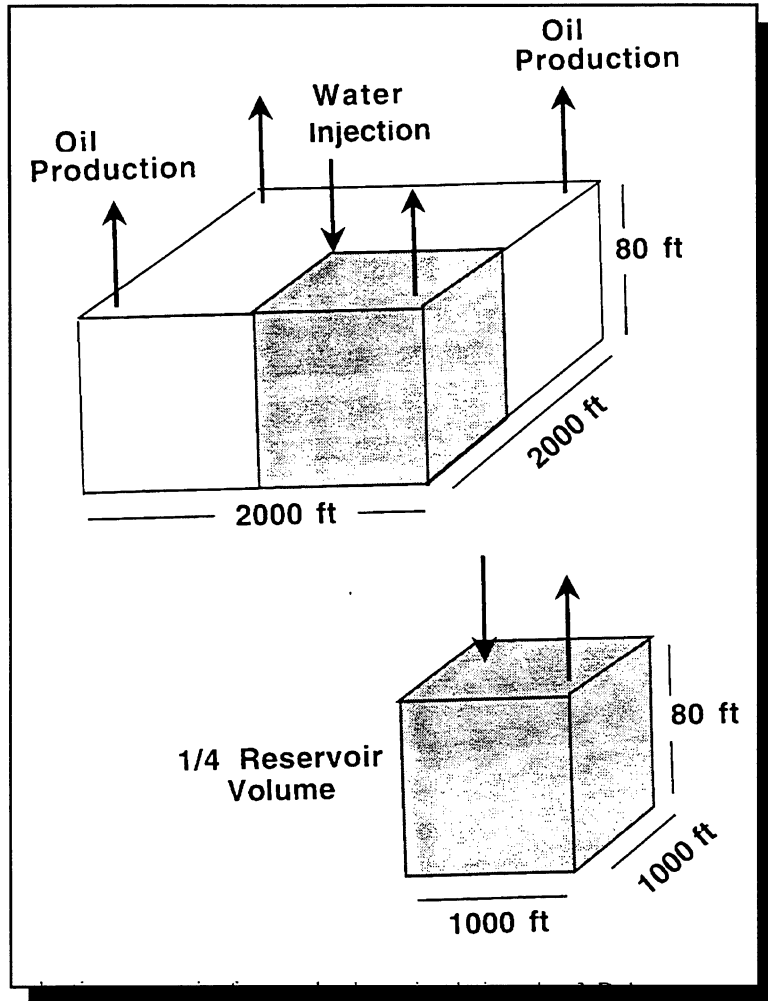


Figure 4.8. Production scenario used when simulating the three-dimensional homogeneous style.

constrained by a maximum bottom-hole injection pressure constraint of 6,000 psia (41,370 kpa). Production at the single corner well in the 1/4-volume is driven by water injected at the opposite corner well. Review of permeability-porosity data collected in the course of the project suggests the following relationship:

$$\text{Eq. 4.3} \quad \log k_{\text{abs}} = (22.72 * \Phi) - 2.64$$

where Φ = porosity expressed as a fraction and k_{abs} = absolute permeability (md). This relationship is used to compute porosity values where corresponding to values of k_{abs} are estimated.

Given that a large number of model runs are anticipated during future sensitivity analyses, it is necessary to determine the minimum number of nodes required to discretize the pressure equations accurately over space. This is especially true for three-dimensional simulations, which can be extremely computationally intensive. In general, the degree of spatial resolution required will

depend on spatial properties of both the physical system being modeled and the flow geometry imposed on the physical system. Steep pressure gradients and extreme variations in permeability, for example, will usually require fine grid resolution. Low gradients and small, gradual changes in permeability over space can be accurately preserved using coarser resolution.

To generate the steepest horizontal gradients common to all three permeability distributions, the geometric mean associated with the lowest permeability, clinoform distal lithofacies (1.48 md) was assigned to the homogeneous model domain. A fairly large water injection rate of 0.0001 PV/day was imposed at the central water-injection well. This combination of low k_{abs} and high injection rate provides worst-case conditions from the perspective of defining a minimum acceptable grid resolution. Specifying initially uniform water and oil saturations, which tend to establish a piston-like pattern of fluid displacement, also contribute to this worst-case scenario.

A number of homogeneous permeability simulations were made using different uniform grid-spacing geometries. In the later stages of each simulation, however, mass balance errors were found to increase beyond acceptable limits. As a consequence, a variable horizontal grid spacing (figure 4.9) was used to alleviate the numerical problems associated with preserving steep horizontal gradients while leaving the computational burden unchanged. A 2-foot (0.6 m) grid spacing is assigned near the injection and production wells. The horizontal grid spacing gradually increases to 202 feet (61.6 m) at the midpoint between the injection and production wells. This discretization scheme produces a grid with 20 feet by 20 feet by 10 feet (6.1x6.1x3.1 m) grid blocks (4,000 finite difference nodes) within the $\frac{1}{4}$ -volume. Small mass balance errors are computed throughout the model domain using this variable grid. This result suggests that the 4,000-node, variable-spacing discretization may be capable of accurately preserving the steepest horizontal pressure gradients that are likely to evolve while simulating each of the three different styles of permeability structure. Note that, when simulating the two heterogeneous styles, one can no longer invoke the $\frac{1}{4}$ -symmetry. As a consequence, when modeling these styles it will be necessary to use at least 16,000 nodes.

Using the optimal grid design based on worst-case conditions (minimum-permeability, maximum pressure-gradient, and piston-like displacement), a set of sample results are computed for the homogeneous, $\frac{1}{4}$ -volume model domain. In this case a homogeneous geometric mean permeability of 3.13 md is assigned to represent the mean permeability of the full three-

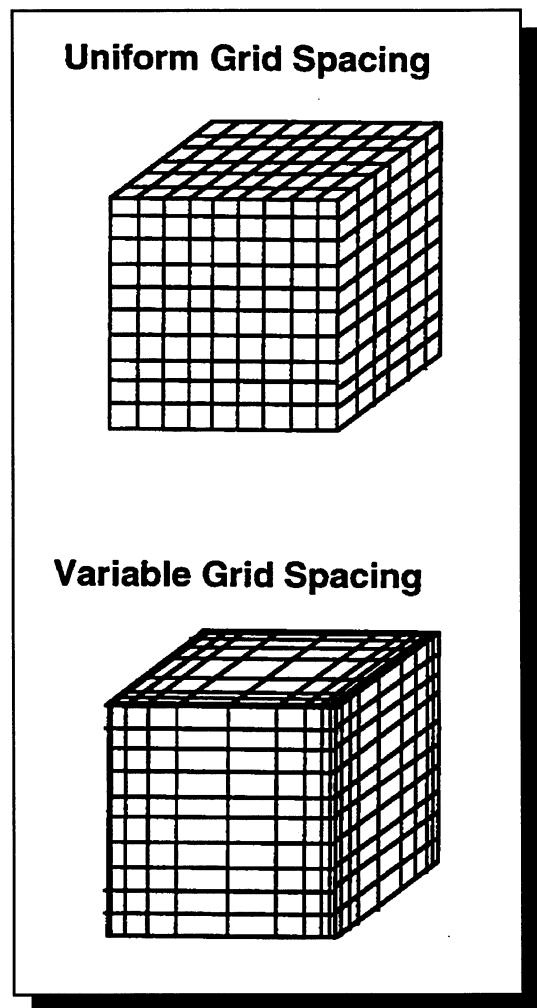


Figure 4.9. Grid spacings used in the $\frac{1}{4}$ -volume three-dimensional model domain shown in figure 4.8.

dimensional volume. A corresponding porosity of 13.8 percent is estimated using the linear correlation relation given by equation 4.3. Computed three-dimensional distributions of oil saturation are shown in figure 4.10 for a series of points in time ranging from 6 months to 20 years. In each three-dimensional saturation plot, the water-injection well is located at the left corner of the model domain, and the oil production well is located in the right corner. White areas correspond to high oil saturations. Thus, one can see the progress of the waterflood through the domain as the dark area, corresponding to high water saturation, expands to fill the model domain.

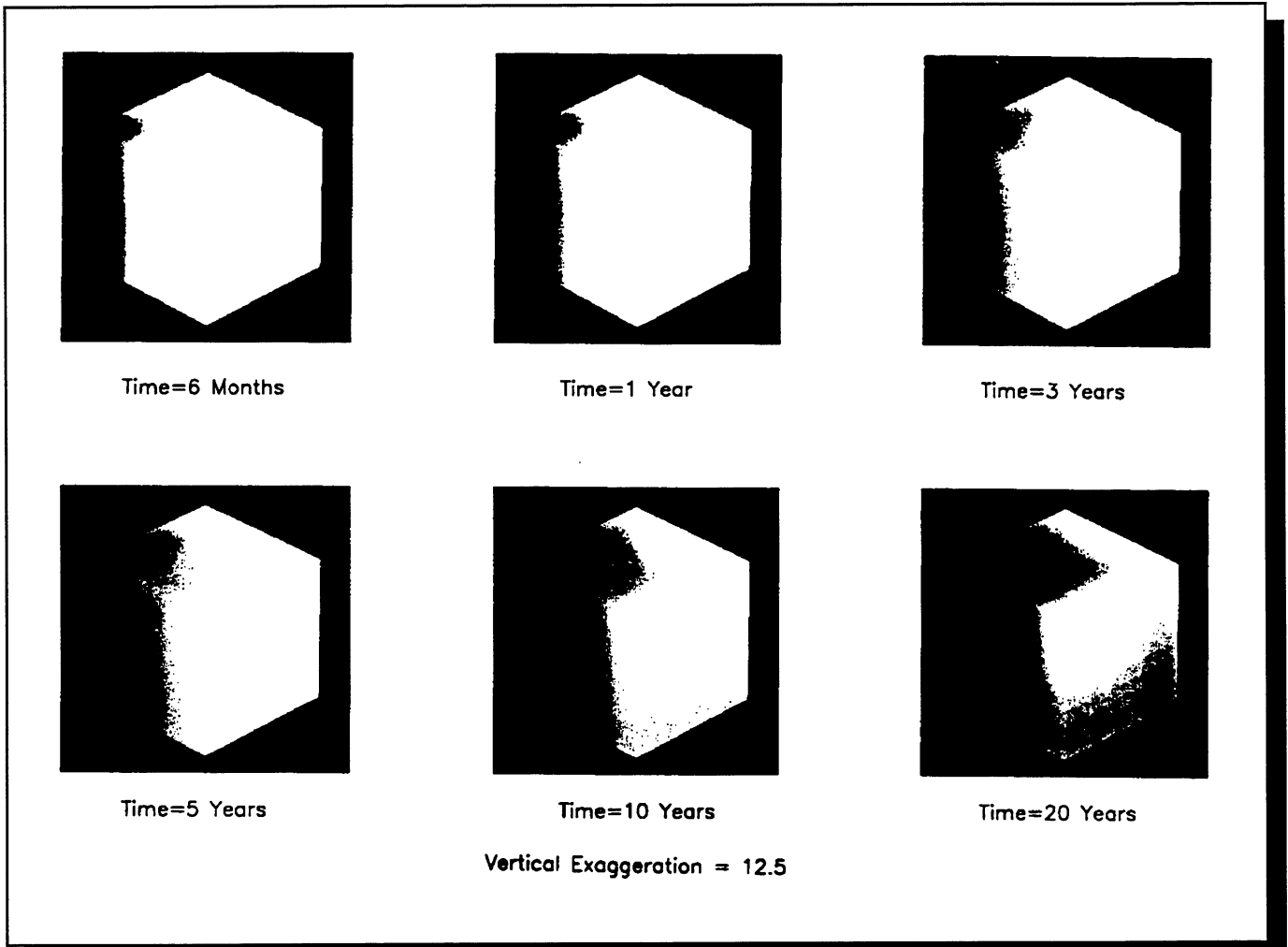


Figure 4.10. Distribution of oil saturation as a function of time for variable grid (horizontal plane) within the three-dimensional model domain. The expanding dark region represents the progress of the water phase through the reservoir during the waterflood. Injection occurs on the left corner of the $\frac{1}{4}$ -volume block. Production occurs on the right corner.

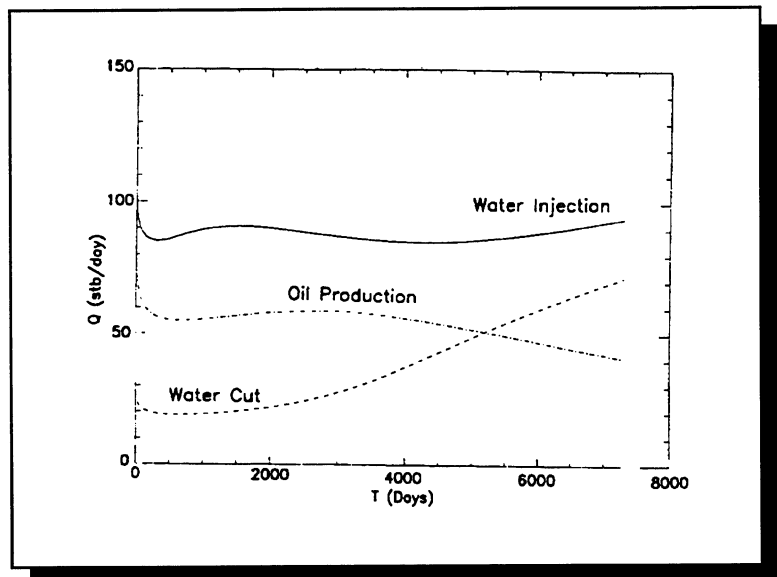


Figure 4.11. Summary plots of water-injection rate, water cut, and oil-production rate as a function of time; computed for the three-dimensional simulation shown in figure 4.10.

The results of the preliminary three-dimensional simulation performed for the homogeneous model domain are summarized in the plots of water-injection rate, oil-production rate, and water cut (figure 4.11). Note that, because only one fourth of the full three-dimensional volume has been simulated, each rate must be multiplied by 4 to obtain reservoir performance measures for the full 2,000-foot by 2,000-foot by 80-foot (610x610x24 m) simulation volume.

Figure 4.12 shows the distribution of absolute permeability assigned in the detailed case. The layered structure (figure 4.13) is a simplified version of the detailed structure constructed

using vertical facies distributions extracted from the detailed model at each of the four corners of the model domain. Permeability and porosity of the layered structure were assigned in the same way as those assigned in the detailed model.

The homogeneous structure is the simplest permeability structure with the absolute permeability computed from the geometric mean of values associated with each facies. The porosity is computed from the same empirical relationship used in the detailed and layered cases.

Relative permeabilities are assigned in the model using relationships developed from laboratory test data reported for samples of Ferron and Berea Sandstones (Miller and others, 1993). Capillary pressures were obtained from the standard water-wet relationships. Fluid properties are defined to be consistent with the initial reservoir fluid pressure of 5,000 psia (34,475 kpa). Wherever possible, fluid properties are specified to be the same as those used to conduct the black oil simulations performed by Odeh (1981). A two-phase oil/water system is assumed, thus the gas phase is not considered.

The 2,000-foot by 2,000-foot by 80-foot-(610x610x24-m-) thick, three-dimensional model grid contains 150,000 rectilinear grid blocks each 20 feet by 2 feet in plan view (6.1x0.6 m) and 4 feet (1.2 m) thick. Thus, there are 15 layers each with a grid of 100 by 100 blocks. Estimated original oil in place differs for each model domain: 2.99 million barrels of oil (MMBO [475,410 m³]) in the detailed styles, 2.67 MMBO (424,530 m³) in the layered heterogeneous style, and 2.07 MMBO (329,130 m³) in the homogeneous style.

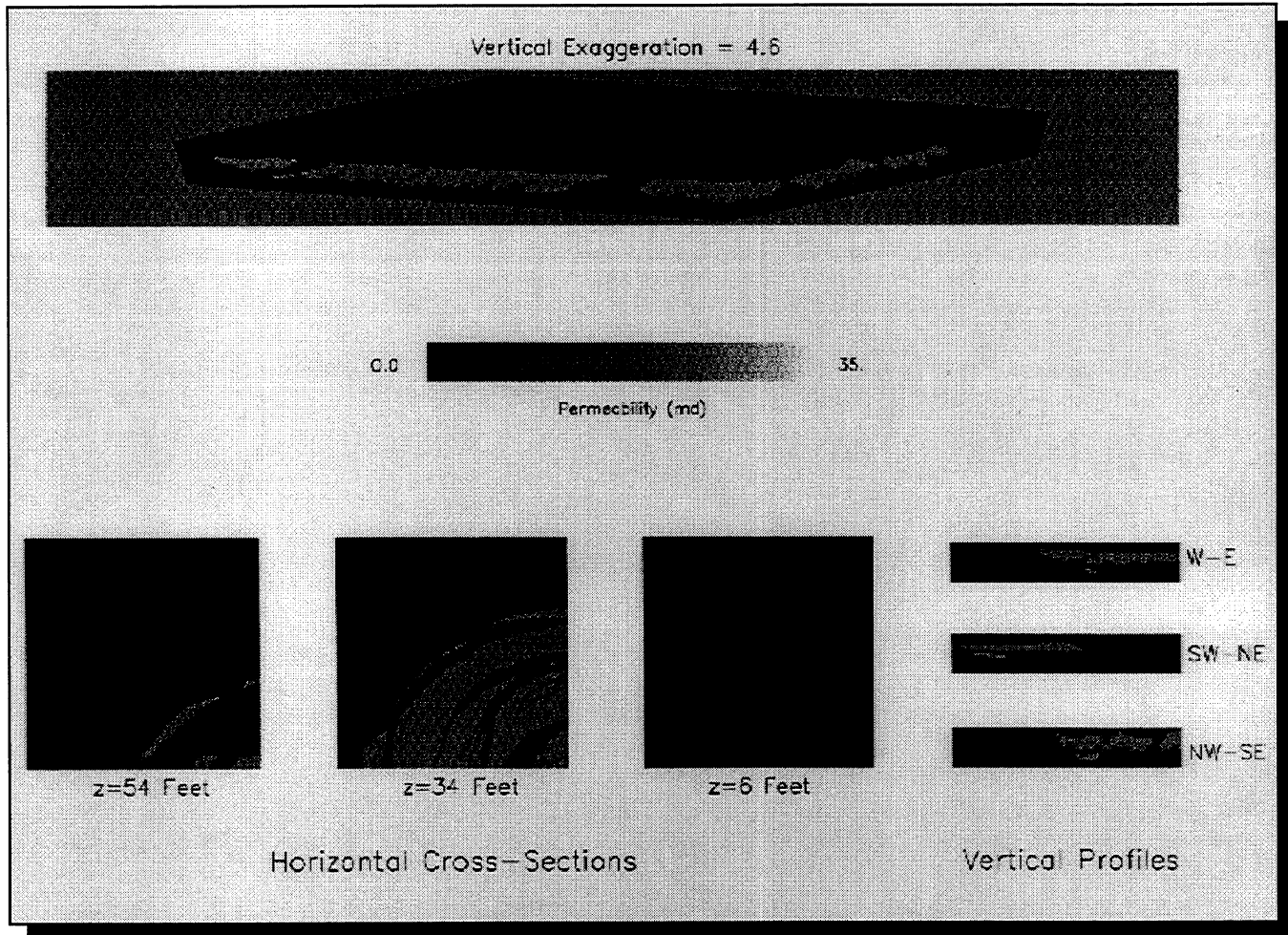


Figure 4.12. Detailed style permeability distribution assigned in the detailed case for the Kf-1-Iv-a parasequence.

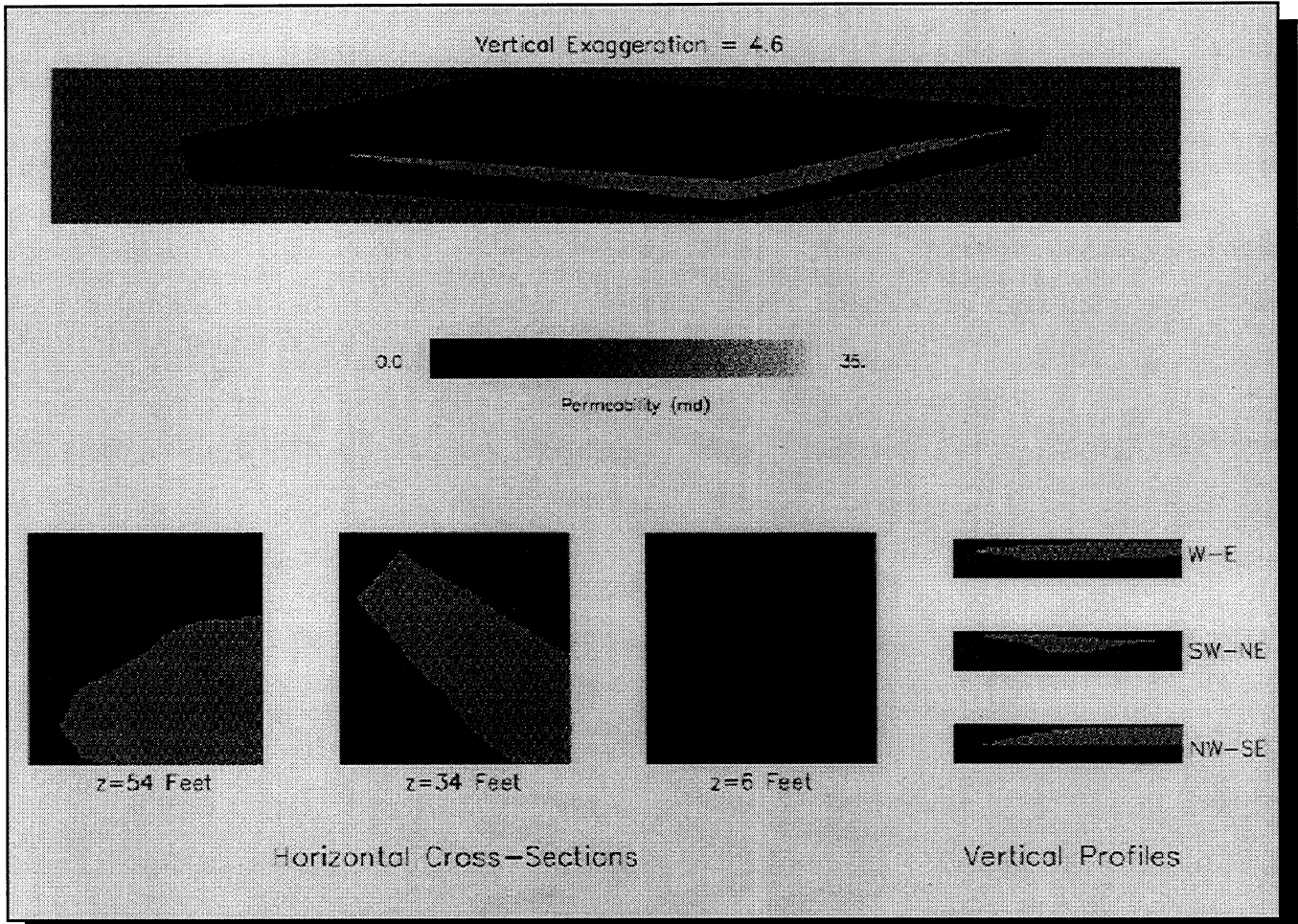


Figure 4.13. Layered heterogeneous permeability distribution for the Kf-1-Iv-a parasequence simplified from the detailed style model.

In order to minimize computer time the primary production stage was bypassed to make all runs in a waterflood mode starting at an initial uniform oil saturation of 50 percent. Four fully-screened production wells were placed at each corner of the model domain with one fully-screened well in the middle of the model.

Sample simulation results are shown as plots of oil saturation at five years after the start of production for both the detailed (figure 4.14) and layered heterogeneous (figure 4.15) styles. The simulation results are consistent with expectations given the assigned input parameters. Preliminary analysis of the results indicates that the homogeneous style requires substantially less water injection to produce a specified volume of oil, however, an extended production time is required to sweep the reservoir. Although the results obtained for the layered heterogeneous and detailed styles differ markedly from those of the homogeneous style, they are similar to one another. After 20 years of production the layered heterogeneous and detailed styles yield about 30 percent of the original oil in place with the layered heterogeneous style providing somewhat better recovery. The detailed style, however, requires slightly less water injection to produce the same amount of oil that is produced in the layered heterogeneous style at a specified point in time.

4.5 References

- Honarpour, Mehdi, Koederitz, Leonard, and Harvey, A.H., 1986, Relative permeability of petroleum reservoirs: Boca Raton, CRC Press, 143 p.
- McCain, W.D., Jr., 1990, The properties of petroleum fluids: Tulsa, Pennwell Publishing Company, p. 325.
- Miller, M.A., Holder, John, Yang, H., Jamal, Y., Gray, K.E., Fisher, R.S., and Tyler, Noel, 1993, Petrophysical and petrographic properties of the Ferron Sandstone: Gas Research Institute Topical Report GRI-93/0219, 257 p.
- Odeh, A.S., 1981, Comparison of solutions to a three-dimensional black-oil reservoir simulation problem: Society of Petroleum Engineers, Paper 9723.

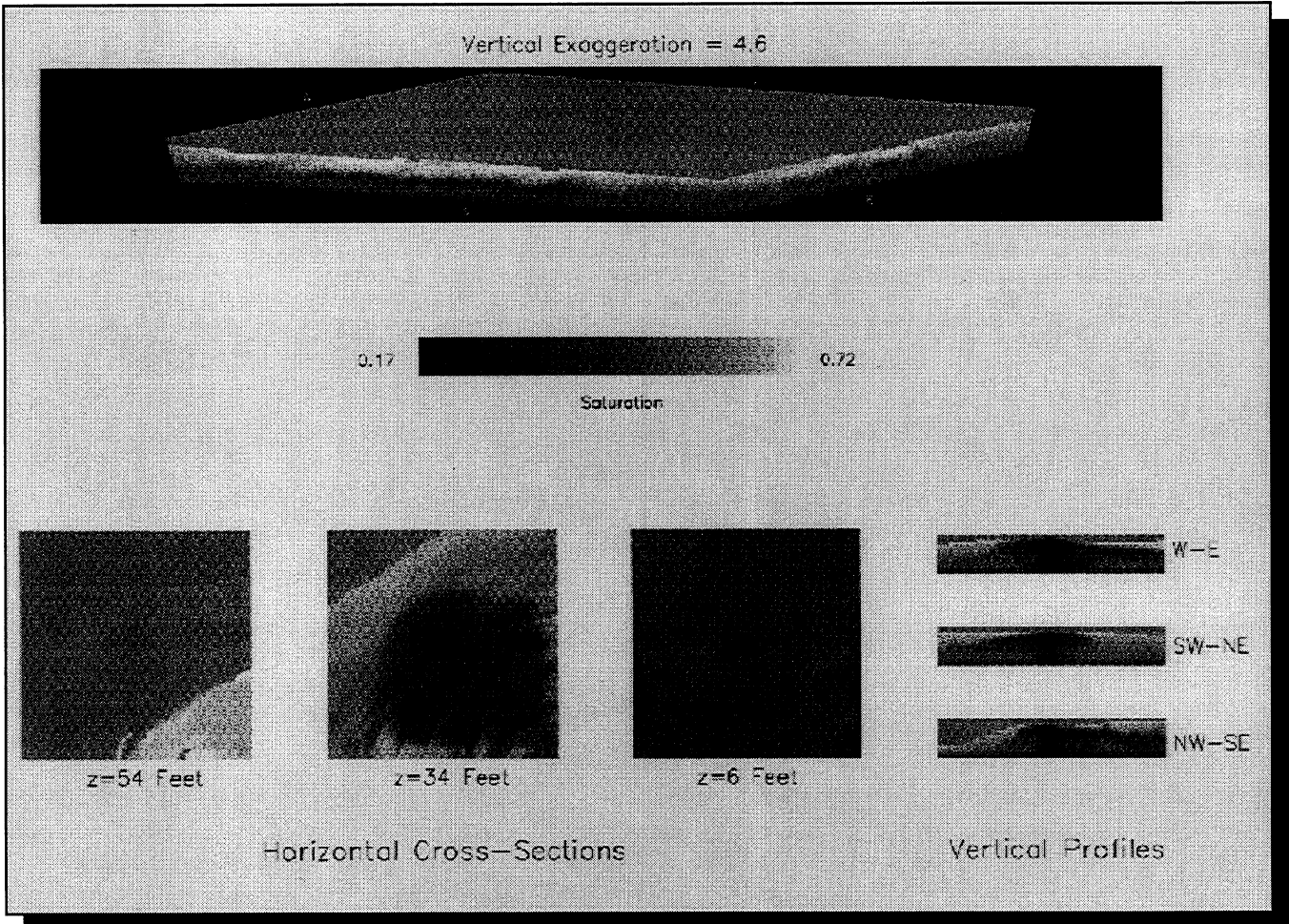


Figure 4.14. Sample plot of oil saturation at five years after the start of production from simulation of the detailed style.

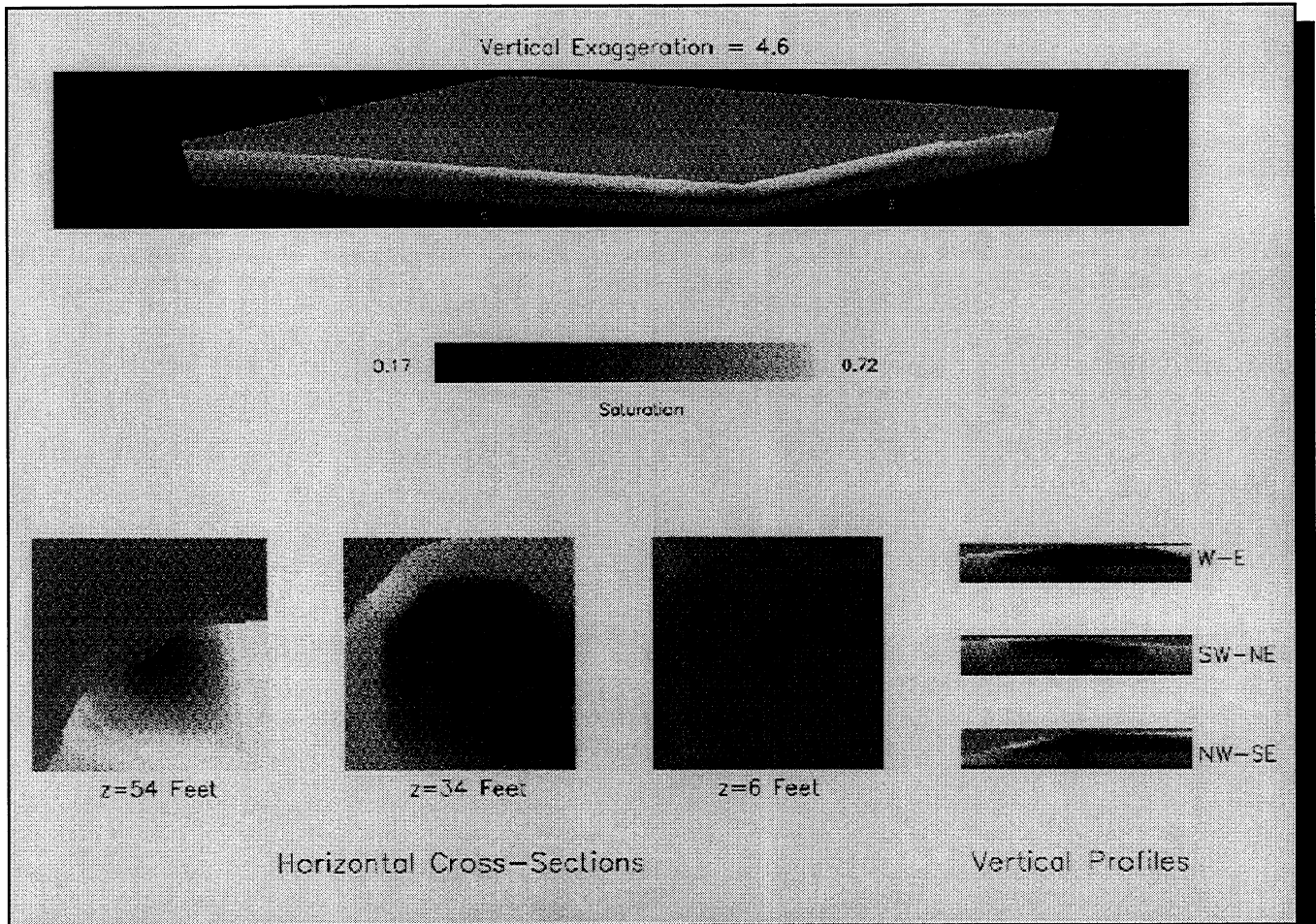


Figure 4.15. Sample plot of oil saturation at five years after the start of production from simulation of the layered heterogeneous style model.

5. TECHNOLOGY TRANSFER

Thomas C. Chidsey, Jr.; Utah Geological Survey

The UGS is the Principal Investigator for three government-industry cooperative petroleum-research projects including the Ferron Sandstone project. The projects are designed to improve recovery, development, and exploration of the nation's oil and gas resources through use of better, more efficient technologies. The projects involve detailed geologic and engineering characterization of several complex heterogeneous reservoirs. Two of the projects will include practical oil-field demonstrations of selected technologies. The U.S. Department of Energy (DOE) and multidisciplinary teams from petroleum companies, petroleum service companies, universities, and State agencies are co-funding the three projects.

Project materials, plans, and objectives were displayed at the UGS booth during the 1997 annual national convention of the AAPG in Dallas, Texas and the 1997 AAPG Rocky Mountain Section meeting in Denver, Colorado. Three to four UGS scientists staffed the display booth at these events. Three abstracts were submitted for a technical presentation at the 1997 Geological Society of America (GSA) national meeting in Salt Lake City, Utah on October 19-22, 1997.

The UGS prepared to present the final results of the project to both academia and industry. Field trips covering the regional stratigraphy and case-study areas will be conducted during the 1997 GSA and 1998 AAPG annual national meetings. The AAPG national meeting will be held in Salt Lake City, Utah on May 17-20, 1998. The field trips have two parts, each with a different emphasis: (1) a review of regional stratigraphy and (2) detailed analysis of depositional environments and permeability trends. The primary objective of day one will be to provide a detailed interpretation of the regional stratigraphy of the Ferron Sandstone outcrop belt from Dry Wash to Last Chance Creek. The primary objective of day two will be to develop a detailed sedimentological characterization of the facies in the Ivie Creek area just north of Interstate 70 (I-70). The Ivie Creek area was selected because it contains abrupt facies changes in the Kf-1 and Kf-2 parasequence sets. Access to the area is excellent because of proximity to I-70. The field trip participants will examine the major reservoir types (mouth-bar complex, wave-modified and fluvial-dominated delta front, distributary channel, and tidal deposits) associated with the Ferron Sandstone. The field trip road logs and Ferron interpretations, titled *Fluvial-Deltaic Sedimentation and Stratigraphy of the Ferron Sandstone*, were published in a two-volume GSA guidebook .

A short course titled *Core and Reservoir Modeling Workshop: Fluvial-Deltaic Nearshore Sands of Ferron Sandstone* will also be offered during the AAPG meeting. The course will take the participants from outcrop to reservoir modeling and flow simulation results of the Ferron project. Integration of geological parameters and methods in setting up a reservoir modeling data set will be presented.

The field trip and short course presented at the AAPG meeting will be sponsored by the UGS, National Petroleum Technology Office - DOE, Mobil Technology Company, and Amoco Production Company.

The UGS has made the collection of core from drill holes in the project area public available at the UGS Sample Library. The Sample Library provides service to all interested individuals and companies who require direct observation of actual samples for their research or investigations. High-quality photographs of the slabbed core surfaces are also available for a nominal fee. The

project core may be examined on site or borrowed for a period of six months. Destructive sampling is occasionally permitted with approval. The UGS requires copies of all reports, photographs, and analyses from these investigations; this information can be held confidential for one year upon request.

The UGS will release all products of the Ferron Sandstone project in a series of formal publications. These will include all the data as well as the results and interpretations. Syntheses and highlights will be submitted to refereed journals, such as the *American Association of Petroleum Geologists (AAPG) Bulletin* and *Journal of Petroleum Technology*, and to trade publications such as the *Oil and Gas Journal*, as well as the UGS *Petroleum News*, UGS *Survey Notes*, and on the project Internet home page of the UGS.

5.1 Utah Geological Survey *Petroleum News*, *Survey Notes*, and Internet Web Site

The purpose of the UGS *Petroleum News* newsletter is to keep petroleum companies, researchers, and other parties involved in exploring and developing Utah energy resources, informed of the progress on various energy-related UGS projects. The UGS *Petroleum News* contains articles on: (1) DOE-funded and other UGS petroleum project activities, progress, and results, (2) current drilling activity in Utah including coalbed methane wells, (3) new acquisitions of well cuttings, core, and crude oil at the UGS Sample Library, and (4) new UGS petroleum publications. *Petroleum News* is published semi-annually.

The purpose of *Survey Notes* is to provide nontechnical information on contemporary geologic topics, issues, events, and ongoing UGS projects to Utah's geologic community, educators, state and local officials and other decision makers, and the public. *Survey Notes* is published three times yearly. Single copies are distributed free of charge and reproduction (with recognition of source) is encouraged.

The UGS maintains a web site on the Internet, <http://www.ugs.state.ut.us>. The *Economic Geology Program* page at this site: (1) describes the UGS/DOE cooperative studies (Ferron Sandstone, Paradox basin, and Bluebell field), (2) contains the latest issue of *Petroleum News*, and (3) has a link to the U.S. Department of Energy web site. Each UGS/DOE cooperative study also has its own separate page on the UGS web site. The Ferron Sandstone project page (<http://www.ugs.state.ut.us/ferron1.htm>) contains: (1) a project location map, (2) a description of the project, (3) a list of project participants and their postal addresses and phone numbers, (4) executive summaries from the first, second, and third annual reports, (5) each of the project Quarterly Technical Progress reports, (6) descriptions of Ferron Sandstone parasequences, (7) a reference list of all publications that are a direct result of the project, and (8) a list of Ferron publications available at the UGS.

5.2 Presentations

The following technical and nontechnical presentations were made during the year as part of the Ferron Sandstone project technology transfer activities. These presentations described the

Ferron project in general and gave detailed information on geostatistics, mathematics of reservoir characterization, sequence stratigraphy, and reservoir models.

Characterization, Facies Relationships, and Architectural Framework in a Fluvial-Deltaic Sandstone: Cretaceous Ferron Sandstone, Central Utah by Ann Mattson; thesis defense, University of Utah, Salt Lake City, Utah, March 1997.

Methods for Characterization of Fluvial-Deltaic Reservoirs by Laura Watkins; 1997 annual spring meeting of the Intermountain Section of the Mathematical Association of America, Utah State University, Logan, Utah, April 1997.

Sandstone Exhumation Effects on Velocity and Porosity: Perspectives from the Ferron Sandstone by R. D. Jarrard and S. E. Erickson; American Association of Petroleum Geologists Annual Convention, Dallas, Texas, April 1997.

Characterization and Upscaling of Sedimentary Depositional Formations Using Archetypal Analysis and Homogenization by Joe Koebbe, Laura Watkins, Thomas, R.; Third IMACS International Symposium on Iterative Methods in Scientific Computation, Jackson Hole, Wyoming, July 1997.

5.3 Publications

Anderson, P.B., Chidsey, T.C., Jr., and Ryer, T.A., 1997, Fluvial-deltaic sedimentation and stratigraphy of the Ferron Sandstone, *in* Link, P.K., and Kowallis, B.J., editors, Mesozoic to Recent geology of Utah: Provo, Brigham Young University Geology Studies, v. 42, pt. 11, p. 135-154.

Chidsey, T.C., Jr., compiler, 1997, Geological and petrophysical characterization of the Ferron Sandstone for 3-D simulation of a fluvial-deltaic reservoir - annual report for the period October 1, 1995 to September 30, 1996: U.S. Department of Energy, DOE/BC/14896-15, 57 p.

Colarullo, S.J., Forster, C.B., Huang, Hongmei, and Mattson, Ann, 1997, From outcrop to simulation in the Ferron Sandstone - 3) impact of 3-D clinoform facies architecture on performance of a fluvial-dominated deltaic-front reservoir [abs.]: Geological Society of America Abstracts with Program, v. 29, no. 6, p. A-465.

Jarrard, R.D., and Erickson, S.E., 1997, Sandstone exhumation effects on velocity and porosity - perspectives from the Ferron Sandstone [abs.]: American Association of Petroleum Geologists Annual Convention, Official Program with Abstracts, v. 6, p. A93.

Mattson, Ann, Chan, M.A., Snelgrove, S.H., Forster, C.B., and Anderson, P.B., 1997, From outcrop to simulation in the Ferron Sandstone - 1) detailed architecture and characterization of a

fluvial-dominated deltaic reservoir analog [abs.]: Geological Society of America Abstracts with Program, v. 29, no. 6, p. A-464.

Snelgrove, S.H., Forster, C.B., Mattson, Ann, and Anderson, P.B., 1997, From outcrop to simulation in the Ferron Sandstone - 2) impact of detailed 2-D clinoform architecture on performance of a fluvial-dominated deltaic-front reservoir [abs.]: Geological Society of America Abstracts with Program, v. 29, no. 6, p. A-464.

Utah Geological Survey, 1997, Ferron project in 3-D simulation phase: Utah Geological Survey Petroleum News (April), p. 2-4.

Utah Geological Survey, 1997, Energy news - oil demonstration programs move into advanced phases: Utah Geological Survey, Survey Notes, v. 30, no. 1, p. 10-11.

U.S. Department of Energy, 1996, Geological and petrophysical characterization of the Ferron Sandstone for 3-D simulation of a fluvial-deltaic reservoir, *in* Contracts for field projects and supporting research on enhanced oil recovery, reporting period July-September 1995: Progress Review No. 84, DOE/BC--95/4, p. 112-120.

U.S. Department of Energy, 1996, Geological and petrophysical characterization of the Ferron Sandstone for 3-D simulation of a fluvial-deltaic reservoir, *in* Contracts for field projects and supporting research on enhanced oil recovery, reporting period October-December 1995: Progress Review No. 85, DOE/BC--96/1, p. 74-78.

U.S. Department of Energy, 1997, Geological and petrophysical characterization of the Ferron Sandstone for 3-D simulation of a fluvial-deltaic reservoir, *in* Contracts for field projects and supporting research on enhanced oil recovery, reporting period January-March 1996: Progress Review No. 86, DOE/BC--96/2, p. 115-120.

